Portions of this dissertation were adapted from the following publications:

Journal of Virology, May 2009, p. 4112–4120 Vol. 83, No. 9

doi:10.1128/JVI.02489-08

Virology, November 2012, p. 157–166, Vol. 433 Iss. 1

http://dx.doi.org/10.1016/j.virol.2012.08.005

Inhibition of the protein kinase R pathway by cytomegalovirus double-stranded RNA binding proteins

Craig J. Bierle

A dissertation

submitted in partial fulfillment of the

requirements for the degree of

Doctor of Philosophy

University of Washington

2012

Reading Committee:

Adam P. Geballe, Chair

Michael Lagunoff

Harmit S. Malik

Program Authorized to Offer Degree:

Molecular and Cellular Biology

University of Washington

Abstract

Inhibition of the protein kinase R pathway by
cytomegalovirus double-stranded RNA binding proteins

Craig J. Bierle

Chair of the Supervisory Committee:
Professor Adam P. Geballe
Division of Human Biology

Double-stranded RNA (dsRNA) that accumulates during many viral infections is recognized by the host cell and elicits an antiviral response. Protein kinase R (PKR) is activated by dsRNA binding, phosphorylates eIF2α, and inhibits translation initiation, potentially blocking the synthesis of viral proteins. Human cytomegalovirus (HCMV) expresses two noncanonical dsRNA binding proteins, TRS1 and IRS, that antagonize PKR. In this study, I investigated the dsRNA-binding properties of TRS1 and related proteins to help clarify their mechanisms of PKR inhibition and roles in viral replication. I found that purified TRS1 specifically bound to dsRNAs as short as 20 base pairs, albeit with a weaker affinity than PKR. However, TRS1 was over 10-fold more abundant than PKR at late times during infection when detectable levels of dsRNA are present. I mutagenized the TRS1 dsRNA binding domain and identified TRS1 variants that impaired dsRNA binding. The TRS1 mutants most deficient for dsRNA binding

did not support the replication of vaccinia virus deleted of its PKR antagonist E3L (VVΔE3L) but did retain the ability to bind PKR. This indicates that while dsRNA and PKR binding are separate functions of TRS1, TRS1 must at least weakly bind dsRNA to antagonize PKR. These results are most consistent with a model in which TRS1 forms a trimolecular complex with dsRNA and PKR to prevent PKR activation. However, it remains possible that the abundance of TRS1 enables it to sequester dsRNA, thereby blocking PKR and other dsRNA-activated pathways. I also investigated whether guinea pig cytomegalovirus (GPCMV), a model of congenital CMV infection, encodes a PKR antagonist. Of the GPCMV dsRNA binding proteins that I identified in a proteomic screen, only gp145 rescued VVΔE3L replication. gp145 reversed the effects of PKR on transfected gene expression and reduced the levels of PKR and eIF2α phosphorylation in VVΔE3L infected cells, demonstrating gp145's capacity to inhibit PKR. Mapping studies demonstrated that gp145 has a dsRNA binding domain homologous to that of TRS1, but also that dsRNA binding by gp145 is not sufficient for PKR inhibition. These studies have demonstrated that dsRNA-binding is a conserved and essential function of the CMV PKR antagonists.

TABLE OF CONTENTS

LIST OF FIGURES AND TABLES

TABLE PAGE

ACKNOWLEDGEMENTS

Science is collaboration, and many people contributed to this work. Despite having e in the Geballe lab almost by accident in my fourth rotation, I could not have found a more patient, helpful, and supportive mentor than I had in Adam. The Geballe Lab's studies of the cytomegalovirus protein kinase R antagonists were initiated by Stephanie Child. Many of the reagents and protocols used in this dissertation were adapted from experiments undertaken by her as well as Morgan Hakki, Emily Marshall, Katie DeNiro, and Pau Mezquita. Katie Semmens has been an active partner on my TRS1 dsRNA binding work. These and other members of the Geballe lab, notably Greg Brennan and Jacquelyn Braggin, provided valued advice and friendship over the years.

My work has also benefited from several healthy collaborations with labs outside of Seattle. I thank Mark Schleiss and Michael Leviton (University of Minnesota) as well as Michael McVoy (Virginia Commonwealth School of Medicine) for introducing me to the guinea pig cytomegalovirus system and for reagents, helpful discussions, and critical review of the gp145 project. Wolfram Brune played an instrumental role in the development of HCMVΔIRS1/ΔTRS1. Additional reagents used in this study were kindly provided by Bertram Jacobs (Arizona State University), Stefan Rothenburg (Kansas State University), and Charles Samuel (University of California, Santa Barbara).

Several labs and core facilities at the FHCRC also contributed to this project. Phil Gafken, Deepa Hegde, and Yuko Ogata of the Proteomics Core assisted with mass spectrometry experiments. Elizabeth Jensen of the Genomic Core gave technical assistance relating to DNA sequencing. Beth Larimore and Bruce Clurman (Fred Hutchinson Cancer Research Center) provided reagents and technical advice on baculovirus expression of proteins. I also thank Erik

Mattsen, and the labs participating in our Herpesvirus, Retrovirus, and Translation Control group meetings for their helpful discussions and feedback. My committee, consisting of Michael Lagunoff, David Morris, Michael Gale, Gabriele Varani, and Harmit Malik, provided valuable guidance throughout my graduate education.

This work was supported by NIH grants AI26672 (to A.P.G) and HD044864 (to M.R.S and A.P.G.).

DEDICATION

For my family**.** The advantage of being one branch of a large tree is the amount of support that the trunk provides. I am especially grateful for the hard work of my parents and grandparents that has provided me with the opportunity to pursue my education far from home. I am also gifted by the love and support of Ilana, who followed me to Seattle and gave me Nolan. I hope that the faith that all of these people have had in me is never disappointed.

CHAPTER 1

Background

Herpesviruses

The herpesviruses are a family of large, double stranded DNA viruses that infect diverse hosts ranging from bivalves to humans. Virions consist of a linear genome from ~120 to 240 kilobases in size that is packaged within an icosahedral capsid that is surrounded by an amorphous tegument and viral envelope. The amplification of the viral genome and packaging of capsids occurs in the nucleus while final virion assembly happens in the cytoplasm. Herpesvirus are capable of both lytic replication, which results in the production of infectious progeny and death of the host cell, and latent infection of host cells, where a subset of viral genes are expressed to maintain the viral genome episomally for an extended period of time (112).

Mammalian herpesviruses have been further characterized into three monophyletic sub-families—the alpha-, beta-, and gammaherpesviruses. These viruses share approximately 40 "core" genes, which are clustered in the middle of the viral genome and are involved in the essential functions of DNA replication, capsid biosynthesis, and virion assembly. Lineage or virus specific genes account for the balance of the viral coding content and confer the viruses with their unique cell or host tropism and replication strategies (142).

Human cytomegalovirus

Human cytomegalovirus (HCMV), also known as human herpesvirus 5, is one of eight herpesviruses known to infect humans. With a genome approximately 235 kilobases in size that encodes over 150 gene products, HCMV has the largest genome coding content of any virus

known to infect humans (103). Like the other herpesviruses, HCMV causes a lifelong infection, although the mechanism of HCMV latency remains less well characterized than in other herpesviruses. Infectious virus is found in most bodily fluids, and is readily spread between individuals who are in close contact with each other. Transmission is frequent between sexual partners, among children in childcare environments, and from infected children to their adult caretakers. Additionally, HCMV is unique among the human herpesviruses in that vertical transmission from mother to child across the placenta, during birth, or in breast milk is quite common (100).

HCMV infection is widespread. Approximately 60% of individuals in the United States are infected and nearly universal infection occurs in some populations (5). In most healthy individuals, infection goes unnoticed, although HCMV can cause a mononucleosis-like disease during primary infection. Severe CMV disease can result from infection of immunocompromised individuals. Prior to the advent of highly active antiretroviral therapies, HCMV was the most common viral opportunistic infection in HIV/AIDS patients and CMV disease is a common complication of solid organ or hematopoietic stem cell transplant and the accompanying immune ablation (100).

Congenital CMV disease can occur following transplacental transmission of HCMV from mother to developing fetus. Fetal infection is most common and CMV disease is generally more severe when primary infection occurs during pregnancy, but congenital CMV infection also occurs in previously immune women following viral reactivation or reinfection. While approximately 90% of congenital CMV infections are asymptomatic, symptomatic infection often results in severe central nervous system sequelae, including vision and hearing loss, cerebral palsy, and mental retardation (100). The human and socioeconomic toll of congenital

CMV, which is estimated to cost $2 billion annually, led the Institute of Medicine to designate congenital CMV as one of the most favorable targets for future vaccine development (135).

Animal models of CMV infection

HCMV and the other betaherpesviruses are species specific viruses that are believed to have coevolved with their hosts (91). This species specificity makes the study of viral infection *in vivo* challenging and has necessitated the development and use of animal viruses as models of HCMV infection. Three viruses that are most widely used in the laboratory are rhesus (RhCMV), mouse (MCMV), and guinea pig cytomegaloviruses (GPCMV). Each of these model systems presents its own set of advantages and disadvantages. The betaherpesviruses are noteworthy for their high rate of gene gain among different viral species; only about 70 genes well conserved between rodent and human cytomegaloviruses (100, 142). As a primate virus, RhCMV is considerably more similar to HCMV than either MCMV or GPCMV, having homologues to approximately 60% of the HCMV genes (100). However, widespread use of the RhCMV model system is limited by the cost and ethical challenges of primate research. There is also little evidence of the vertical transmission of RhCMV during natural infection, making the virus a poor model of congenital CMV disease (4).

MCMV has been the most studied of the animal CMVs. The mouse model benefits from the availability of knockout mice and other genetic tools. However, MCMV does not infect or spread across the placenta during pregnancy. MCMV models of congenital CMV infection have relied on direct injection of the virus into the developing fetus (70, 128). In contrast, GPCMV is more genetically similar to primate CMVs than MCMV (129). Moreover, the guinea pig placenta is morphologically very similar to that of humans, and GPCMV can spread

transplacentally during natural infection (129). This has led to the development of GPCMV as a model for congenital CMV disease (128).

The innate immune response to dsRNA

The capacity for a cell to differentiate between self and non-self plays a central role in the innate immune response to pathogens. Biomolecules that are not normally produced by or are mislocalized in mammalian cells serve as pathogen associated molecular patterns (PAMPs). PAMPs elicit an immune response by binding to and activating a variety of cell surface and cytoplasmic pathogen recognition receptors (PRRs), which stimulate the production of cytokines including interferon that induce an anti-pathogen state in the host. Several foreign nucleic acid species are recognized by mammalian cells as PAMPs, including unmethylated or cytoplasmic DNA, single stranded RNAs that lack features of normal eukaryotic mRNA processing, and double-stranded RNA (dsRNA) (78).

The response of mammalian cells to dsRNA is length dependent (48). dsRNAs that are shorter than 30 base pairs play important roles in regulating gene expression, mRNA translation, and RNA stability during development and normal cell growth (48). Longer dsRNAs are only found in the nucleus of uninfected cells, where they are compartmentalized away from PRRs (10). Cytoplasmic or extracellular dsRNA that exceeds 30 base pairs in length generally occur as a result of viral infection and can stimulate the production of interferon following binding and recognition by PRRs (48). Additionally, several interferon-stimulated genes (ISGs) are also activated by this long dsRNA to induce an antiviral state in infected cells.

The viral origin of dsRNA

dsRNA seems to be an unavoidable consequence of viral replication, although the source of dsRNA depends on the viral genome type. In dsRNA viruses, the viral genome itself is comprised of perfectly duplexed RNA (63). For ssRNA viruses, dsRNA is an intermediate of genome replication (63). Fully duplexed RNA has not been detected during retrovirus infection, but regions of secondary structure in the viral genome, such as HIV TAR, can activate dsRNA binding antiviral pathways (87).

The genomes of DNA viruses are densely packed with open reading frames, which often overlap. Bidirectional transcription can result in the accumulation and annealing of sense and antisense mRNAs to form dsRNA. Sense and antisense viral transcripts have been detected during the replication of poxviruses (14), herpesviruses (51, 65), and adenoviruses (114), although it has not yet been determined whether these transcripts form duplexes *in vivo*. Viral transcripts with complex secondary structures also might be able to elicit an antiviral response.

Detection of viral dsRNAs *in vivo* has relied on dsRNA-specific antibodies (130). Measurable quantities of dsRNA have been detected in cells infected by dsRNA viruses, positive strand ssRNA viruses, and DNA viruses (144). Surprisingly, dsRNA was not detected in cells infected with negative strand ssRNA viruses (144). Given that negative strand ssRNA viruses encode factors that inhibit dsRNA-activated pathways, such as the influenza protein NS1 (85), and that quantities of cytoplasmic dsRNA as low as a single molecule per cell can have an impact on cell physiology (89), dsRNA may be produced during infections by negative-stranded ssRNA viruses at quantities below the limits of detection of immunofluorescence.

Detection of dsRNA by pattern recognition receptors

Mammalian PRRs detect both cytoplasmic and extracellular dsRNA to elicit an immune response. The Toll-like receptors (TLRs) were initially characterized for their involvement in innate immunity against bacterial pathogens, but several of the receptors are activated by viral PAMPs, including virion proteins and nucleic acids (138). TLR3, which is localized both on the cell surface and in endosomal compartments, is activated by dsRNA (141). The TLR3-dsRNA interaction and subsequent TLR3 activation requires an acidic pH, suggesting that the receptor is activated when the cell internalizes extracellular dsRNA by endocytosis (141). While most TLRs recruit and signal through MyD88, TLR3 functions exclusively through TRIF signaling to activate IRF3 and NFκB and stimulate the production of interferon (138).

The RIG-I-like helicases are PRRS that detect intracellular dsRNA. The helicases RIG-I and MDA5 each recognize and are activated by a different set of viruses (78). This differential activity can be explained by the ligand specificities of the proteins—RIG-I is activated by shorter dsRNAs and 5' triphosphates (60) while MDA5 binds to and is activated by longer dsRNAs (71). Ligand binding by either helicase results in conformational changes that expose the protein's CARD domains and allow interaction with the CARD containing, mitochondrial surface protein IPS-1, which in turn activates IRF3 and NFκB signaling to induce interferon production (78).

dsRNA-activated interferon stimulated genes

The production and action of interferon causes the upregulation and synthesis of interferon stimulated genes and the induction of an antiviral state in cells. Several ISGs are activated by dsRNA binding. These ISGs can make the cell inhospitable to viral replication either by editing viral messages to destroy the genetic information contained in viral genomes or transcripts or by inhibiting translation and preventing the synthesis of viral proteins.

RNA adenosine deaminases (ADARs) bind dsRNA and catalyze the deanimation of adenosine (A) to inosine (I), destabilizing the duplexed RNA. The human genome encodes 3 ADAR genes, two of which express catalytically active protein, and one isoform of ADAR1 is interferon inducible (125). dsRNA binding proteins including ADAR generally bind dsRNA in a sequence independent manner. Although A to I editing can cause the hyper-mutation of perfectly duplexed RNAs at any site, complex RNA secondary structure such as bulges can target ADARs to specific bases to achieve site-selective RNA editing. Nontargeted, A to I hypermutation, as observed during infection by viruses including measles and hepatitis C, is decidedly antiviral (125). In contrast, targeted A to I editing can have either a proviral effect or be essential to viral replication. For example, during hepatitis D virus replication A to I editing is necessary for the synthesis of a second form of a viral protein and, ultimately, virion packaging (17).

The RNA interference (RNAi) pathway plays a central role in the antiviral response of plant and invertebrate cells (36). Whether the pathway plays an important antiviral role in mammalian cells remains controversial. Dicer expression is regulated by cell stresses and interferon (146), and many mammalian viruses encode factors that can inhibit Dicer activity (36). However, Dicer competes for cytoplasmic viral dsRNAs with the other antiviral dsRNA binding PRRs and ISGs and there is no evidence that long viral dsRNA is processed by the ribonuclease during infection (36). While RNAi may not be important for innate immunity in mammals, some viruses, including HCMV, encode their own miRNAs (46) or require the expression or modulation of cellular miRNAs for replication (69, 109), illustrating the importance of the RNAi/miRNA pathway to viral replication.

Cytoplasmic dsRNA activates two interferon-induced antiviral pathways that regulate translation. 2'-5' oligoadenylate synthetase (2'-5' OAS, (61)) binds to dsRNA and catalyzes the formation of 2'-5'-linked oligomers of adenosine, which in turn activate the latent ribonuclease L (RNase L). Activated RNase L then degrades rRNA and mRNAs of either viral or cellular in origin, potentially inhibiting viral replication.

Protein Kinase R

Protein kinase R (PKR) is one of four cellular kinases that phosphorylate the α-subunit of the eukaryotic initiation factor 2 (eIF2). eIF2 forms a ternary complex with GTP and the initiating methionine tRNA (Met-$tRNA_i$) that then binds to the 40s ribosomal subunit to form the translation preinitiation complex. After a mRNA binds to the preinitiation complex, base paring between the Met-$tRNA_i$ and the mRNA results in hydrolysis of eIF2·GTP to eIF2·GDP by eIF5. eIF2·GDP is then released from the assembling ribosome and must be recycled back to eIF2·GTP before it can recruit another Met-$tRNA_i$ and initiate another round of translation. The recycling of eIF2 is carried out by the guanine nucleotide exchange complex eIF2B. eIF2 is a trimer, and phosphorylation of eIF2 on its α-subunit at serine 51 causes the affinity of the complex for eIF2B to increase 100-fold, outcompeting unphosphorylated eIF2 for eIF2B binding (50). Because eIF2B is present at limiting quantities in the cell, elevated levels of phospho-eIF2α prevents recycling of eIF2 by eIF2B's, leading to a block of translation at initiation and inhibiting the synthesis of most proteins once available ternary complex has been depleted (59).

PKR is comprised of two canonical double-stranded RNA binding domains and the eIF2α kinase domain. In the absence of dsRNA, PKR exists as a monomer in a conformation where the dsRNA binding domains block the PKR dimerization interface. While PKR can bind dsRNA as

short as 20 bp in length, a duplexed RNA of at least 30 bp is required to engage both dsRNAs and elicit a conformational change in the protein that allows dimerization of PKR. Dimerized PKR rapidly autophosphorylates, stabilizing dimerization and increasing the catalytic activity of the kinase on eIF2α (50).

In addition to dsRNA substrates, PKR is activated by relatively unstructured RNAs that have a 5'-triphosphate (ppp-ssRNA) (104). Most RNA viruses replicate in the cytoplasm and ppp-ssRNAs are often produced as a byproduct of viral replication. These RNAs are recognized by RIG-I in addition to PKR to elicit an antiviral response (60). PKR activation by ppp-ssRNAs appears to both require the dsRNA binding domain and a second triphosphate binding site elsewhere in PKR's structure (139).

Viral PKR antagonists

Viruses depend on the host translation machinery to replicate and have evolved a variety of strategies to evade or exploit the PKR pathway. Every step of the PKR activation pathway is targeted by one or more viral antagonists. Several viruses express dsRNA binding proteins to sequester dsRNA away from PKR. Some viral dsRNA binding proteins, including vaccinia E3L, bind dsRNA using a canonical dsRNA binding motif (132), while other proteins such as influenza NS1 (85) and herpes simplex (HSV) US11 (75) interact with dsRNA using atypical protein structures. Many of these dsRNA binding proteins also interact directly with PKR to either block dimerization and activation or to inhibit eIF2α phosphorylation (83, 132). However, dsRNA binding is not a prerequisite for proteins to bind and inhibit PKR, and several protein antagonists act exclusively by binding to PKR, such as the hepatitis C virus (HCV) proteins E2 and NS5A (147).

Instead of sequestering dsRNA away from PKR, some viruses encode structured RNAs that bind to but fail to activate PKR. RNA inhibitors of PKR activation include the adenovirus VAI (76) and Epstein-Barr virus EBER RNAs (32). These structured RNAs interact with the PKR dsRNA binding domain, blocking the binding of other RNAs, while preventing PKR dimerization and autophosphorylation (93). In addition to these competitive inhibitors of PKR-dsRNA binding, viruses also express eIF2α mimics that act as competitive inhibitors of eIF2α phosphorylation. PKR antagonists encoded by the pox- and ranaviruses (74, 79, 80) have considerable homology to the N-terminus of eIF2α, which allows the antagonists to effectively compete with eIF2α for PKR binding (79).

Some viruses allow the activation of PKR and subsequent eIF2α phosphorylation but prevent the downstream antiviral consequences. For example, both the HSV γ34.5 and human papillomavirus E6 proteins manipulate the cellular protein phosphatase 1α to dephosphorylate eIF2α and permit viral replication (79, 101). Alternatively, viruses can exploit PKR activation to create a cellular environment more hospitable to replication. Viral internal ribosome entry sites (IRES) can allow translation initiation independent of normal eIF2 function. For example, PKR is activated during HCV replication, shutting down ISG production in infected cells, but viral protein synthesis continues thanks to the viral IRES (49).

Like many genes involved in immunity, PKR has been evolving under strong positive selection, presumably driven to adapt under evolutionary pressure from viral PKR antagonists (45, 123). PKR is evolving much more rapidly than the other cellular eIF2α kinases (123), which are evolving under strong purifying selection (45). An effect of the arms race between PKR and its antagonists has been the evolution of species-specific interactions between proteins. This has been best characterized with the vaccinia eIF2α mimic K3L. The PKR antagonists E3L

and K3L have long been known to be determinants of vaccinia host range (80), but more recently individual amino acids in PKR that are evolving under positive selection have been identified as conferring either resistance or susceptibility to K3L (45, 123).

HCMV TRS1 and IRS1 antagonize PKR

HCMV was first demonstrated to encoded a PKR antagonist when it was found to rescue the replication of vaccinia virus lacking its dsRNA-binding PKR antagonist, E3L (27). Infecting human fibroblasts with HCMV prior to VVΔE3L reduced phosphorylation of eIF2α, inhibition of translation, and activation of RNase L (27). To identify the gene or genes that were acting as PKR antagonists, a series of VVΔE3L mutants expressing fragments from a HCMV genome library were analyzed for replication (25). A single recombinant virus was isolated after serial passage in VVΔE3L-nonpermissive human fibroblasts. This recombinant virus included the HCMV TRS1 gene along with part of the adjacent J1S ORF. When viruses that expressed TRS1, J1S, or frameshifted TRS1 were cloned, only the virus that expressed TRS1 rescued VVΔE3L replication (25).

HCMV has the complex class E herpesviral genome structure characterized by long, inverted repeat sequences at the ends of the unique long (UL) and unique short (US) genome regions (39). TRS1 is partially encoded in the repeat sequences that flank the US region of the HCMV genome and is thus closely related to the gene IRS1. The proteins are identical over N-terminal 559 codons and share approximately 50% homology in their divergent C-terminal thirds (25, 55). When expressed in VVΔE3L, IRS1 had the same effects as TRS1 on reversing translation inhibition, eIF2α phosphorylation, and RNase L activation (25).

To determine the role TRS1 and IRS1 played during HCMV replication, a series of viruses lacking TRS1 and/or IRS1 were constructed. Deletion of IRS1 had no impact on viral replication while deletion of TRS1 resulted in a modest decrease in titer, thought to be caused by a replication defect late in infection related to impaired virion packaging (12). Deletion of both IRS1 and TRS1 (HCMV[ΔI/ΔT]) resulted in a virus that is unable to replicate in normal fibroblasts. HCMV[ΔI/ΔT] infection caused the inhibition of translation and eIF2α phosphorylation as early as 24 hours post infection (90). This result suggested that IRS1 and TRS1 are functionally redundant as PKR antagonists. Notably, the replication defect of HCMV[ΔI/ΔT] was also found to be complemented by the PKR antagonist from another virus, vaccinia E3L (90).

Mapping of TRS1 functions required for PKR inhibition

Betaherpesviruses are noteworthy for their large genomes, high rate of gene acquisition, and the presence of several unique gene families (40, 142). TRS1 and IRS1 are members of the US22 gene family (40, 145). The US22 gene family is the largest of these gene families to be conserved across both the cytomegaloviruses and the related roseoloviruses (40). The US22 family is postulated to have originated following the gene capture of a bacterial SUKH family protein (148). There is no obvious homology between the US22 domain and eukaryotic proteins. In TRS1 and IRS1, the US22 domain spans amino acids 116 to 510 and includes two SUKH domains in tandem (148) (Fig. 1.1).

The functional domains of TRS1 and IRS1 have been mapped by truncation (Fig. 1.1). A double-stranded RNA binding domain mapped to residues 74 and 246, roughly corresponding to the N-terminal half of the US22 domain and the first SUKH domain (54, 148). This dsRNA-

binding domain has no detectable homology with the canonical double stranded RNA binding motif or with other known dsRNA binding structures (19, 54). TRS1 N-terminal truncations that disrupt the dsRNA binding domain cannot rescue VVΔE3L (54). However, C-terminal truncations that retain wildtype levels of dsRNA binding also fail to rescue VVΔE3L, suggesting that dsRNA binding by TRS1 is necessary but not sufficient to antagonize PKR (54).

As with many viral dsRNA-binding PKR antagonists, including vaccinia E3L (132) and influenza NS1 (83), TRS1 was also found to interact directly with PKR (55). The precise boundaries of the TRS1-PKR interface have not been mapped, but the TRS1 C-terminus between AAs 679-738 is required for efficient binding (55). TRS1 also causes some PKR to relocalize from the cytoplasm to the nucleus, but whether PKR relocalization is plays role in HCMV replication remains unknown (55). Even though TRS1 and IRS1 have divergent C-termini, IRS1 also binds to PKR and requires its C-terminus for this interaction (55).

Other Functions of TRS1 and IRS1

TRS1 and IRS1 are tegument proteins, which are packaged into the virion and delivered to cells immediately upon infection (120). The TRS1 and IRS1 genes are expressed at immediate early times and accumulate throughout the entire viral replication cycle (121). The proteins were initially described to be transcriptional transactivators. In transfection based assays, neither TRS1 nor IRS1 increased transcription significantly when expressed individually, but either protein could enhance transcription mediated by the immediate early 1 and 2 proteins when cotransfected (62, 120, 121, 133). However, since transfection results in a localized activation of PKR (72, 73), it is possible that the apparent effect of TRS1 or IRS1 on transcription is in fact mediated by blocking transfection-induced translational inhibition

mediated by local PKR activation. Similarly, in transfection based assays TRS1 or IRS1 was required for efficient DNA synthesis from the HCMV oriLyt (110, 111). This effect could also result from TRS1 or IRS1 inhibiting PKR activation following transfection, but the viral proteins have been found interact with the HCMV DNA polymerase processivity factor UL44 (134). Thus whether TRS1 and IRS1 play a role in viral DNA replication remains unclear.

While TRS1 and IRS1 are redundant PKR antagonists, some differences have been identified in proteins' other functions. As noted earlier, HCMV[ΔTRS1] has a replication defect late in infection while HCMV[ΔIRS1] replicates to wild type titers (12). HCMV[ΔTRS1] displayed defective assembly of DNA filled capsids and virus-induced nuclear reorganization (1). A second, in-frame open reading frame is expressed from the unique C-terminus of IRS1 (120). This protein product, called pIRS1^{263}, can antagonize the activity of immediate early CMV transcriptional transactivators (121). Finally, TRS1 interacts with the autophagy regulating protein, Beclin 1, to block autophagosome formation and inhibit autophagy (20). While this binding reaction requires the N-terminus of TRS1, which is identical to IRS1, it is not yet known if IRS1 can also inhibit autophagy (20).

PKR antagonists expressed by other cytomegaloviruses

Since the discovery of HCMV TRS1/IRS1, the PKR antagonists of several other cytomegaloviruses have been identified and characterized. The MCMV genome is in the class A configuration, which comprised of a single unique region flanked by terminal direct repeats. While MCMV does not encode a genome-terminal US22 family protein homologous to TRS1 (119), deletion of either of the US22 family proteins m142 or m143 resulted in replication incompetent viruses (94) that caused the phosphorylation of PKR and inhibition of protein

synthesis during infection (140). The m142 and m143 deletion viruses could be rescued by either by the expression of the PKR antagonists TRS1, vaccinia E3L, or HSV λ34.5, or by growing the viruses PKR deficient fibroblasts (16, 140).

While the US22 domain is relatively conserved between m143/m143 and TRS1/IRS1, m142 and m143 are only 55 and 70% of the length of TRS1, respectively (140). Further investigation of m142/m143 function revealed that they and several other MCMV US22 proteins bind dsRNA (26). Rescue of VVΔE3L was also dependent on expression of both proteins, which bind dsRNA cooperatively (26), complex as a heterotetramer in cells, and bind to and relocalize PKR to the nucleus (24).

Like MCMV, RhCMV has a class A genome structure, but, unlike MCMV, a TRS1 orthologue, rhTRS1 (also called rh230), is found at the end of the viral chromosome (57). Characterization of rhTRS1 in VVΔE3L rescue experiments revealed that it and HCMV TRS1 have species-specific activity against PKR (23). TRS1 antagonized PKRs from great apes but not old world monkeys while rhTRS1 antagonized African green monkey PKR but not great ape PKRs (23). The activity of TRS1 and rhTRS1 against PKRs from nonprimate origin has not been fully explored, but it is interesting to note that TRS1 can apparently support MCMV replication (140). Curiously, while TRS1 and m142/m143 bind to inactive, unphosphorylated PKR (24, 55), rhTRS1 appears to only bind to the phosphorylated form of PKR (23).

In summary, studies of the CMV PKR antagonists from three viruses have revealed that one or more of the US22 family proteins has evolved as a PKR antagonist in each virus. dsRNA binding and PKR interaction are conserved functions in all identified CMV PKR antagonists. However, differences between the species specificity of the CMV PKR antagonists and whether

multimerization is required for protein function suggest that each virus has adapted its PKR antagonist(s) to best suit replication in their modern host.

Project Aims

Our studies have previously demonstrated the essential role that TRS1 and IRS1 play as PKR antagonists during HCMV replication (90). Viruses that lack a normal PKR response have been explored as vaccine strains (68), and we believe that the HCMVΔI/ΔT virus could potentially be a useful live-attenuated or disabled infectious single cycle vaccine. However, our current understanding of how TRS1 and IRS1 function during HCMV infection is incomplete and *in vivo* models of HCMVΔI/ΔT infection have been limited to MCMV infections, which do not replicate the pathogenesis of HCMV congenital infection.

As TRS1/IRS1 require both direct PKR interaction and dsRNA binding to rescue VVΔE3L replication, we hypothesize that the proteins form a trimolecular complex with dsRNA and PKR to block PKR activation. To test this model, the first project discussed herein investigated the formation of dsRNA during HCMV infection and dsRNA binding by TRS1. I examined the kinetics and length requirements of dsRNA binding by TRS1. Finally, I mutagenized TRS1 and identified amino acids that are involved in TRS1-dsRNA binding. I then examined the effect of partial or complete loss of TRS1's dsRNA binding activity on binding to and inhibition of PKR by TRS1.

The study of MCMV m142/m143 has provided valuable insights into the conserved functions of TRS1, but the virus is a poor model for congenital CMV infection. Because preventing congenital CMV is a primary goal of HCMV vaccine development, in a second project I sought to determine whether GPCMV encodes a PKR antagonist. After identifying the

US22 family protein gp145 as a GPCMV antagonist the PKR pathway, I characterized the similarities and differences between gp145 and the PKR antagonists of HCMV, RhCMV, and MCMV.

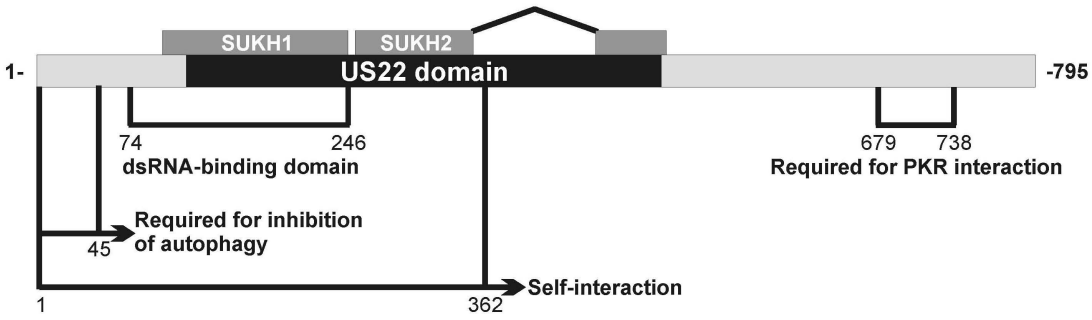

Figure 1.1. Map of TRS1. The approximate boundaries of the TRS1 US22 and SUKH domains are shown in black and gray. Also indicated are the amino acid boundaries of minimal TRS1 fragments that are sufficient for dsRNA binding (TRS1[74-246]) and self-interaction (TRS1[1-362]). TRS1 amino acids between 1-45 and 679-738 are required for inhibition of autophagy by TRS1 and TRS1-PKR interactions, respectively.

CHAPTER 2

Double-stranded RNA production and binding by human cytomegalovirus

SUMMARY

Protein kinase R (PKR) is an antiviral protein that inhibits translation in response to the detection of cytoplasmic double-stranded RNA (dsRNA). Once activated by dsRNA binding, PKR phosphorylates eIF2α, and thereby inhibits the formation of eIF2-$tRNA_i^{Met}$-GTP ternary complex, which is needed for translation initiation. Human cytomegalovirus (HCMV) expresses two proteins, IRS1 and TRS1, which bind to dsRNA and PKR to antagonize PKR during infection. We investigated the formation of dsRNA during HCMV infection and tested the dsRNA binding properties of TRS1. We observed that dsRNA accumulation correlates temporally with the activation of PKR in cells infected with HCMV[ΔIRS1/ΔTRS1]. Using the electrophoretic mobility shift assay we found that TRS1 interacts with dsRNAs as short as 20 base pairs in length and determined that TRS1 binds dsRNA with a lower affinity than PKR. By mutagenizing amino acids in the TRS1 dsRNA binding domain, we identified TRS1 point mutants that were unable to bind dsRNA and tested their ability to bind or antagonize PKR. These results indicate that dsRNA and PKR binding are separate functions of TRS1 and that at least weak dsRNA binding activity is required for TRS1 to antagonize PKR.

INTRODUCTION

Double-stranded RNA (dsRNA) is a pathogen associated molecular pattern commonly associated with viral infection (144). Cytoplasmic or extracellular dsRNA is detected by the pattern recognition receptors TLR3, RIG-I, and MDA5 to stimulate the production of interferon and interferon-stimulated genes (48). Several of the latter, including protein kinase R (PKR), are activated by dsRNA to elicit an antiviral response in the infected host cell. PKR activates upon dsRNA binding, phosphorylates eIF2α, and inhibits translation initiation by preventing the formation of eIF2-$tRNA_i^{Met}$-GTP ternary complex (50).

Viruses depend on the host translation machinery for protein synthesis, and thus PKR activation has the potential to stop viral replication. Viruses have evolved a variety of strategies to antagonize the activation of PKR including PKR degradation and expression of RNA inhibitors of PKR, eIF2α pseudosubstrates, or dsRNA binding proteins (79). Viral dsRNA-binding proteins (dsRBPs) sequester dsRNA to prevent PKR activation and frequently interact directly with PKR to inhibit its function (79).

dsRNA adopts the A-form helical structure, with a relatively deep and narrow major groove and shallow minor groove relative to the B-form helix. dsRBPs bind dsRNA in a sequence non-specific manner by recognizing these characteristic differences in the nucleic acid structure (47). Most cellular and many viral dsRBPs utilize the canonical dsRNA binding motif, which is characterized by an αββββα fold that binds 12 to 16 consecutive RNA base pairs (19). However, not all dsRBPs utilize this fold to interact with dsRNA; notable exceptions include influenza NS1 (143) and herpes simplex US11 (75).

Human cytomegalovirus expresses two functionally redundant dsRNA-binding PKR antagonists, IRS1 and TRS1 (90). These proteins are members of the viral US22 gene family,

which is unique to betaherpesviruses and has no obvious homology to other known proteins. The minimal dsRNA binding domain of TRS1 has been mapped to its N-terminal third by analyses of truncations and deletions (54). The C-terminal end of TRS1, which is dispensable for dsRNA binding, is required for TRS1 to bind and antagonize PKR, suggesting that dsRNA binding is necessary but not sufficient for TRS1 to function as a PKR antagonist (55).

We hypothesize that TRS1 must bind to both PKR and to dsRNA in a trimolecular complex to antagonize PKR (90). This project sought to ascertain the kinetics both dsRNA formation during HCMV infection and binding by TRS1. To test our trimolecular model of TRS1 function, we also aimed to identify TRS1 mutants that disrupt dsRNA binding and determine their effect on TRS1 function as a PKR antagonist. Using dsRNA specific immunofluorescence assays, we found that dsRNA accumulates during HCMV infection and that the kinetics of dsRNA formation correlate temporally with the activation of PKR in cells infected with HCMV deleted for IRS1 and TRS1 (90). We examined the dsRNA binding properties of TRS1 using an electrophoretic mobility shift assay and observed that TRS1 binds dsRNAs as short as 20 base pairs with an affinity weaker than PKR. After identifying TRS1 point mutants deficient in dsRNA binding, we observed that dsRNA binding is required for TRS1 function as a PKR antagonist but not for TRS1-PKR interactions.

RESULTS

dsRNA accumulates during HCMV infection

Detectable levels of dsRNA accumulation have been observed during the infections of many viruses, including the large dsDNA viruses herpes simplex and vaccinia (144), and we sought to determine whether dsRNA accumulates during HCMV infection. Human fibroblasts

were infected with HCMV[AD169] and the presence of dsRNA was assayed at several time points post infection by immunofluorescence using the well-characterized dsRNA-specific monoclonal antibody, J2 (130, 144), as described in Materials and Methods. J2 binds dsRNA in a largely sequence independent manner, although it has some binding preference for A- and U-rich sequences and the ends of dsRNA molecules (13).

We detected J2 reactivity in HCMV infected cells by 24 h p.i. and observed only limited amounts of background fluorescence in mock-infected cells or in infected cells stained with an isotype-matched control antibody (Fig. 2.1A). No dsRNA was detected at 7 h. p.i. or after infection in the presence of cycloheximide (data not shown), suggesting that dsRNA is not delivered with virions or the result of viral immediate early gene transcription. The intensity of the immunofluorescence was not substantially altered by ganciclovir treatment, indicating that late-gene expression is not required for dsRNA production.

We then treated cells with RNase III and RNase A to evaluate the specificity of the J2 antibody for dsRNA in HCMV infection (Fig. 2.1B). The dsRNA-specific RNase III eliminated most of the immunofluorescence signal. Additionally, J2 signal was lost by digestion with RNase A under low-salt but not high-salt conditions—RNase A is generally considered to be a single-strand specific RNase, but it can digest dsRNA under low-salt conditions (107). The ribonuclease susceptibility of J2 immunofluorescence and lack of signal using an isotype matched control antibody supports our conclusion that HCMV infection generates dsRNA.

Deletion of IRS1 and TRS1 from the HCMV genome (HCMV[ΔI/ΔT]) results in a virus incapable of replication in normal fibroblasts. Phospho-eIF2α accumulates in infected cells by 24 h.p.i. and protein synthesis is strongly inhibited by 48 h.p.i. (90). Therefore, the timing of

PKR activation in corresponds with the accumulation of dsRNA in HCMV infected cells. We observed that dsRNA accumulated in cells infected with HCMV[ΔI/ΔT] with similar kinetics as we observed in wild type HCMV (Fig. 2.1C). These data demonstrate that dsRNA is produced by 24 h post-HCMV infection and highlight the importance of viral dsRNA binding proteins to inhibit PKR activation and allow viral replication (16).

Expression of TRS1 in bacteria and yeast

The HCMV dsRBPs TRS1 and IRS1 play an essential role during HCMV replication (90), but we know very little about how they bind dsRNA because the proteins are not homologous to most dsRBPs. While truncating the termini of TRS1 provided some insight into the dsRNA (54) and PKR (55) binding properties of TRS1, we cannot easily differentiate truncations that disrupt individual functional domains from those that destroy the normal folding of the protein because we don't know the structure of TRS1. Before attempting to engineer point mutants into the TRS1 dsRNA binding domain, we first sought to develop a protocol to express full length TRS1 to study its RNA binding properties.

We first attempted to express of TRS1 in *E. coli*. However, the HCMV TRS1 gene was not expressed in bacteria, possibly because of the high G+C content of the natural open reading frame. We collaborated with the Seattle Structural Genomics Center for Infectious Disease (SSGCID) to test the expression of TRS1 that had been codon optimized for bacteria. Full length TRS1 again failed to express, and, of the several truncations tested, significant amounts of soluble protein were only produced from a construct expressing a short C-terminal region, TRS1[615-795]. Since this construct excludes TRS1's US22 domain and is unlikely to bind dsRNA or antagonize PKR, it was not useful for our analyses.

The minimal dsRNA-binding domain (dsRBD) of TRS1, amino acids 74-246, includes roughly half of the US22 domain and one of two SUKH domains in the protein (148). We constructed two bacterial codon optimized constructs to express TRS1 dsRBD (TRS1[45-250] and [71-250]) with an N-terminal GST fusion domain and tested the expression of these constructs in a variety of *E. coli* strains. Soluble GST-TRS1[71-250] was purified using glutathione conjugated agarose beads following expression of the construct in BL21 RIL cells. GST-TRS1[71-250] bound to poly I:C agarose beads, but cleaving GST from TRS1[71-250] with thrombin resulted in loss of dsRNA binding activity (data not shown). As TRS1[74-246] binds dsRNA after *in vitro* translation, it is not clear why cleaved GST-TRS1[71-250] would not bind. Perhaps that GST dimerization enhances dsRNA binding by mimicking multimerization that may occur during dsRNA binding by full-length TRS1.

We next sought to test TRS1 expression in eukaryotic protein expression systems. As with *E. coli*, the HCMV TRS1 gene was not expressed when introduced to the yeast *S. cerevisiae*. However, yeast codon optimized TRS1 is expressed and has been used for two-hybrid analysis of TRS1-PKR interactions (23). His-tagged TRS1 was expressed under the control of a galactose-inducible promoter in yeast and affinity purified protein using nickel-NTA agarose. While TRS1 was detectable by α-His immunoblot in the yeast lysate and elutant, the final yield of TRS1 was low and contained numerous impurities (data not shown). Because neither *E. coli* nor *S. cerevisiae* expressed useful quantities of full-length TRS1, we next sought to test the expression of TRS1 using a baculovirus expression system.

Purification of TRS1 from insect cells

The baculovirus polyhedron gene is highly expressed during the late stages of replication and plays an important role in the viral transmission among insects via occluded virus (77, 86). Disruption of the polyhedron gene and transgene expression using the polyhedron promoter does not interfere with the lytic replication and can result in the production of large quantities of the transgenic protein (77, 86). We engineered recombinant baculovirus expressing either His-tagged HCMV or yeast codon-optimized TRS1 genes (23). Both viruses expressed TRS1, but the highest levels of protein expression were observed using the baculovirus that expressed the HCMV gene (Fig. 2.2A). After optimizing infection and nickel affinity purification protocols, we tested purified TRS1 for dsRNA binding and found that TRS1 produced from baculovirus infected cells interacts with poly I:C conjugated but not control naked agarose beads (Fig. 2.2B). Similarly, PKR expressed in and purified from *E. coli* also bound to the dsRNA beads (33).

To confirm that TRS1 expressed from insect cells has similar dsRNA binding properties as TRS1 expressed either in mammalian cells or by *in vitro* translation using reticulocyte lysate (23, 54), we subjected TRS1 to limited proteolysis with trypsin or chymotrypsin either before or after binding to poly I:C beads. To detect the protease treated TRS1, we immunoblotted using either antibodies to the C-terminal His tag or the N-terminal dsRBD (90). We observed that the His tag was lost at all but the lowest protease concentrations, but the TRS1 fragments retained reactivity to the dsRBD specific antibody (data not shown). These results indicate that baculovirus-expressed TRS1 binds dsRNA through an N-terminal region, similar way results from experiments utilizing expression by transfection in mammalian cells or by *in vitro* translation.

Characterization of TRS1 dsRNA binding by electrophoretic mobility shift assay

dsRNA binding viral PKR antagonists often bind PKR, but the proteins vary considerably in their protein structure, affinities for dsRNA, and the relative importance of dsRNA binding versus PKR interaction. For example, E3L binds dsRNA using a canonical dsRNA binding motif, and its dsRNA binding domain alone is sufficient to support viral replication in cell culture (132). In contrast, the influenza PKR antagonist NS1 binds dsRNA at a low affinity using a noncanonical dsRBD. Because it cannot effectively compete with PKR for dsRNA binding, NS1 requires direct PKR interactions to function (83). To better understand the importance of TRS1 dsRNA binding versus PKR interactions, we sought to determine the affinity of TRS1 for dsRNA by electrophoretic mobility shift assay (EMSA).

We synthesized RNA hairpins 20, 29, and 39 base pairs (bp) in length and incubated them with increasing quantities of purified TRS1 (Fig. 2.3A) (9). TRS1 bound to all three dsRNAs, although with a higher affinity to the 29 and 39 bp hairpins than the 20 bp. We calculated the dissociation constant (K_d) of TRS1 for the dsRNA by plotting the fraction of RNA bound against the TRS1 concentration in the binding reaction and fitting the binding curve by nonlinear least-squares regression (Fig. 2.3C) (124). TRS1 binds to the 20, 29, and 39 bp dsRNAs with K_Ds of approximately 440, 230, and 260 nM respectively. PKR binds to dsRNA through cooperative interactions between its two dsRBDs (88). Under similar conditions as were used in TRS1 EMSA, PKR bound to the 29 and 39 bp dsRNAs at a K_D of approximately 100 nM (Fig. 2.3B).

The specificity of TRS1 for dsRNA had initially been demonstrated using poly I:C binding assays, where incubation with free poly I:C prevented binding to poly I:C agarose while incubation with either single-stranded poly C or I did not (54). Similarly, addition of an equal or greater mass of cold competitor poly I:C to EMSA binding reactions with the 29 bp hairpin

prevented TRS1 binding (Fig. 2.3C) while neither tRNA nor poly C, even at a 30-fold mass excess, affected the interaction between TRS1 and dsRNA. These EMSA experiments confirmed that TRS1 specifically binds dsRNA, albeit with a weaker affinity than PKR.

Quantification of TRS1 and PKR during HCMV infection

Because TRS1 binds dsRNA with a weaker affinity than PKR, whether TRS1 could sequester dsRNA away from PKR depends on the relative concentration of the two proteins during infection. To estimate the concentrations of both proteins, human fibroblasts (HFs) were infected at an MOI of 3 with HCMV or mock infected. The cells were harvested at 2, 8, 24, 48, 72, and 96 hours post infection and lysates were separated by SDS-PAGE along with known quantities of purified TRS1 or PKR and visualized by immunoblotting (Fig. 2.4). The intensity of the PKR and TRS1 bands were compared with the purified protein standards to estimate the molar ratio of full length TRS1 plus IRS1 to PKR at each time point.

The concentration of TRS1 and IRS1 exceeded that of PKR at 24 hours post infection and later, when detectable levels of dsRNA are observed in HCMV infected cells (90). At these time points, TRS1 and IRS1 were at molar concentrations estimated to be at least 10 fold higher than PKR. We also observed of TRS1 or IRS1 fragments throughout the infection. This was most significant at 2 and 8 hours post infection, when the fragments were more abundant than the full length proteins. Whether these fragments represent alternatively processed or degraded TRS1/IRS1 and what function they have during HCMV replication remains unclear. Because TRS1 and IRS1 were detected using an antibody specific to their N-termini, these fragments are not $IRS1^{263}$ (12). Additionally, these bands are not detected during HCMV[ΔI/ΔT] infection, suggesting that they are not the result of antibody cross-reactivity (90). In conclusion, the

relative abundance of TRS1 and IRS1 during HCMV infection would suggest that the proteins could potentially function as a stoichiometric inhibitor of PKR after 24 hours post infection despite the relatively weaker affinity of the viral proteins for dsRNA. However, it remains unclear whether dsRNA is present at undetectable but biologically significant levels earlier in infection when full length TRS1 and IRS1 are less abundant.

Modification of TRS1 arginines disrupts dsRNA binding

Our previous delineation of the dsRNA- and PKR-binding activities of TRS1 have relied on truncating TRS1 (54, 55). Because truncating TRS1 and disrupting either of these activities results in a protein that cannot antagonize PKR, we hypothesized that TRS1 complexes with PKR and dsRNA in a trimolecular interaction to function as a PKR antagonist. However, because data from our previous experiments testing the affinity of TRS1 for dsRNA and its relative abundance compared to PKR prevents us from excluding the possibility that TRS1 functions by sequestering dsRNA exclusively, we sought to engineer point mutations into TRS1 to disrupt dsRNA binding and test their effect. However, our limited knowledge of TRS1 structure made selecting which amino acids to mutate a challenge.

Charged amino acids are commonly found on the surface of proteins, often playing a role in protein-protein or protein-nucleic interactions, and mutagenizing these residues is unlikely to disrupt protein structure (30). Since arginine is the most represented basic amino acid in TRS1, we tested the effect of covalent modification of arginines on TRS1 dsRNA binding. We incubated purified TRS1 or PKR with increasing concentrations of *p*-hydroxyphenylglyoxal (HPG) either before (Fig. 2.5A) or after (Fig. 2.5B) binding to poly I:C agarose (92, 95). HPG modification of both TRS1 and PKR prior to incubating the proteins with poly I:C beads

prevented their association with dsRNA. To our surprise, TRS1 appeared resistant to HPG modification once bound to dsRNA while PKR was not, perhaps reflecting differences between the dsRNA binding domains of the two proteins. Nonetheless, these results suggest that arginine plays an important role in dsRNA binding by TRS1.

Site-directed mutagenesis of TRS1

Knowing both the rough boundaries of a minimal TRS1 dsRBD and that arginine is involved in dsRNA binding, we constructed two sets of alanine point mutants in the minimal TRS1 dsRBD, which has been mapped to TRS1[74-246] (54). Truncation of the C-terminal end of the TRS1 dsRBD between amino acids 240 and 246 resulted in a dramatic loss of dsRNA binding while truncation of the N terminal end caused a gradual loss of binding activity (54). Using this information we constructed the following series of point mutants in the TRS1[240-246] region: G241A, E242A, V243A, V244A, R245A, and V246A.

While the TRS1 dsRBD has no homology to dsRNA binding proteins found outside of the betaherpesviruses, related PKR antagonists from mouse (26, 140), rhesus(23), and guinea pig (11) CMVs have been characterized as dsRNA binding proteins. These proteins vary considerably in length and differ in how they interact with PKR, but their US22 domains, which include the minimal TRS1 dsRBD, are conserved. We used a homology based approach to identify conserved basic amino acids in TRS1[74-246]. After constructing an alignment comprised of one known or predicted HCMV PKR antagonists from 13 CMVs (Fig. 2.6), we compared the pattern of amino acid conservation with a second alignment that included the homologues of 4 additional US22 family proteins from the same viruses: US22. US23. US24, and US26 (data not shown). This allowed us to identify 4 classes of basic residues: 1) unique to

human and chimpanzee TRS1, 2) conserved primarily in TRS1s from primate CMVs, 3) widely conserved in TRS1 homologues but not in other US22 family proteins, or 4) widely conserved in all US22 family proteins examined. For this study, we mutagenized the six residues widely conserved in TRS1 homologues (R121, R124, K125, R129, R150 and R162) and two residues conserved only among the TRS1 homologues of primate CMVs (R230 and R245).

dsRNA binding by TRS1 point mutants

We tested the effect of the TRS1 point mutants on dsRNA binding. TRS1 dsRNA binding was originally characterized by using proteins produced in rabbit reticulocyte lysates and tested for binding to poly I:C agarose (54). However, this protocol has recently failed to replicate results we originally published with several key TRS1 truncations, notably TRS1[Δ86-246], a difference that might be due to differences between batches of reticulocyte lysates or poly(I:C) agarose. Regardless, we utilized a modified dsRNA binding assay in which the protein is produced by transfection and then bound to dsRNA beads (23, 54). We observed that TRS1[V244A] and [R245A] both bound dsRNA at levels comparable to wild type TRS1(Fig. 2.7). The majority of the remaining point mutants, along with TRS1[1-679] and [1-648], bound weakly but detectably to the poly I:C beads. TRS1[R230A], [E242A] and [V243A] had no detectable dsRNA binding in shown experiment, although [E242A] and [V243A] have weakly bound in repeated experiments (data not shown).

We were not surprised that most single amino acid changes had only a modest impact on dsRNA binding. It is likely that multiple protein-nucleic acid contacts are involved in dsRNA binding. Charge-cluster-to-alanine mutagenesis has previously been used to identify functionally important residues in HCMV genes (131), and we constructed two multi-residue mutants.

TRS1[R121A/R124A/ K125A] (Triple) mutated a cluster of conserved basic residues while TRS1[G241A/E242A/V243A/R245A] (Quad) mutated four bases in the TRS1[240-246] region. Neither of these mutants had detectable levels of dsRNA binding.

TRS1 point mutants fail to rescue VVΔE3L

Having identified several TRS1 point mutants that either diminish or eliminate dsRNA binding, we tested the mutants for their ability to antagonize PKR by measuring rescue of vaccinia that lacks its PKR antagonist E3L (VVΔE3L). VVΔE3L infection activates PKR in many cell types, restricting viral replication (7). Viral replication can be rescued by transfecting cells with TRS1 prior to infection (54), and we tested each point mutant for its ability to rescue VVΔE3L (Fig. 2.8). To clone the point mutants in the TRS1[240-246] region, a silent ClaI site cutting at position 741 was introduced into the TRS1 gene (WT+ClaI). As expected, this mutation had no effect on VVΔE3L rescue. Most of the single amino acid to alanine changed had a modest effect on VVΔE3L, rescuing viral replication at least 50% as much as wild type TRS1. Two mutants had a more severe phenotype and rescued VVΔE3L replication no more than 25% of wild type TRS1—R150A and, in low MOI infections (data not shown), G241A. Both the triple and quadruple mutants also failed to rescue VVΔE3L replication.

While expression of the TRS1 mutants was variable, protein expression levels did not correlate with rescue. Notably, the quadruple mutant was poorly expressed in this experiment, but has expressed well in other experiments and still failed to rescue VVΔE3L replication (data not shown). In summary, total loss of dsRNA binding resulted in a greatly diminished capacity for TRS1 to rescue VVΔE3L replication. However, partial loss of dsRNA binding activity caused only in a modest decrease in vaccinia replication.

dsRNA binding and PKR interactions may be independent functions of TRS1

We next sought to determine what impact the loss of dsRNA binding would have on interactions between PKR and TRS1. Previous studies observed that truncating the N- and C-termini of TRS1 disrupt dsRNA and PKR interactions respectively (54, 55), leading us to hypothesize that TRS1 point mutants that disrupt dsRNA binding could still retain the ability to bind PKR. To assay PKR interaction, cells were transfected with plasmids expressing a TRS1 variant along with kinase-dead, biotinylation signal tagged PKR. Following cell lysis, biotin-tagged PKR, along with any associated TRS1, was pulled down using avidin beads (Fig. 2.9).

TRS1[R150A] and the triple mutant both interacted with PKR, while the Quad mutant did not. However, TRS1[1-679], the longest TRS1 truncation tested that failed to interact with PKR in our previous study (55), also bound PKR in this assay. TRS1[1-679]-PKR interactions were initially assayed by pulling down transfected TRS1 and detecting associated endogenous PKR (55). Therefore, the differences between results from the two PKR interaction protocols could be attributable to PKR overexpression. Regardless, the PKR binding by all tested mutants with the exception of the quadruple mutant may suggest that the quadruple mutant has a grossly disrupted structure. These results indicate that dsRNA binding and PKR interactions are separate functions of TRS1. While interactions between PKR and TRS1 alone are not sufficient to rescue VVΔE3L, weak dsRNA binding activity plus PKR interaction can allow TRS1 to antagonize PKR.

DISCUSSION

PKR is activated by dsRNA that accumulates during viral infection, potentially inhibiting translation by the blocking the formation of ternary complex and translation initiation. Most

viruses must inhibit the PKR pathway to replicate, and HCMV is no exception. Deletion of the viral dsRNA binding proteins TRS1 and IRS1 results in a virus incapable of replication in normal fibroblasts (90). While interactions with dsRNA (54) and PKR (55) appear to be necessary for TRS1 function, the structure of the protein is not known and we do not completely understand the mechanisms TRS1 uses to bind either substrate and antagonize PKR.

dsRNA accumulates during the replication of many viruses (144), but our understanding of why dsRNA accumulates during DNA virus infection remains incomplete. We found that, as with other herpesviruses (16, 144), dsRNA accumulates during HCMV infection and is presumably responsible for the activation of PKR in cells that are infected with HCMV[ΔI/ΔT] (90). Several studies have found that a many viral transcripts that are produced during HCMV infection are antisense to known or predicted viral open reading frames (51, 149), suggesting that dsRNA may be a consequence of bidirectional transcription of the viral genome. It remains to be seen whether these transcripts anneal *in vivo* to activate PKR.

dsRBPs are essential for HCMV (90) and MCMV (16) replication, and we sought to better understand how TRS1 interacts with dsRNA. We used EMSA to determine both the affinity and length requirements of dsRNA-binding by purified TRS1. We observed that TRS1 bound dsRNA with a weaker affinity than PKR. However, we also found that TRS1 is much more abundant in infected cells than PKR at time points when dsRNA has been detected during infections (90). For this reason, we cannot exclude the possibility that TRS1 functions as a stoichiometric inhibitor of PKR at late time points when TRS1 is most abundant. We also observed that TRS1 binds dsRNAs as short as 20 bp in length, suggesting that TRS1 could interfere with cellular miRNA pathways.

Our ability to express and purify TRS1 also gives us a valuable tool for future structural studies of TRS1. We have successfully expressed TRS1 on a milligram scale using adherent insect cells, and further optimizing protein production in suspension cells could yield enough protein for crystallization trials. Alternatively, we have successfully demonstrated that TRS1 can be modified by HPG, and envision that HPG modification could be used to probe the nucleic acid or PKR binding interfaces of TRS1 by mass spectrometry (92). We are also interested in purifying TRS1 mutants so that we directly compare their dsRNA binding affinity to the wild type protein. However, the time investment needed to engineer a baculovirus and prepare viral stocks is considerable, and an alternative approach for protein expression should be developed for the routine analysis of TRS1 mutants.

We also identified TRS1 point mutants defective for dsRNA binding, a function of TRS1 that has been widely conserved in TRS1 homologues from both rodent and primate CMVs (11, 23, 26, 54). We mutagenized residues found either at the boundary of the minimal TRS1 dsRNA binding domain (54) or basic residues that have been conserved across CMV evolution. Mutations that eliminated dsRNA binding also greatly reduced TRS1 activity against PKR, as measured by VVΔE3L rescue. Additionally, while partial loss of dsRNA binding activity only had a modest effect on VVΔE3L rescue, we found that combining 3 or 4 of the less severe dsRNA binding mutants also resulted in proteins that did not function as PKR antagonists.

Two point mutants that lacked dsRNA binding activity, TRS1[R150A] and [R121A/R124A/ K125A], remained able to bind to PKR. These results suggest that dsRNA binding is not a prerequisite for TRS1 interaction with PKR and that interactions between TRS1 and PKR are not sufficient to antagonize PKR function. However, low levels of dsRNA binding by TRS1 are sufficient to rescue VVΔE3L replication if the protein can also bind PKR. While

these results support our trimolecular model of TRS1 function. Identification of TRS1 or PKR point mutants that disrupt the interaction between the two proteins would help to further clarify how TRS1 functions.

TRS1, like many other viral proteins, is multifunctional. In addition to binding dsRNA and antagonizing PKR, TRS1 has been described to play a role in viral transcription (133), virion packaging (1), and inhibition of autophagy (20). While PKR is activated by infection with HCMVΔI/ΔT, we do not know for certain that inhibition of PKR is the (or only) essential role of TRS1 and IRS1 during replication. In future studies, we are eager to determine the impact that disrupting TRS1 dsRNA and/or PKR interaction domains has on these other functions. Additionally, TRS1 can antagonize the 2'-5' oligoadenylate synthetase/RNase L pathway during VVΔE3L infection (90) and it remains to be seen whether TRS1 similarly interferes with this and other dsRNA activated pathways aside from PKR during HCMV replication.

MATERIALS AND METHODS

Cells and Virus

Human fibroblasts (HF), COS-7 (ATCC CRL-1651), and HeLa cells were propagated on Dulbecco's modified Eagle's medium supplemented with 10% NuSerum (BD Biosciences) as previously described (25). SF9 cells (from Bruce Clurman, FHCRC) were grown on propagated either in Grace's Insect Media (Invitrogen) supplemented with 10% fetal bovine serum or in SF-900 III (Invitrogen). VVΔE3L was obtained from Bertram Jacobs and propagated and titered in BHK cells (6, 25). HCMV[AD169] (ATCC, VR-538) and HCMV[Towne] (ATCC, VR-977) were propagated and titered on HFs, while HCMV[ΔI/ΔT] was propagated and titered on HF-944.5 cells (90).

Plasmids

pEQ1257 was cloned by digesting pEQ1180 with BamHI and PmeI and ligated into pFastBac Dual (Invitrogen) that was digested with BamHI and StuI. pEQ1258 was cloned by digesting pEQ1236 (pUC57 containing yeast codon optimized TRS1 [GenScript]) with EcoRI and PstI and cloned into pFastBac Dual linearized with EcoRI and PstI.

pEQ1196 was cloned by amplifying pEQ1180 with PCR primers #88 (5'-AGGCGTGTACGGTGGGAGGTCTAT-3') and #695 with Phusion polymerase (New England Biolabs). The resulting fragment was cut with HindIII and ligated into pEQ1180 that had been linearized with HindIII and PmlI. A second PCR reaction was primed with primers #652 and #694 and also used pEQ1180 as template. The resulting product was digested with BsrG1 and ClaI and ligated into pEQ1195 that had been linearized with the same enzymes. pEQ1209 was cloned by amplification of pEQ1180 with primers #88 and #720 (5'-TTGCATCGATACACCCGCACCACCTCGGGCGCGCCGTGCCGAAACCA-3'). The resulting PCR product was digested with HindIII and ClaI and ligated into pEQ1196 that had been linearized with the same enzymes. This introduced an AseI restriction site and TRS1[G241P] mutation.

TRS1 point mutants were cloned by digesting pEQ1209 with AseI and ClaI and ligating in the following annealed primer pairs: pEQ1216 (TRS1[G241A], #725, 5'-CGCGGCGGAGGTGGTGCGGGTGTAT-3' and #726, 5'-CGATACACCCGCACCACCTCCGC-3'), pEQ1217 (TRS1[E242A], #727, 5'-CGCGGGCGCGGTGGTGCGGGTGTAT-3' and #728, 5'-CGATACACCCGCACCACCGCGCC-3'), pEQ1220 (TRS1[R245A], #731, 5'-

CGCGGGCGAGGTGGTGGCGGTGTAT-3’ and #732, 5’-CGATACACCGCCACCACCTCGCC-3’), pEQ1223 (TRS1[V243A], #736, 5’-CGCGGGCGAGGCGGTGCGGGTGTAT-3’ and #737, 5’-CGATACACCCGCACCGCCTCGCC-3’), pEQ1224 (TRS1[V244A], #738, 5’-CGCGGGCGAGGTGGCGCGGGTGTAT-3’ and #739, 5’-CGATACACCCGCGCCACCTCGCC-3’), pEQ1225 (TRS1[V246A], #740, 5’-CGCGGGCGAGGTGGTGCGGGCGTAT-3’ and #741, 5’-CGATACGCCCGCACCACCTCGCC-3’)and pEQ1370 (TRS1[G241A/E242A/V243A/R245A], #929, 5’-CGCGGCTGCCGCTGTGGCCGTGTAT-3’ and #930, 5’-CGATACACGGCCACAGCGGCAGC-3’).

Additional TRS1 point mutants were cloned by stitch PCR using complementary forward and reverse primer pairs for each mutant. For the first set of PCR reactions, using pEQ1196 as a template, oligonucleotide #88 (5’- AGGCGTGTACGGTGGGAGGTCTAT-3’) was combined with each reverse primer while primer #450 (5’-CACCGCGCCCAGCGCCAGCCA-3’) was combined with each forward primer. PCR products were purified using Geneclean II (MP Bio) and used for a second round of PCR where the products for each matching set of reactions were combined and amplified with primers #88 and #450. The final stitch PCR products were digested with HindIII and ClaI and ligated into pEQ1196 that had been linearized with the same enzymes. This protocol was used to clone the following plasmids: pEQ1424 (TRS1[R121A], #1016f and #1017r, 5’ CCAACAGCACGGGCGCCGCCATGCGCAAG 3’), pEQ1425 (TRS1[R124A], #1018f and #1019r, 5’-CGGGCCGCGCCATGGCCAAGTGGTCGCAGCG-3’), pEQ1426 (TRS1[K125A], #1020f and #1021r, 5’-GCCGCGCCATGCGCGCGTGGTCGCAGCGCG-3’), pEQ1427 (TRS1[R121A/R124A/

K125A] , #1022f and #1023r, 5'-CCAACAGCACGGGCGCCGCCATGGCCGCGTGGTCGCAGCGCG-3'), pEQ1428 (TRS1[R129A], #1024f and #1025r, 5'-CGCAAGTGGTCGCAGGCCGACGCGGGCACGC-3'), pEQ1429 (TRS1[R150A], #1026f and #1027r, 5'-CGCGGGTGACGCCGGCCAGCCAGATGAACGGC-3'), pEQ1430 (TRS1[R162A], #1028f and #1029r, 5'-GCGCGACGGACCTGGCGCAGCTGTCGCCGCG-3'), and pEQ1431 (TRS1[R230A], #1030f and #1031r, 5'-GATCCTGGCGGCGGCCGACGCGGACGAGTG-3')

HCMV infections

HF were infected with HCMV at MOIs ranging from 3 to 5 PFU/cell, depending on the experiment. Virus was diluted in medium and allowed to adsorb to cells for 2 hours, after which the inoculum was aspirated and replaced with fresh medium. For HCMV[ΔI/ΔT] infection, cells were infected using spin inoculation. Virus was diluted in medium sufficient to cover the cells and the plates were centrifuged at 700 x *g* for 30 min at 7°C. The plates were then incubated at 37°C for an additional 30 min, after which the inoculum was aspirated and fresh medium was added.

Immunofluorescence

HF were seeded into 12-well plates containing glass coverslips. The cells were infected at an MOI of 5 as described above. The coverslips were rinsed with PBS, fixed with 4% formaldehyde in PBS for 30 min at 4°C, and rinsed three times with PBS. The cells were permeabilized with 0.5% Triton X-100 (Sigma) in PBS, rinsed, and then blocked using 3% bovine serum albumin (BSA) in PBS for 30 min at room temperature (RT) and rinsed. The coverslips were incubated with J2 mouse monoclonal antibody (1:1,000 in 3% BSA in PBS; English and Scientific

Consulting) or isotype-matched β-galactosidase mouse monoclonal antibody (Promega; Z378A) for 30 min at RT and rinsed three times in PBS before being stained with fluorescein isothiocyanate-labeled goat anti-mouse antibody (1:1,000 in 3% BSA in PBS) for 30 min at RT. Hoechst no. 33342 (5 μg/ml; Invitrogen) was used to stain nuclei. RNase treatments were completed after the blocking step using 8 U/ml ShortCut RNase III (New England Biolabs; M0245S) in the manufacturer-supplied buffer or 50 μg/ml RNase A (Sigma; R5503) in either 0.1X SSC (1X SSC is 0.15 M NaCl plus 0.015M sodium citrate) (low salt) or 2X SSC (high salt). After the addition of RNase, the coverslips were incubated at 37°C for 1 h before being washed with PBS and stained with J2 as described above. Ganciclovir (30 μM/ml; Syntex) was added at 1 h p.i. and remained on the cells throughout the infection.

Construction of recombinant baculovirus

Competent DH10Bac cells (Invitrogen) were prepared using the calcium chloride method (58). These cells were transformed with pFastBac Dual, pEQ1257, and pEQ1258 and grown on LB agar plates containing kanamycin (50 ug/ml), gentamicin (7 ug/ml), tetracyclin (10 ug/ml), X-Gal (40 ug/ml), and IPTG (40 ug/ml). Recombinant bacmid containing colonies were picked and assigned new numbers—pFastBac Dual became pEQ1263, pEQ1257 became pEQ1266, and pEQ1262. Bacmid DNA was isolated using the Invitrogen's Bac to Bac protocol. SF9 cells were transfected with bacmid DNA using Lippofectamine 2000. The media from the transfection was harvested 8 days later and used to infect SF9 cells and media harvested at 72 hours post infection. Virus was titered on SF9 cells according to Invitrogen's instruction. Subsequent baculovirus passages used an infection of 0.1-0.5 and harvested media at 72 hours post infection.

Purification of TRS1 from insect cells

Confluent SF9 cells were infected with BVEQ1266 at a MOI of 0.5. At 72 hours post infection, cells were sloughed off of the plate, pelleted at 500 x *g*, and washed with PBS. After pelleting again at 500 x g and removing the PBS, the cells were lysed in buffer containing 500 mM NaCl, 50 mM sodium phosphate pH 7.0, 1% NP-40, and 20 mM imidazole by incubating for 15 minutes on ice. The lysate was then clarified by centrifugation at 15800 x *g*. PerfectPro NiNTA agarose or superflow (5Prime) beads were washed with lysis buffer prior to addition to clarified lysate and incubated for 2 hours at 4°C with rotation. The beads were then pelleted at 500 x *g* and the unbound lysate discarded. Wash buffer, containing 500 mM NaCl, 50 mM sodium phosphate pH 7.0, 1% NP-40, and 50 mM imidazole, was added to the beads, which were incubated at 4°C with rotation for 15 minutes before transferring to a centrifuge column (Pierce) and centrifuging at 500 x *g*. The beads were then washed four additional times by addition of wash buffer and centrifuging at 500 x *g*. Elution buffer 1 (500 mM NaCl, 50 mM sodium phosphate pH 7.0, and 100 mM imidazole) was then added to the beads, incubated for 5 minutes at 4°C, and collected after centrifugation at 500 x *g*. This step was repeated once more with elution buffer 1, and twice with elution buffer 2 (500 mM NaCl, 50 mM sodium phosphate pH 7.0, and 250 mM imidazole). Final protein concentrations were determined by measuring absorbance at 280 nm using the Nanodrop 2000 and by the fluoraldehyde o-phthalaldehyde (OPA, Pierce) assay (53).

Preparation of PKR

Active PKR was expressed and purified from bacteria as previously described (33). Protein quantifications were determined by either the Bradford or OPA assay.

dsRNA binding assay

dsRNA [poly(rI · rC)] agarose beads were prepared as described previously (81). Purified protein was either directly added to Buffer A or harvested transfected cells were lysed by incubating in Buffer A for 20 minutes on ice and pelleting the nuclei by centrifuging (16,000 x *g*) for 15 minutes at 4°C. The samples were split between a mixture of 10% dsRNA agarose beads in carrier Sepharose CL-6B (Sigma-Aldrich) or with control Sepharose CL-6B alone and incubated for 2 hours at 4°C on a rotating mixer. After binding, the beads were pelleted (845 x *g*, 3 min) and washed in Buffer A 3-4 times after which bound proteins were denatured, separated on 10% SDS-PAGE gels and visualized either by coomassie staining or immunoblot.

Electrophoretic mobility shift assay

The following oligonucleotides were annealed and transcribed *in vitro* (MAXIscript, Ambion), labeling with α-^{32}P-UTP (EasyTides, Perkin-Elmer), according to the manufacturer's instructions: 675 (5'-TAATACGACTCACTATAG-3') and 807 (5'-GGGCGAAUUGGAGCUCCACCGCGGUGGCGGCCGCUCUAGAGGACUAGAGCGGCCGCCACCGCGGUGGAGCUCCAAUUCGCCC-3'), 675 and 890 (5'-GGGCGAAUUGGAGCUCCACCGCGGUGGCGAGGACGCCACCGCGGUGGAGCUCCAAUUCGCCC-3'), 675 and 891 (5'-GGGCGAAUUGGAGCUCCACCAGGAGGUGGAGCUCCAAUUCGCCC-3'). The concentrations of hairpin RNA were calculated using the LS 6500 scintillation counter (Beckman Coulter). For binding reaction, between 0.25 to 1 pmol of hairpin RNA was incubated in EMSA buffer (325 mM NaCl, 32.5 mM sodium phosphate (pH 7.0), 162.5 mM imidazole, 0.1 µg/ul sonicated salmon sperm DNA, 0.2 µg/ul BSA, 0.2% Triton X-100, and 2 mM DTT) with TRS1 at a final concentration between 10 and 1000 nM at room temperature for 15 minutes. For

competition experiments, 29 bp hairpin was incubated as described above with 316 nM TRS1. Between 2 and 63.2 ng of Poly I:C, Poly C, or tRNA was added to each binding reaction. 3X no dye loading buffer (325 mM NaCl, 32.5 mM sodium phosphate (pH 7.0), 162.5 mM imidazole, 0.2% Triton X-100, 2 mM DTT, and 15% glycerol) was added to the binding reactions and separated 10% Mini-PROTEAN TBE Precast Gels (Bio-RAD) with 0.5X TBE. Gels were dried and visualized by phosphorimager analysis (Typhoon Trio [GE Healthcare]) and bands quantified using the ImageQuant software. Binding curves were calculated using GraphPad Prism 6.

HPG modification of TRS1

PKR or TRS1 was modified with *p*-hydroxyphenylglyoxal (HPG, Thermo) either before or after binding to poly I:C agarose beads. Samples were incubated in HPG buffer (50 mM Hepes, pH 8, 50 mM boric acid, 150 mM NaCl) containing between 1 and 50 mM of HPG (92). After dsRNA binding, samples were separated by SDS-PAGE and proteins detected by immunoblot.

TRS1 alignment

US22 genes, including the known or predicted TRS1 homologues, from human herpesvirus 6A (NC_001664.2) and cytomegaloviruses that originated from the following mammals were aligned using ClustalX2: rat (*R. nor*., NC_002512.2), mouse (*M. mus*., NC_004065.1), three-striped night monkey (*A. tri*., FJ483970), common squirrel monkey (*S. sci*., FJ483967), grivet monkey (*C. aet*., FJ483969), olive baboon (*P. cyn*. AC090446.27), rhesus macaque (*M. mul*., NC_006150.1), crab-eating macaque (*M. fas*., JN227533), common chimpanzee (P. tro., NC_003521.1), human (H. sap., NC_006273), common treeshrew (T. glis, NC_002794.1), common bent-wing bat (M. sch., JQ805139), and guinea pig (C. por., NC_011587.1)

VVΔE3L rescue

Triplicate wells of subconfluent HeLa cells were transfected with the indicated plasmid using Lipofectamine 2000 (Invitrogen) according to the manufacturer's instructions. 24 hours post transfection, cells were infected with VVΔE3L at a MOI of 5 and viral replication was quantified by 4-methylumbelliferyl β-D-galactopyranoside (MUG) assay at 24 hours post infection as described previously (54).

PKR binding assay

Subconfluent COS-7 cells in 6 well plates were transfected using Lipofectamine 2000 with a mixture of 1.3 μg of each of 3 plasmids: 1) pCS2+BirA, 2) Bio/His-tagged, kinase-dead PKR (pEQ1068) and 3) a plasmid expressing 6X-His-tagged TRS1 variants or GFP. Biotinylated PKR and associated proteins were pulled-down as previously described (11) and detected by α-His immunoblot.

Immunoblot analyses

Unless otherwise noted, cells were lysed with 2% SDS, DNA sheared with a Bransonic bath sonicator, and protein concentrations were determined using fluoraldehyde *o*-phthalaldehyde (OPA, Pierce) assay (53). Equivalent amounts of protein were separated by SDS-PAGE prior to transfer to polyvinylidene difluoride membranes (GE Life Sciences) by electroblotting. Proteins were detected using the Western-Star™ chemiluminescent detection system (Applied Biosystems) according to the manufacturer's instructions using a 1:5000 dilution of α-TRS1 (αp999) (90) or using the following commercial primary antibodies diluted 1:1000: Actin (Sigma A-2066), Penta-His (Qiagen, 34660), PKR (Santa Cruz Biotechnology, Inc. sc-6282 and sc-707; R&D systems, clone #HL71/10),

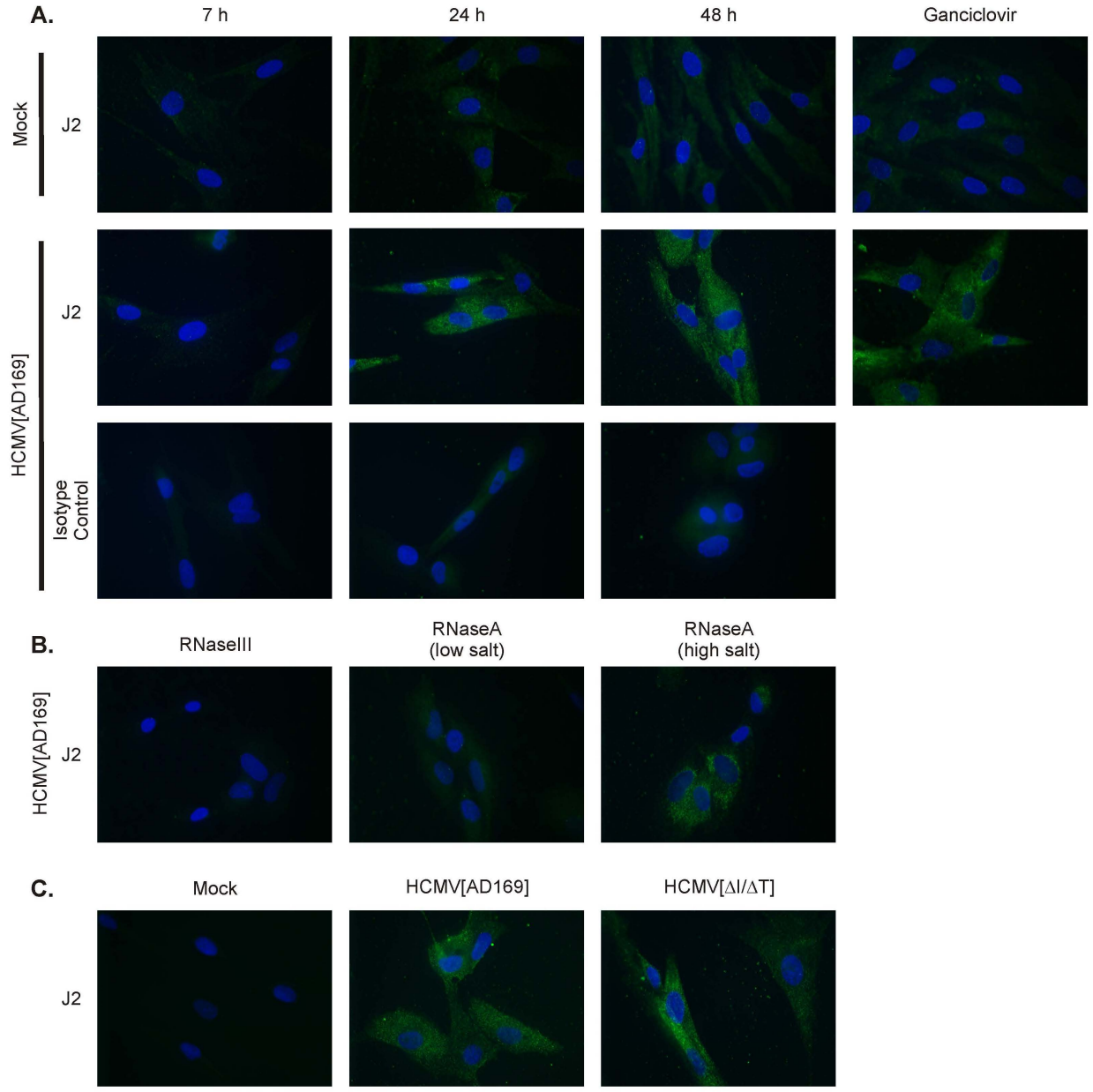

Figure 2.1. dsRNA production during HCMV infection. HF were mock infected or infected with HCMV at an MOI of 5 without (A and B) or with (C) spin inoculation and stained with the dsRNA-specific J2 antibody or an isotype matched control antibody (green), as described in Materials and Methods. Nuclei were stained using Hoechst no. 33342 (blue). (A) HCMV[AD169] or mock-infected HF were stained using J2 at 7, 24, or 48 h p.i. (top rows) or with an isotype matched control antibody (bottom row). Mock infected and infected cells were also treated with ganciclovir, preventing viral late protein synthesis, and stained at 48 h p.i. (right). (B) HF infected with HCMV[AD169] for 48 h were incubated with dsRNA specific RNase III (left) or RNase A under low-salt (center) and high-salt (right) conditions before being stained with J2. (C) HF were mock infected or infected with HCMV[AD169] (center) or HCMV[ΔI/ΔT] (right) and stained with J2 at 48 h.p.i.

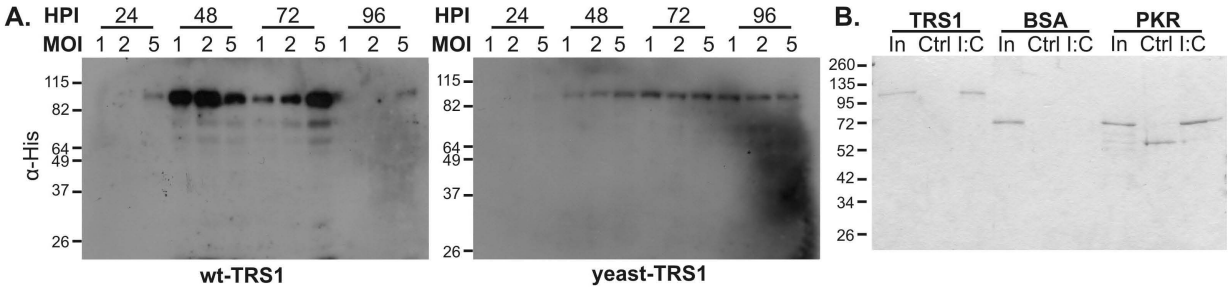

Figure 2.2. Expression and purification of TRS1 from insect cells. SF9 cells were infected with baculoviruses expressing either the wild type HCMV TRS1 or a yeast codon-optimized TRS1 genes at a MOI of 1, 2, or 5. Cells were harvested at 24, 48, 72, or 96 hours post infection and immunoblotted for TRS1 production with α-His (A). Following purification using Ni-NTA beads, TRS1 was incubated with either control or poly I:C agarose beads before SDS-PAGE and coomassie staining (B). TRS1 and PKR purified from bacteria bound poly[I:C] beads but not control beads, while BSA does not bind to either bead. Input (In) lane contains10% (150 ng) of the protein used in each binding reaction.

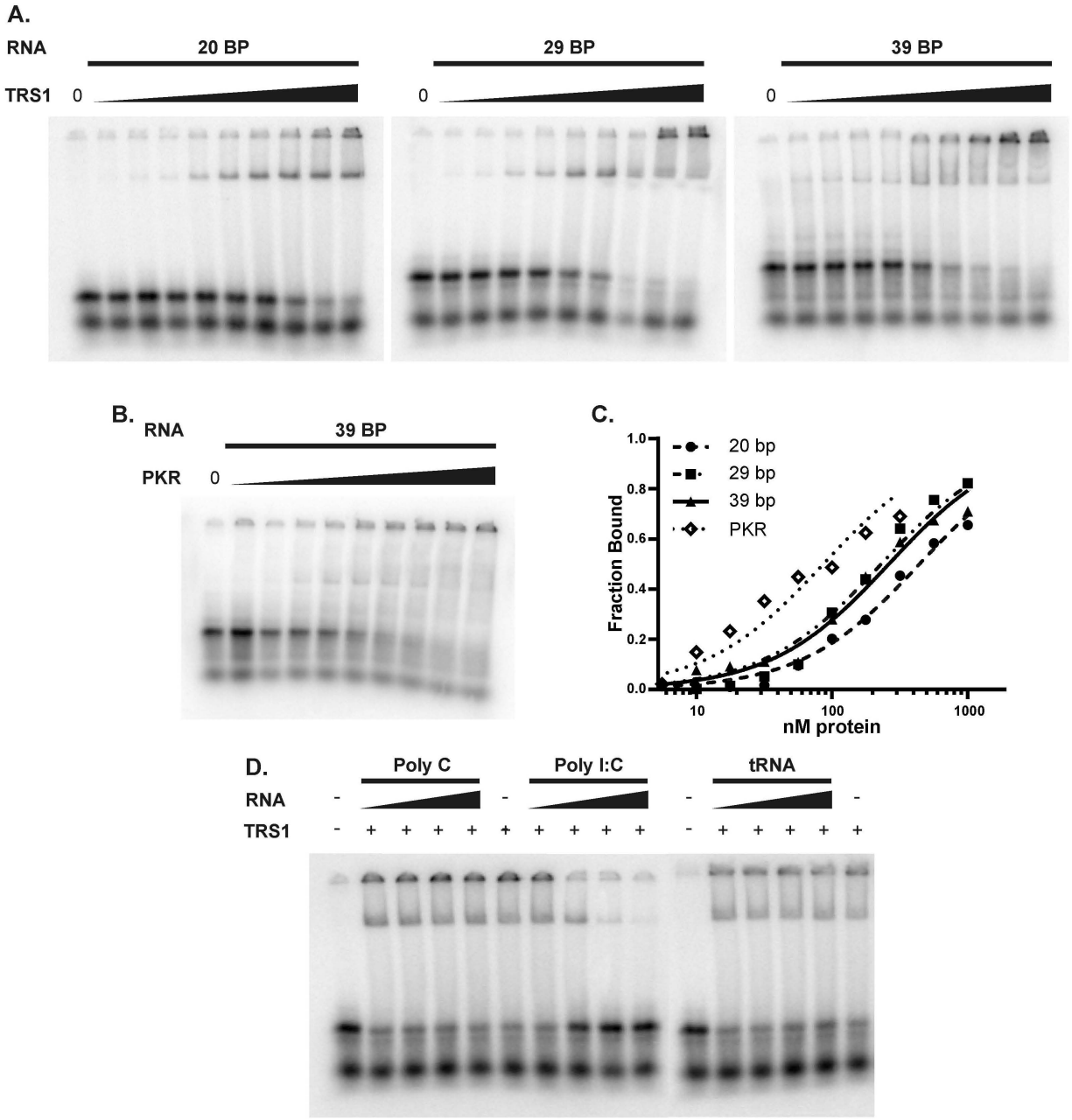

Figure 2.3. TRS1 binds dsRNAs as short as 20 bp. Native gel shift experiments using ^{32}P labeled hairpin RNAs 20, 29, or 39 bp in length that were incubated with increasing quantities of purified TRS1 (A) or PKR (B) prior to separation by TBE-PAGE and visualization The fraction of each hairpin bound by TRS1 was calculated after phosphorimaging, plotted, and binding curves calculated using nonlinear least-squares fit regression (C). Cold competitor poly C, poly I:C, or tRNA was incubated along with TRS1 and the 29 bp hairpin in binding reactions to illustrate the specificity of TRS1 for dsRNA (D).

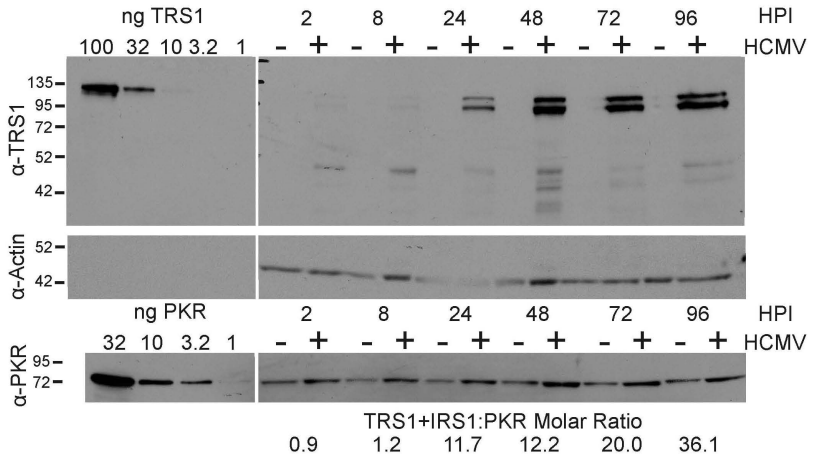

Figure 2.4. TRS1 and PKR production during HCMV infection. HFs were infected with HCMV at a MOI of 3 or mock infected. Cells were lysed at the indicated hour post infection (HPI). Lysates plus the indicated quantities of purified TRS1 or PKR were separated by SDS-PAGE and visualized by immunoblot with antibodies against TRS1, Actin, or PKR. Intensities of the full-length TRS1 and IRS1 bands were compared with PKR bands to estimate the molar ratios of the viral and cellular proteins present during infection.

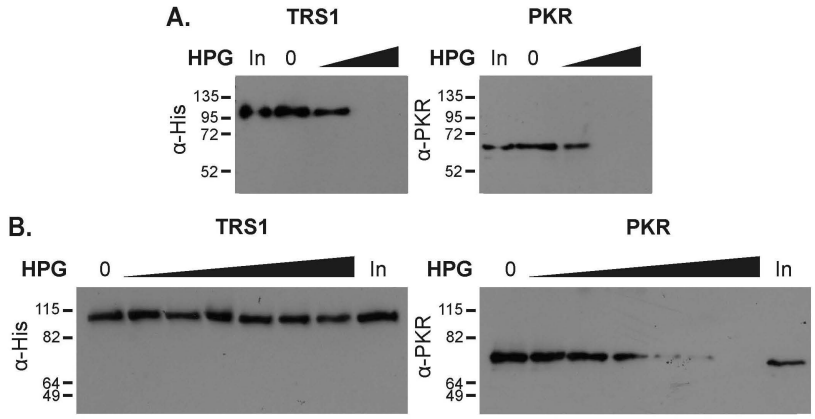

Figure 2.5. dsRNA binding is inhibited by HPG treatment. Purified TRS1 or PKR was treated with increasing quantities of *p*-hydroxyphenylglyoxal as described in Materials and Methods either before (A) or after (B) incubation and pull-down with poly I:C agarose beads. Binding was visualized by either α-His or α-PKR immunoblot.

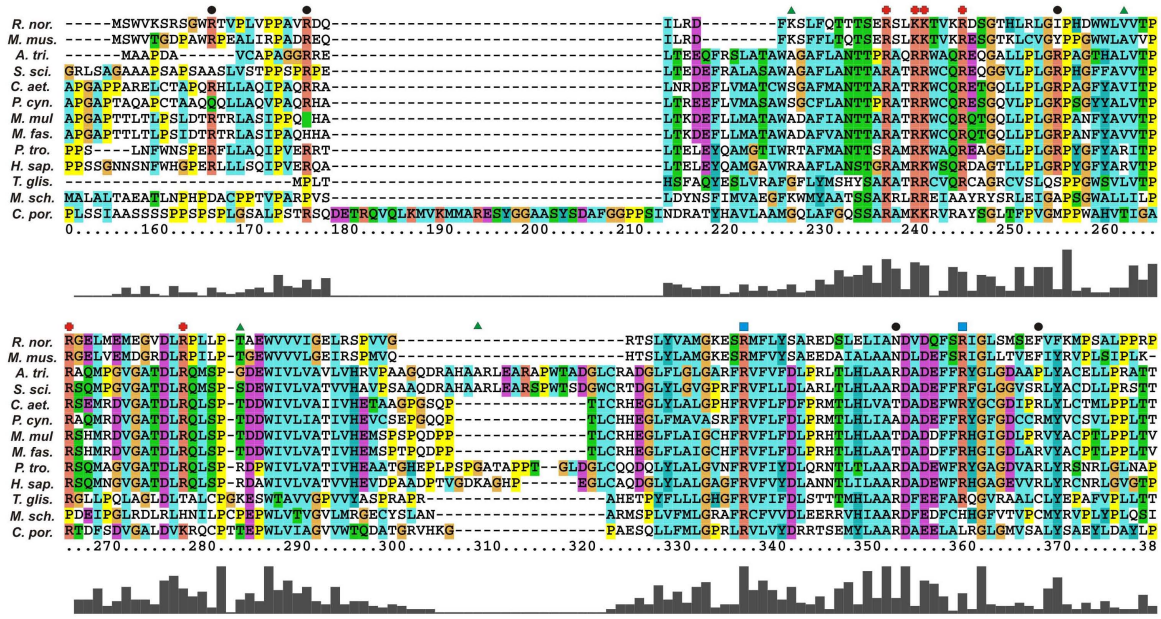

Figure 2.6. Conserved basic amino acids in TRS1 homologues. The TRS1 homologues from 13 cytomegaloviruses were aligned using ClustalX2. Above the alignment, basic amino acids from TRS1 are indicated as either unique to human and chimpanzee CMV (▲), conserved primarily in primate CMVs (●), widely conserved in TRS1 homologues but not other US22 family proteins (✚), or widely conserved in US22 family proteins (■). Cytomegaloviruses originated from rat (*R. nor.*), mouse (*M. mus.*), three-striped night monkey (*A. tri.*), common squirrel monkey (*S. sci.*), grivet monkey (*C. aet.*), olive baboon (*P. cyn.*), rhesus macaque (*M. mul.*), crab-eating macaque (*M. fas.*), common chimpanzee (*P. tro.*), human (*H. sap.*), common treeshrew (*T. glis*), common bent-wing bat (*M. sch.*), and guinea pig (*C. por.*).

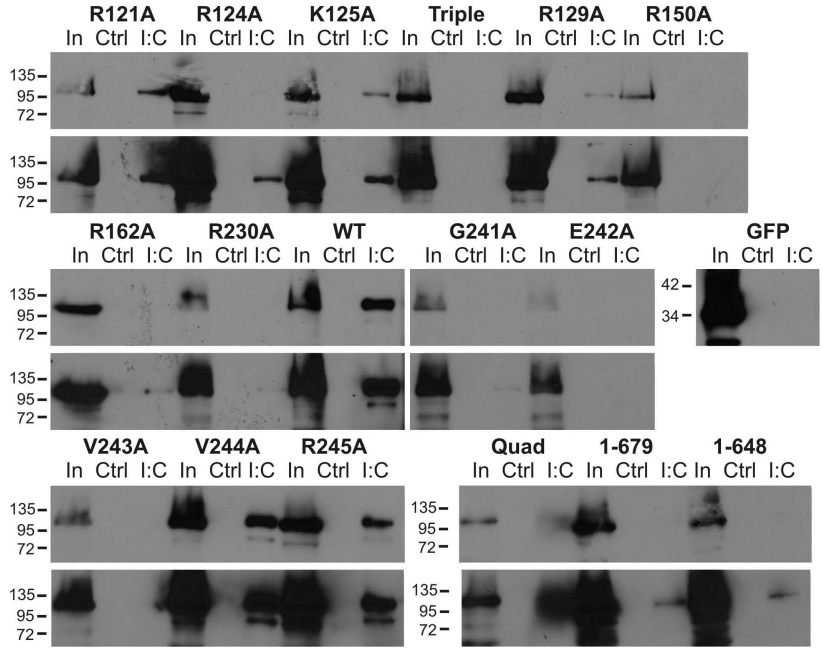

Figure 2.7. dsRNA binding by TRS1 point mutants. HeLa cells were transfected with the indicated TRS1 mutants, lysed, and the lysate bound to naked (Ctrl) or poly I:C agarose beads. The bound protein, along with input protein equal to 10% of the amount used in binding reactions (In), was separated by SDS-PAGE and visualized by α-His immunoblot. Two exposures of the immunoblot are shown to best differentiate strong versus weak versus non-binders. Triple is TRS1[R121A/R124A/ K125A], Quad is TRS1[G241A/E242A/V243A/R245A].

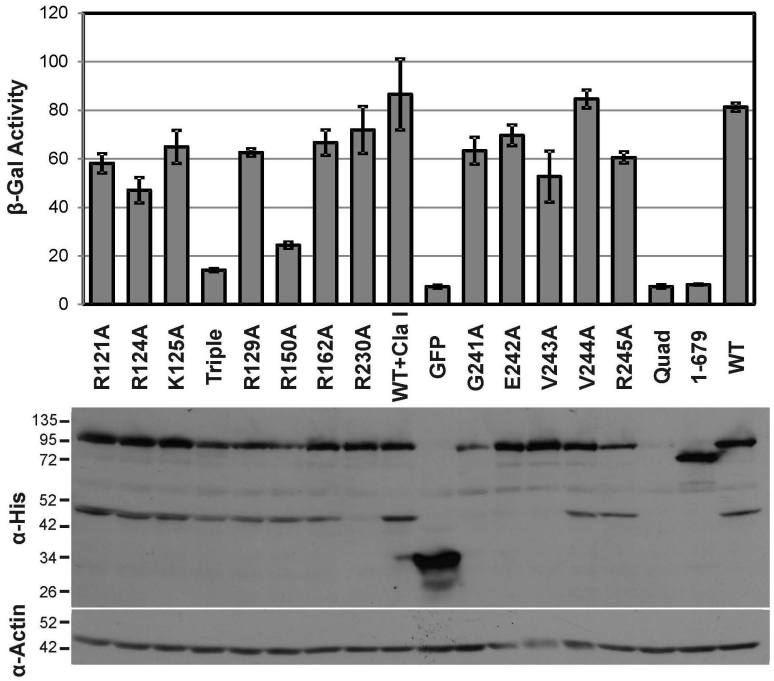

Figure 2.8. Mutation of TRS1 impairs VVΔE3L rescue. HeLa cells were transfected with the indicated TRS1 mutants and infected with VVΔE3L 24 hours later. Viral replication was measured at 24 hours post infection and the expression of the transfected proteins was measured by α-His immunoblot.

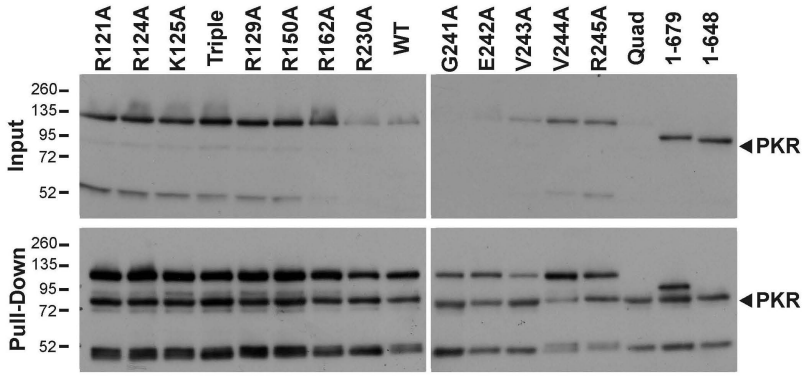

Figure 2.9. PKR binding by TRS1 point mutants. Cos7 cells were transfected with plasmids that expressed biotin ligase, biotin signal and 6XHis-tagged, kinase dead PKR, and His tagged TRS1 mutants. Biotinylated PKR and any associated proteins were pulled down with avidin agarose following lysis. Proteins were detected by α-His immunoblot following SDS-PAGE.

CHAPTER 3

Antagonism of the protein kinase R pathway by the guinea pig cytomegalovirus US22-family gene *gp145*

SUMMARY

Viral double-stranded RNA (dsRNA) activates protein kinase R (PKR), which phosphorylates eIF2α and inhibits translation. In response, viruses have evolved various strategies to evade the antiviral impact of PKR. We investigated whether guinea pig cytomegalovirus (GPCMV), a useful model of congenital CMV infection, encodes a gene that interferes with the PKR pathway. Using a proteomic screen, we identified several GPCMV dsRNA-binding proteins, among which only gp145 rescued replication of a vaccinia virus mutant that lacks E3L (VVΔE3L). gp145 also reverses the inhibitory effects of PKR on expression of a cotransfected reporter gene, and reduces the levels of PKR and eIF2α phosphorylation in VVΔE3L infected cells. Mapping studies demonstrated that the gp145 dsRNA-binding domain has homology to the PKR antagonists of other CMVs. However, dsRNA binding by gp145 is not sufficient for it to block PKR. gp145 differs from the PKR antagonists of murine CMV in that it functions alone and from those encoded by human CMV in functioning in cells from both primates and rodents.

INTRODUCTION

Human cytomegalovirus (HCMV) is the most common viral infection in newborns, infecting between 0.5 and 2% of infants *in utero* (41). Each year in the United States there are over 5500 congenital HCMV infections that result in permanent neurologic disability or death (5). HCMV is thought to have coevolved with humans (91) and replicates well only in human cells. This species-specificity precludes the study of HCMV in animal models and has led to the development of several primate and rodent CMVs as models for studying pathogenesis of and immunity to HCMV (4, 116, 128). Among these, guinea pig cytomegalovirus (GPCMV) is a particularly valuable model to study congenital infection since, like HCMV, GPCMV crosses the placenta and infects the developing fetus *in utero* (128). Application of the GPCMV model requires an understanding of the similarities and differences between GPCMV and HCMV genes and mechanisms, particularly those involved in evasion of rapidly evolving host defense systems.

Double-stranded RNA (dsRNA), which accumulates during the replication of HCMV and many other viruses (90, 144), activates several cellular antiviral pathways, including one mediated by protein kinase R (PKR). Upon binding to dsRNA, PKR dimerizes and autophosphorylates to form active PKR, which then phosphorylates the α-subunit of eukaryotic initiation factor 2 (eIF2α). Phosphorylated eIF2α inhibits the activity of the guanine nucleotide exchange factor eIF2B and thereby limits formation of the eIF2α-$tRNA_i^{Met}$-GTP ternary complex, inhibiting translation initiation and viral replication (50).

To counteract the effects of PKR, many viruses have evolved factors that block the pathway at one or more steps (79, 102). In the case of HCMV, two genes, *IRS1* and *TRS1*, encode proteins that bind both to dsRNA and to PKR, preventing PKR activation in human cells (25, 54, 55). *TRS1* and *IRS1* are members of the β-herpesvirus US22 gene family, which also

includes PKR antagonists of MCMV (*m142* and *m143*) and RhCMV (*rhTRS1*). The proteins encoded by these genes all bind to dsRNA and interact with PKR with varying species-specificities (16, 23, 26, 140). Deletion of both the PKR antagonists of HCMV or either one from MCMV eliminates viral replication (90, 140). Productive infection can be restored to these viruses by providing an active PKR antagonist in *cis*- or *trans*- (90, 140) or, in the case of MCMV, by abolishing PKR activity in infected cells (16).

To better understand the function and evolution of PKR inhibition by CMVs, we sought to identify a PKR antagonist encoded by GPCMV. We found that gp145, a member of the US22 protein family, binds to dsRNA and inhibits the PKR pathway. gp145 shares a noncanonical dsRNA-binding domain and an ability to multimerize with TRS1 and m142/m143. Also, like TRS1, dsRNA-binding and self-association by gp145 are insufficient to antagonize PKR. Our results reveal that while dsRNA binding is a conserved feature of the CMV PKR antagonists, mechanistic differences between GPCMV gp145 and the PKR antagonists of other rodent and primate CMVs may reflect adaptations to evolutionary changes in the PKR genes of their host species.

RESULTS

Identification of GPCMV dsRNA-binding proteins

To test whether GPCMV encodes a PKR antagonist, we initially investigated whether GPCMV infection could rescue a vaccinia virus mutant (VVΔE3L) that lacks its PKR antagonist E3L and thus replicates poorly in many cell types (7). VVΔE3L replication can be rescued by coinfection with a second virus that blocks PKR (64), as was observed previously by coinfection with HCMV and VVΔE3L (27). However, VVΔE3L replication was much less restricted in guinea pig lung fibroblasts (GPL) and other GPCMV-permissive cell lines than it is in other cell

types such as human fibroblasts or HeLa cells. Prior infection with GPCMV did not further increase VVΔE3L replication in GPL cells (data not shown). We also tested whether a second vaccinia protein, K3L (8), might be acting as the primary PKR antagonist in GPL cells but found that VVΔK3L also displayed only a modest growth defect in GPL cells and prior infection with GPCMV resulted in no substantial rescue of VVΔK3L (data not shown). Thus we were unable to utilize rescue of VVΔE3L in GPCMV-permissive cell lines to determine whether GPCMV encodes a PKR antagonist.

The unusually weak phenotypes of VVΔE3L and VVΔK3L viruses in GPCMV-permissive cell lines led us to explore alternative means to screen for a GPCMV PKR antagonist. Because the PKR antagonists of many viruses are dsRNA-binding proteins (23, 26, 54, 79, 102), we hypothesized that a GPCMV PKR antagonist might also bind dsRNA. To identify GPCMV dsRNA-binding proteins, we incubated lysates from mock or GPCMV-infected GPL cells with poly I:C agarose beads (Fig. 3.1) as described in Materials and Methods. Several bands unique to GPCMV infection were detected, and these likely represented either viral or virally-induced host dsRNA-binding proteins. To identify these proteins, the prominent bands were excised, digested with trypsin, and subjected to liquid chromatography–tandem mass spectrometry (Table 1). Several cellular dsRNA-binding proteins were detected in this experiment, including mammalian Staufen and ILF3 (15, 117), supporting the specificity of the poly I:C pull-down assay. The most intense bands (~72 and ~47 kDa) corresponded to the GPCMV proteins gp145 and GP44. gp145 is a member of the US22 gene family and has been annotated as a possible homologue of HCMV TRS1, while GP44 is homologous to UL44, a HCMV DNA polymerase accessory protein that has been previously shown to interact with TRS1 (129, 134). gp145 was detected in multiple samples that migrated above and below the predicted molecular weight of

the protein, suggesting that multiple or modified forms of the gp145 might be produced during infection. Alternatively, the smaller fragments could be degradation products generated during sample preparation. Other abundant GPCMV proteins identified in this screen included gp3, a US22 family protein with no obvious homologue in HCMV, and GP122, the GPCMV homologue of the HCMV IE2 transcriptional transactivator. A third US22 family protein identified in this experiment, gp139 (129), was not detected when this experiment was repeated.

We next sought to differentiate direct dsRNA-binding by GPCMV proteins from indirect binding as part of a multi-protein complex. In addition to testing gp3, gp44, and gp145, we also tested the dsRNA-binding of three additional US22 family proteins that have some sequence similarity to TRS1 (gp141, gp144, and gp146) but that were not detected in the proteomic analysis. The GPCMV proteins were expressed by *in vitro* translation and analyzed by the dsRNA-binding assay. With the exception of gp141, which failed to express either by *in vitro* translation or transient transfection, all of the GPCMV proteins tested bound to the poly I:C beads (Fig. 3.2 and data not shown). To test the specificity of the observed dsRNA-binding, the *in vitro* translation products were preincubated with either DNA or poly I:C prior to incubation with poly I:C beads. As expected, E3L binding to the poly I:C beads was competed by dsRNA but not by DNA, and gp145 binding was also more strongly competed by preincubation with dsRNA. The opposite pattern was observed from gp3 and GP44, suggesting that these proteins preferentially bind to DNA. These experiments demonstrated GPCMV encodes several dsRNA binding proteins, although only gp145 appears to preferentially bind dsRNA over DNA.

gp145 rescues VVΔE3L

Having identified GPCMV proteins capable of dsRNA-binding, we next tested their ability to inhibit the PKR pathway by measuring the impact of the individual proteins on

VVΔE3L replication (64). We transfected HeLa cells with plasmids expressing the GPCMV proteins, infected the cells with VVΔE3L, and measured viral replication at 24 hours post infection. Of the GPCMV proteins tested, only gp145 rescued the replication of VVΔE3L (Fig. 3.3A). Similar results were also observed in African green monkey cells (COS-7, data not shown). Unlike the MCMV proteins m142 and m143, which function as a heteromeric complex (26), gp145 was both stably expressed and sufficient to rescue VVΔE3L when expressed by itself. We tested whether VVΔE3L rescue by gp145 might be enhanced by cotransfection of HeLa cells with both gp145 and either gp3, GP44, gp144, gp146, or GFP, but observed no further increase in VVΔE3L replication by mixed transfection of GPCMV proteins over the gp145 plus GFP control (data not shown).

Because GPCMV evolved in guinea pigs and its PKR antagonist is likely to be most active against guinea pig PKR, we sought to identify a guinea pig cell line with which we could assess rescue of VVΔE3L replication by transfection. We found that GPC-16 cells (ATCC CCL-242), a transformed line of guinea pig epithelial cells, are highly restrictive to VVΔE3L replication. This cell line is not permissive to GPCMV replication (108) and so we could not use it to test whether GPCMV infection could rescue VVΔE3L replication. However, transient transfection of either gp145 or E3L did rescue VVΔE3L replication in GPC-16 cells (Fig. 3.3B). TRS1 failed to rescue VVΔE3L in GPC-16 cells, suggesting that TRS1 may be inactive against guinea pig PKR. These results demonstrated that gp145 can rescue VVΔE3L replication in human, African green monkey, and guinea pig cells and suggest that gp145 activity against PKR is less species-specific than the PKR antagonists of primate CMVs (23). Additionally, gp145 is more similar to the HCMV and RhCMV PKR antagonists than to MCMV m142/m143 in that a single protein is sufficient to block the PKR pathway.

gp145 antagonizes PKR

Because E3L interferes with a number of cellular antiviral pathways in addition to PKR (113), the ability of a protein to rescue VVΔE3L is only an indirect measure of PKR antagonism. We sought additional evidence demonstrating specific activity of gp145 against PKR, but the lack of available guinea pig reactive reagents prevented us from assaying whether gp145 can prevent phosphorylation of guinea pig PKR. Therefore, we tested whether gp145 can block PKR by measuring its ability to reverse the inhibitory effects of PKR on expression of cotransfected reporter genes (64, 123). We transfected plasmids expressing secreted alkaline phosphatase (SEAP), human PKR or GFP, and either GFP, E3L, TRS1, or gp145 into HeLa cells in which endogenous PKR has been stably knocked down by an shRNA (151). Expression of PKR with SEAP resulted in a 12-fold reduction in protein expression relative to the GFP control (Fig. 3.4). E3L, TRS1, and gp145 all rescued SEAP expression when coexpressed with human PKR.

We observed that PKR expression was higher in cells that also expressed a PKR antagonist. This suggests that active antagonists enable increased expression of all transfected genes, including PKR and the SEAP reporter, and has been observed by others (123). We suspect that the increase in PKR expression ultimately overwhelms the antagonists and prevents the full recovery of SEAP levels. To exclude the possibility that increased SEAP expression is the result of an increased level of transcription, we assessed the abundance of SEAP mRNA by northern blot. While transfection of E3L and gp145 both increased the abundance of SEAP mRNA, this effect did not result in a significant increase in SEAP production in the absence of PKR. Surprisingly, although TRS1 has previously been described as a transcriptional transactivator (121, 133), expression of TRS1 inhibited SEAP mRNA and protein production in

the absence of PKR. These results support to our conclusion from the previous VVΔE3L rescue experiments that gp145 antagonizes the PKR pathway.

gp145 blocks PKR and eIF2α phosphorylation

Previous studies have found that the CMV PKR antagonists utilize different mechanism to inhibit PKR activation. For example, HCMV TRS1 blocks both PKR and eIF2α phosphorylation, but RhTRS1 blocks eIF2α phosphorylation while allowing PKR phosphorylation. Additionally, RhTRS1 appears to bind only to the phosphorylated form of PKR (23). We sought to determine whether gp145 blocks either PKR or eIF2α phosphorylation. Transfection based assays cannot be used to assay for the phosphorylation status of either PKR or eIF2α. When transfected cells are infected at a high MOI, only a subset of cells express the transfected protein while all cells are infected. Upon lysis, these cell populations mix and we would expect to observe, at best, only a modest decrease in PKR or eIF2α phosphorylation. TRS1 expressed from either a transduced retroviral vector or as a recombinant transgene in VVΔE3L rescues VVΔE3L replication while providing a more uniform level of TRS1 expression in all cells, and we tested both approaches with gp145.

A LNCX based retroviral vector (99) expressing gp145 was constructed and used to transduce human fibroblasts (HF). gp145, under the control of the vaccinia 7.5k promoter, was also introduced into the VVΔE3L genome by homologous recombination, disrupting the vaccinia thymidine kinase gene. The genome structure of the resulting recombinant vaccinia was verified by southern blot (Fig. 3.5) and gp145 expression from both the transduced cell line and recombinant virus was verified by western blotting (Fig. 3.6).

VVΔE3L replication in gp145 transduced HFs was rescued relative to control cells (Fig. 3.6). Likewise, VVΔE3L+gp145 replication was higher than the parental VVΔE3L virus.

However, the level of VVΔE3L rescue by gp145 was reduced relative to the level of rescue in TRS1-HF cells or by VVΔE3L+TRS1 infection. TRS1, as a tegument protein, is delivered to infected cells immediately upon infection. However, it is unlikely that that TRS1 and other herpesvirus tegument proteins would be packaged into vaccinia particles. While we do not know if gp145 is a tegument protein, we nonetheless attempted to simulate the delivery of gp145 as part of the tegument by infecting gp145-HF cells with VVΔE3L+gp145. gp145 expression from both cellular and viral sources had an additive effect on rescue that was not observed with TRS1, although the level of vaccinia rescue by gp145 was still lower than by TRS1.

Compared to VVΔE3L infection, VVΔE3L+gp145 had a clear effect on reducing the level of both eIF2α and PKR phosphorylation observed during VVΔE3L infection and increasing the level of vaccinia protein synthesis (Fig. 3.6). This effect was not observed when transduced gp145 was the only source of the protein. However, there were still elevated levels of phospho-eIF2α and PKR and somewhat lower levels of translation in cells where VVΔE3L was rescued with gp145 relative to VVΔE3L rescue by TRS1.

Because transfection of gp145 but not TRS1 can rescue VVΔE3L in guinea pig cells (Fig. 3.3), we were eager to determine if it was acting by blocking the PKR pathway in these cells. While we were unable to identify antibodies reactive to guinea pig phospho-eIF2α or PKR, infection of gp145-transduced guinea pig cells or infection of wild type guinea pig cells with VVΔE3L+gp145 demonstrated that gp145 rescues protein synthesis during VVΔE3L infection. However, GPC-16 cells were both refractory to transduction and did not support the replication of VVΔE3L rescue viruses that express E3L, gp145, or TRS1 using the 7.5k promoter (data not shown).

In conclusion, gp145 blocks VVΔE3L-stimulated PKR and eIF2α phosphorylation to rescue vaccinia protein expression in human cells, but it is a less effective antagonist of human PKR than TRS1. While we were unable to compare the effectiveness of gp145 and TRS1 against guinea pig PKR, we suspect that the differences in rescue between the two proteins reflect species-specific adaptations of the CMV PKR response.

dsRNA-binding activity maps to the gp145 US22 domain

Having demonstrated the anti-PKR activity of gp145, we next sought to identify its functional domains. To delineate the dsRNA-binding domain of gp145, we engineered a series of N- and C-terminal gp145 truncations and analyzed their dsRNA-binding properties (Fig. 3.7). gp145[187-632], [1-355], and all longer C-terminal truncations bound to poly I:C beads at a level similar to that of full length gp145 while the deletion of residues 1-355 (gp145[356-632]) eliminated dsRNA-binding activity. Both gp145[1-186] and gp145[187-355] retain the ability to bind dsRNA, although the level of binding is substantially reduced. dsRNA binding in TRS1 also maps to the N-terminus. Of note, the TRS1 minimal dsRNA-binding fragment (TRS1[74-246]) and gp145[187-355] are among the most similar regions of the two proteins, having ~45% amino acid sequence similarity (54). These data suggest that the gp145[187-355] and TRS1[74-246] are a homologous dsRNA-binding domain and that that the common ancestor of these proteins predates the divergence of human and guinea pig CMVs.

dsRNA-binding by gp145 is not sufficient to rescue VVΔE3L

In addition to the N-terminal dsRNA-binding domain, TRS1 requires most of its C-terminal end to rescue VVΔE3L replication and to bind to PKR (54, 55). Outside of the shared US22 domain, gp145 and TRS1 are highly divergent and gp145 lacks similarity to the C-terminal end of TRS1 that is necessary for PKR interactions. We hypothesized that gp145

functions primarily by binding and sequestering dsRNA; such a mechanism is sufficient for E3L to limit PKR activation in cell culture (132). To evaluate the requirement of dsRNA-binding and/or other regions of gp145 to antagonize PKR, we tested a selection of gp145 truncations for their ability to rescue VVΔE3L replication following transfection of COS-7 cells. Only full length gp145 and gp145[187-632] rescued the replication of VVΔE3L (Fig. 3.8). Notably, gp145[1-355], gp145[1-512] and gp145[1-566] all failed to rescue VVΔE3L replication despite having dsRNA-binding activity comparable to full length gp145 (Fig. 3.7). Similar results were observed in VVΔE3L rescue experiments in both HeLa and GPC-16 cells (data not shown). These data led us to suspect that the C-terminus of gp145 provides some function other than dsRNA-binding that is required for VVΔE3L rescue.

Because direct interaction with PKR appears to be a necessary function of the PKR antagonists expressed by HCMV, MCMV, and RhCMV (23, 24, 55), we investigated whether gp145 could bind to PKR. In cotransfection experiments, we detected only weak and inconsistent binding of gp145 to either human or guinea pig PKR (data not shown). Thus, whether gp145 interacts with PKR remains unclear, but we suspect there is a weak protein-protein interaction between gp145 and PKR that might be facilitated by a dsRNA tether.

gp145 and TRS1 self-interact

Because MCMV m142 and m143 cooperatively bind dsRNA and both are needed to block PKR (26, 140), we hypothesized that gp145 may need to multimerize to antagonize PKR. To test for self-interaction, we transfected COS-7 cells with plasmids expressing biotin ligase and biotinylation signal-tagged gp145 along with full length or truncated 6X-His-tagged gp145 expression plasmids. Following avidin pull-down of the biotinylated gp145, we detected co-precipitated 6X-His-tagged proteins by immunoblot assay (Fig. 3.9A). Three gp145 constructs—

full length, gp145[187-632] and gp145[1-566]—co-precipitated with full length gp145, while the shorter C-terminal truncations did not. Because gp145[1-566] interacted with full length gp145 but did not rescue VVΔE3L replication (Fig. 3.8), gp145 self-interaction appears to be insufficient for PKR inhibition. Additionally, gp145 self-interaction cannot be explained as exclusively mediated by a dsRNA bridge as several truncations that bind dsRNA fail to self-interact, such as gp145[1-355] and gp145[1-512].

Using this approach, we also found that TRS1 self-interacted (Fig. 3.9) and we determined that TRS1[1-362] is the minimal TRS1 fragment capable of self-interaction (Fig. 3.9B). Like gp145[1-566], TRS1[1-362] fails to rescue VVΔE3L but retains dsRNA binding activity (data not shown). We also explored whether TRS1 self-interacts during HCMV infection. Lysates from HCMV infected HFs were subjected to separation by a glycerol density gradient. While TRS1 self-interacted in the biotin pull-down assay, its apparent size on the density gradient was consistent with TRS1 monomers (data not shown), suggesting that TRS1 does not multimerize during HCMV infection.

In summary, dsRNA-binding and self-interaction are common features shared between gp145, TRS1, and the other known CMV PKR antagonists. While these activities may be necessary for gp145 function they appear to be insufficient to rescue VVΔE3L. C-terminal residues of gp145 not required for dsRNA-binding may either participate in another currently unidentified protein interaction or enhance dsRNA-binding to facilitate gp145 rescue of VVΔE3L replication. It is also unclear at this time whether gp145 or TRS1 self-interact during CMV infection.

DISCUSSION

PKR recognizes dsRNAs that accumulate during viral infection and can inhibit viral replication by shutting down protein synthesis (50, 144). Viral dependence on the host translation machinery to replicate has led to the evolution of numerous viral strategies to antagonize PKR function. In response, PKR has evolved rapidly during speciation, presumably driven by selection to evade viral antagonists (44, 123). The cytomegaloviruses are believed to have cospeciated with their respective hosts over the past 105 million years (91). As the diversity of available host and viral genome sequences increases, CMVs present a unique model to study the coevolution of host defenses and viral countermeasures. Prior to this study, the PKR antagonists of two primate viruses (HCMV and RhCMV) and one rodent virus (MCMV) had been characterized (16, 23, 90, 140). In this study, we demonstrate that the GPCMV protein gp145 antagonizes the PKR pathway.

The ability to bind to dsRNA is a common feature of the PKR antagonists encoded by many RNA viruses, poxviruses, and herpesviruses (18, 23, 26, 54, 101, 115). Thus, we suspected that a dsRNA-binding protein may contribute to PKR inhibition in GPCMV, where no single protein could be identified as an obvious homologue to either TRS1 or m142/m143. We identified several viral dsRNA-binding proteins present in GPCMV-infected cell lysates by mass spectrometry and assessed their ability to rescue VVΔE3L replication, a surrogate measure of PKR antagonism (64). The GPCMV protein gp145 was detected in this proteomic screen and subsequently found to bind dsRNA when translated *in vitro*, to decrease PKR and eIF2α phosphorylation during VVΔE3L infection to rescue viral replication, and to reverse the inhibitory effects of PKR activation on the expression of a cotransfected reporter gene.

Like the PKR antagonists of HCMV, RhCMV, and MCMV, gp145 is a member of the US22 gene family, which is one of several gene families unique to beta herpesviruses (22, 57,

119, 129, 145). A recent study included the US22 family in the SUKH gene superfamily, which predominantly includes bacterial nuclease toxin-immunity systems (148). Most US22 family proteins are comprised of 2 SUKH domains in tandem, which are referred to here as SUKH1 and SUKH2 of TRS1 and gp145 (Fig. 3.10). Little is known about either the function of most US22 family proteins or the shared structural domain(s) of these proteins (94). However, we found dsRNA binding maps to the gp145 US22 domain, specifically to SUKH1, as is the case for TRS1 (Fig. 3.10). As with MCMV, several GPCMV US22 proteins bind dsRNA but only a subset of these proteins can antagonize PKR (26). It remains to be seen whether binding to dsRNA or other nucleic acids plays a central role in the presently uncharacterized functions of the other US22 proteins.

In addition to binding dsRNA, TRS1, rhTRS1, and m142/m143 all directly interact with PKR, in some cases in a species-specific manner (16, 23, 24, 55). gp145 lacks residues homologous to the C-terminal end of TRS1 that are essential for interaction with human PKR and for VVΔE3L rescue. Our failure to identify robust gp145-PKR interactions led us to speculate that the activity of gp145 against PKR utilizes a mechanism that relied exclusively on dsRNA binding and sequestration. However, we observed that the C-terminal half of gp145, which is dispensable for dsRNA-binding, is required for VVΔE3L rescue (Fig. 3.10). We speculated that, similar to m142 and m143, gp145 may need to multimerize to function. While gp145 does self-interact, the region of gp145 that is sufficient for self-interaction is incapable of rescuing VVΔE3L. It remains unclear whether the function of the gp145 C-terminus in intact cells is to potentiate binding to dsRNA or PKR, self-interaction, or for some other interaction.

PKR has been found to be evolving under strong positive selection in several mammalian lineages (44, 123). Complex patterns of species-specificity have been observed in the

sensitivities of the vaccinia virus eIF2α mimic K3L (44) and more recently in the anti-PKR response of the TRS1 genes of HCMV and RhCMV (23). While human and rhesus CMV TRS1s are only active against PKRs originating from close relatives of each virus's natural host (23), gp145 appears to have activity against human, African green monkey, and guinea pig PKRs. As previous studies have found that MCMV m142 and m143 are active against human and mouse PKR (26, 140), rodent CMVs may have maintained a broader range of activity against PKR genes than have the primate CMVs (23). Nonetheless, GPCMV and MCMV PKR differ in their requirement for one versus two proteins to antagonize PKR (26, 140). Such differences are not entirely surprising since mice and guinea pigs last shared a common ancestor approximately 65 million years ago ago (96) and the GPCMV genome appears to be more similar to primate CMVs than to MCMV (129).

Deletion of the PKR antagonists of either HCMV or MCMV results in a replication incompetent virus. While this study does not address whether gp145 is essential for GPCMV replication, a previous study found that GPCMVΔgp138-149 had an approximately three-log replication defect compared to wild type virus while both Δgp123-143 and Δgp147-149 viruses replicated to normal titers (35). These results are consistent with the possibility that gp145 plays a critical role in efficient GPCMV replication. It is surprising that GPCMVΔgp138-149 can replicate at all in normal cells, since HCMVΔIRS1/ΔTRS1 and MCMVΔm142 or Δm143 cannot. However, the Δgp138-149 virus was propagated in GPL cells, which we found also support the replication of VVΔE3L and VVΔK3, and it is possible that GPL cells are less sensitive to dsRNA accumulation or PKR activation than many other cell types. Alternatively, as is the case for herpes simplex virus and vaccinia virus (38, 101), GPCMV may encode a second PKR

antagonist that has yet to be identified. Future analyses of a gp145 knockout virus will help clarify these issues.

Viruses that lack a normal PKR response, such as VVΔE3L, have been explored as potential live-attenuated or disabled infectious single cycle vaccines (68). The urgent need for an effective vaccine to prevent congenital CMV infection and the known replication defect of HCMVΔIRS1/ΔTRS1 (90) make GPCMVΔgp145 an attractive model for vaccine development. GPCMV has an advantage over MCMV in that the virus better models congenital infection and may require only a single protein to antagonize PKR. That said, many viral proteins are multifunctional and TRS1 is no exception. Previous studies have demonstrated possible roles for TRS1 as a coactivator with IE1 and IE2 transcriptional transactivators (121, 133), in virion assembly (1), in viral DNA replication (111, 134), and in viral manipulation of autophagy (21). Determining whether gp145 shares any of these additional activities will be of great interest for understanding the conserved roles of TRS1 and related US22 family proteins in viral replication and pathogenesis.

MATERIALS AND METHODS

Cells and viruses

HeLa PKR knockdown cells (HeLa PKR^{KD}) cells were provided by Charles Samuel (University of California, Santa Barbara) (151). GPL (ATCC CCL-158), HeLa, GPC-16 (ATCC CCL-242), HeLa PKR^{KD}, and COS-7 (ATCC CRL-1651) cells were propagated on Dulbecco's modified Eagle's medium supplemented with 10% NuSerum (BD Biosciences) as previously described (25). VC2 ((137) and VVΔE3L were obtained from Bertram Jacobs (Arizona State University) and propagated and titered in BHK cells (6, 25). GPCMV strain 22122 (ATTC VR682) was

propagated and titered on GPL cells. Retroviral vectors produced from pLNCX and pEQ1301 were used to transduce human fibroblasts (HFs) as previously described (90).

Plasmids

GPCMV genes were PCR amplified using the following oligonucleotide pairs and cloned into pcDNA3.1/V5-His-TOPO (Invitrogen): pKTS777 (gp141, 5'-ACCATGTGGCGACTGAACAG-3' and 5'-TATCAGGTAGCTAGAAAAGT-3'), pKTS778 (gp44, 5'-ACCATGGAACGTAAGACGTC-3' and 5'-GGCGGAACATTTCTGCTTCTT-3'), pKTS780 (gp3, 5'-ACCATGAAGCGATCGGAAGC-3' and 5'-ATCGAGATCCAGTTCGAACG-3'), pKTS784 (gp144, 5'-ACCATGCCCAAGCTCGTCTC-3' and 5'-GTTCTGATGTTTTCTCGGCG-3'), pKTS786 (gp145, 5'-ACCATGACCGAGGCGTTTC-3' and 5'-GGAACACTCCTCGTCGCTGG-3'), and pEQ1396 (gp146, #960 5'-ACCATGTCGCGTTCTGTATCTCG -3' and #961 5'- CGCGAGTCCCGTCGGG -3').

Two E3L-expressing plasmids were used in this study: pMTE3L (18), generously provided by Bert Jacobs, was used for transient transfections while pEQ1119 (23) was used for *in vitro* translation and dsRNA binding assays. TRS1 was expressed using pEQ1180 (formerly pEQ981) (54). An EGFP construct tagged with 6X-His only, pEQ1159, was cloned from pEQ1100 (26), which expresses GFP tagged with both a biotinylation signal and 6X-His (Bio-His), by digestion with EcoRV and SacII, blunted with Klenow, and ligated to excise the biotinylation signal. Knockdown-resistant human PKR (SR#329) was generously provided by Stefan Rothenburg (Kansas State University) (123). The SEAP expression vector (pEQ886) has been previously described (66). pEQ1338 was cloned by removing the CMV and T7 promoters of the EGFP expressing pEQ1100 by digestion with SspI and Asp718 and inserting a PvuII - Asp718 fragment from SR#329 containing the SV40 promoter and β-Globin intron.

gp145 expressing retroviral vectors were constructed by digesting pKTS786 with HindIII and PmeI and ligating the gp145-containing fragment into pLNCX that had been linearized with HindIII and HpaI, resulting in pEQ1301 (99). A gp145 expressing vaccinia recombination cassette was prepared by digesting pKTS786 with Asp718 and AgeI and ligating the gp145 containing fragment into pEQ1233 that had been linearized with the same enzymes (23). Similarly, a vaccinia recombination vector expressing TRS1 with an N-terminal 6X-His tag was prepared by annealing oligonucleotides #417 (5'-GATCACCATGGCCCATCATCACCATCACCATAA-3') and #418 (5'-GATCTTATGGTGATGGTGATGATGGGCCATGGT-3'), digesting with BamHI, and ligating into pEQ904 linearized with BamHI (25).

gp145 truncations were amplified from pKTS786 using either the PCR Extender System (5 Prime) or Phusion (New England Biolabs) polymerases with the following oligonucleotide pairs before cloning into pcDNA3.1/V5-His-TOPO (Invitrogen): pEQ1336 (gp145[187-632], #899 5'-ACCATGGCCAGGGAAAGCTACG-3' and #900 5'-GGAACACTCCTCGTCGCTGG-3'); pEQ1337 (gp145[356-632], #901 5'-ACCATGGCCTATCTGCCCGCCAGC-3'and #900); pEQ1412 (gp145[1-186], #902 5'-ACCATGCACCGAGGCGTTTC-3' and #988 5' CATCTTGACCATCTTCAGCTGCA 3');pEQ1353 (gp145[1-355], #902 and #903 5'-GTCCAGGTACTCGGCGCT-3'); pEQ1347 (gp145[1-512], #902 and #904 5'-GAGATACGTGTTTCCCGGCAG-3'); pEQ1352 (gp145[1-566], #902 and #905 5'-GTCGTAGCGCTCGTCGGTG-3'); pEQ1355 (gp145[187-355], #899 and #903).

pCS2+BirA expressing the *Escherichia coli* biotin ligase was obtained from Bruce Clurman (FHCRC). Biotinylation signal (Bio) tagged TRS1[1-738] , pEQ1133, was engineered

by digesting the Bio-His tagged pEQ1068 (24) with PmeI and BstBI, blunting with the Klenow fragment, and re-ligating. This plasmid was then digested with Asp718 and NotI and TRS1 was replaced with gp145 excised from pKTS786 using the same enzymes to make pEQ1376, Bio-tagged gp145. TRS1 [1-351] was amplified using primers #356 and #450 (5'-CACCGCGCCCAGCGCCAGCCA-3') before cloning into pcDNA3.1/V5-His-TOPO (54). Additional TRS1 truncations were cloned by PCR amplification with the following primers, digestion with HindIII and XhoI, and ligation into pEQ1180 backbone that had been digested with the same enzymes: pEQ1181 (TRS1[1-384], #88 5'-AGGCGTGTACGGTGGGAGGTCTAT-3' and #690 5'-GCATCTCGAGCTCGCCCCCGCCGGCAA-3'), pEQ1192 (TRS1[1-362] #88, and #696 5'GCATCTCGAGCCCGCCGCGCAGCCCAGCCA-3'), and pEQ1193 [TRS1[1-372], #88 and #697 5'- GCATCTCGAGGCCGTCGTCCCCGCCGTCAT-3').

GPCMV Infection

Confluent GPL cells were infected with GPCMV at a multiplicity of infection (MOI) of 3. Virus was allowed to adsorb to the cells for 2 hours at 37°C before the inoculum was aspirated and replaced with fresh media. At 4 days post infection, cells were either harvested directly for dsRNA-binding assays or radiolabeled with EasyTag Express^{35}S Protein Labeling Mix (50 μCi/ml; Perkin-Elmer) for 2 hours, washed once with PBS, harvested by scraping, and lysed with Buffer C (200 mM KCl, 20 mM HEPES [pH 7.5], 10% glycerol, 5 mM MgOAc, 1 mM dithiothreitol, 1 mM benzamidine (Sigma), and1% NP-40) (54).

dsRNA-binding assay

dsRNA [poly(rI · rC)] agarose beads were prepared as described previously (81). Binding assays using GPCMV-infected cells were performed by harvesting the cells and lysing in Buffer A by

incubating for 20 minutes on ice and pelleting the nuclei by centrifuging (16,000 x *g*) for 15 minutes at 4°C. The lysate was split between samples containing a mixture of 10 or 20% dsRNA agarose beads in carrier Sepharose CL-6B (Sigma-Aldrich) or with control Sepharose CL-6B alone and incubated for 2 hours at 4°C on a rotating mixer. After binding, the beads were pelleted (845 x *g*, 3 min) and washed in Buffer A 3-4 times after which bound proteins were denatured, separated on 10% SDS-PAGE gels and visualized either by silver-staining or autoradiography. To test the dsRNA binding of an individual protein, the indicated plasmid was *in vitro* translated using the TNT Quick Coupled Transcription/Translation System (Promega) and radiolabeled with [^{35}S] (Easy Tag Express^{35}S Protein Labeling Mix, Perkin-Elmer) per reaction. The *in vitro* translated protein was then diluted with Buffer A and subjected to the above binding assay. For competition assays, samples were incubated with either 200 μg of free poly(rI · rC) (Sigma) or salmon sperm DNA (Sigma) competitor for 1 hour at 4 °C on a rotating mixer before addition of the dsRNA bead mixture. Following separation on 10% SDS-PAGE gels and fluorographic enhancement (EN3HANCE [PerkinElmer]), samples were visualized by autoradiography.

LC-MS/MS analysis

Samples from a GPCMV infection that had been subjected to a dsRNA-binding assay were run on a 10% SDS-PAGE gel before being stained and destained using the SilverQuest kit (Invitrogen). The bands were excised, dehydrated using acetonitrile, and digested overnight with 5 ng/μL trypsin (Promega) in 50 mM ammonium bicarbonate at 37 °C. The peptides were first extracted using 5% v/v formic acid in water after 30 min incubation, then with acetonitrile. The pooled extracts were dried in a speed vac and cleaned using ZipTip™ C18 (Millipore) before mass spectrometry (MS).

Liquid chromatography (LC)–tandem mass spectrometry (MS/MS) analysis was performed using a LTQ Orbitrap mass spectrometer (Thermo Fisher Scientific). The LC system was configured in a vented format consisted of a fused-silica nanospray needle packed in-house with Magic C18 AQ 100A reverse-phase media (Michrom Bioresources Inc.) and a trap containing Magic C18 AQ 200A reverse-phase media (84). The peptide samples were loaded onto the column and chromatographic separation was performed using a two-mobile-phase solvent system consisting of 0.1% formic acid in water (A) and 0.1% acetic acid in acetonitrile (B). The mass spectrometer operated in a data-dependent MS/MS mode over the *m/z* range of 400-1800. For each cycle, the five most abundant ions from each MS scan were selected for MS/MS analysis using 35% normalized collision energy. Selected ions were dynamically excluded for 45 seconds.

Raw MS/MS data were submitted to the Computational Proteomics Analysis System (CPAS), a web-based system built on the LabKey Server and searched using the X! Tandem search engine against a protein database derived from the GPCMV genome sequence (GenBank ID: NC_011587.1) and the guinea pig protein database (Broad Institute: cavPor3), which also included additional common contaminants such as human keratin (34, 118). The search output files were analyzed and validated by ProteinProphet (106). Proteins and peptides with a probability score of 1.0 were accepted.

VVΔE3L rescue by transient transfection

Triplicate wells of subconfluent HeLa, GPC-16, or COS-7 cells were transfected with the indicated plasmid using Lipofectamine 2000 (Invitrogen) according to the manufacturer's instructions. 24 hours post transfection, cells were infected with VVΔE3L at a MOI of 1 and

viral replication was quantified by 4-methylumbelliferyl β-D-galactopyranoside (MUG) assay at 24 hours post infection as described previously (54).

HeLa PKR^{KD} reporter gene rescue assay

Subconfluent HeLa PKR^{KD} cells in 24 well plates were transfected with 2 µl Lippofectamine 2000 (Invitrogen) per well and the following amounts of plasmid DNA: 0.05 µg of SEAP reporter (pEQ886), 0.1 µg of knockdown resistant PKR or EGFP (SR#329 or pEQ13384), and 0.65 µg of EGFP or PKR antagonist (pEQ1159, pMTE3L, pEQ1180, or pKTS786) and (123). The transfection medium was replaced with fresh medium after 24 hours and at 48 hours post transfection, the medium was harvested and SEAP activity was measured as described previously (66).

Northern Blot

RNA was harvested from transfected HeLa PKR^{KD} cells using Trizol reagent (Invitrogen) and resolved on a 1% formaldehyde agarose gel prior to capillary transfer to a supported nitrocellulose membrane (Optitran, GE Healthcare). Northern hybridization was performed as described previously (25) using a probe specific to SEAP, which was generated from a fragment of pEQ886 gel isolated following digestion with XhoI and HindIII. The blot was visualized by phosphorimager analysis (Typhoon Trio [GE Healthcare]) and bands quantified using the ImageQuant software.

gp145 expressing recombinant vaccinia virus

pEQ942 and pEQ1317 were used to generate VVΔE3L+gp145 as previously described (23, 25). Vaccinia DNA was isolated from BHK cells infected with VC2, VVΔE3L, or VVΔE3L+gp145, digested with Asp718 or Hind III, and analyzed by Southern blotting using a probe generated from pEQ1317 (25).

Infections of transduced cell lines

HF-LNCX, HF-gp145, and HF-TRS1 cells were infected at a MOI of 5 with VVΔE3L, VVΔE3L+gp145, VVΔE3L+TRS1, or mock infected. Each condition was prepared in triplicate, and the cells were subjected to MUG assay at 24 hours post infection. One well of each condition was radiolabeled with EasyTag Express^{35}S Protein Labeling Mix (50 μCi/ml; Perkin-Elmer) for 2 hours. Cells were harvested with 2% SDS and the protein concentrations were measured by OPA assay prior to SDS-PAGE and visualizing the proteins by autoradiography or immunoblot.

Avidin agarose pull-down

Subconfluent COS-7 cells in 6 well plates were transfected using Lipofectamine 2000 with a mixture of 1.3 μg of each of 3 plasmids: 1) pCS2+BirA, 2) Bio-tagged TRS1 (pEQ1133) or gp145 (pEQ1376), and 3) a plasmid expressing 6X-His-tagged protein. 24 hours post transfection, the transfection medium was replaced with medium supplemented with 35 μM Biotin (Sigma). At 48 hours post transfection, cells were harvested by trypsanization and lysed in 110 μl of radioimmunoprecipitation assay buffer ([RIPA] 50 mM Tris-HCl, 150 mM NaCl, 0.1% sodium deoxycholate, 0.05% SDS, and 1% Triton X-100) by incubation for 20 minutes on ice followed by centrifugation (16,000 x *g*) for 15 minutes at 4°C to pellet the nuclei. After reserving a portion, the lysate was added to avidin agarose (Pierce) and incubated on a rotating mixer at 4°C for 2 hours. After binding, the beads were pelleted (845 x *g*, 3 min) and washed 3X with RIPA buffer before denaturing and separation by 10% SDS-PAGE and visualization by immunoblot as described below.

Immunoblot analyses

Unless otherwise noted, cells were lysed with 2% SDS, DNA sheared with a Bransonic bath sonicator, and protein concentrations were determined using fluoraldehyde *o*-phthalaldehyde (OPA, Pierce) assay (53). Equivalent amounts of protein were separated by SDS-PAGE prior to transfer to polyvinylidene difluoride membranes (GE Life Sciences) by electroblotting. Proteins were detected using the Western-Star™ chemiluminescent detection system (Applied Biosystems) according to the manufacturer's instructions using the following commercial primary antibodies diluted 1:1000: Actin (Sigma A-2066), Penta-His (Qiagen, 34660), PKR (Santa Cruz Biotechnology, Inc. sc-6282), phospho-PKR (T446; 1120-1; Epitomics), and phospho-eIF2α (S51; 9721; Cell Signaling Technology) Biotinylated proteins were detected using avidin-alkaline phosphatase conjugate (Avidx-AP, Applied Biosystems).

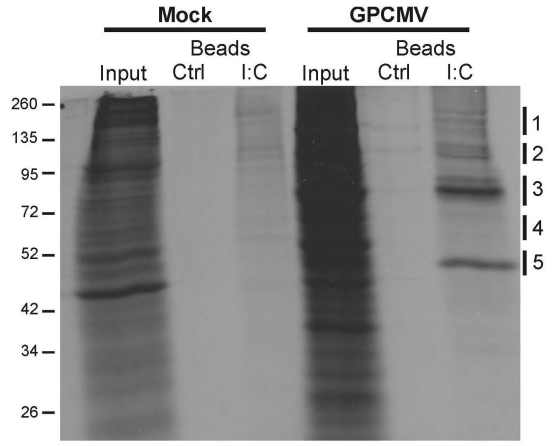

Figure 3.1. dsRNA-binding proteins produced during GPCMV infection. GPL cells infected with GPCMV were radiolabeled with ^{35}S-methionine at 4 days post infection, lysed, and proteins bound to control or poly I:C conjugated agarose beads. Proteins were visualized by autoradiography following SDS-PAGE. Regions indicated on the right (1-5) correspond to samples isolated from a second experiment that were analyzed by mass spectrometry (see Table 1).

Table 3.1.
dsRNA-binding proteins in GPCMV infected cells.

Sample[a]	Gene	# Pep.[b]	% Cov.[c]	MW (kDa)	Gene function
	ILF3	22	21.9	95.3	interleukin enhancer binding factor 3
	gp3	13	14.5	87.7	homology to THV T5b; US22 superfamily
1	gp145	10	12.0	68.9	homology to HCMV IRS1/TRS1; US22 superfamily
	GP69	7	7.0	116.3	UL69 homolog
	GP122	6	13.7	35.4	UL122 homolog; HCMV IE2
	ILF3	32	21.7	95.3	interleukin enhancer binding factor 3
2	gp145	12	16.1	68.9	homology to HCMV IRS1/TRS1; US22 superfamily
	gp139	5	6.5	79.5	homology to THV T5b; US22 superfamily
3	gp145	38	24.4	68.9	homology to HCMV IRS1/TRS1; US22 superfamily
	STAU1	22	23.7	62.2	staufen, RNA binding protein, homolog 1
4	GP55	12	12.7	102.2	UL55 homolog; glycoprotein B
	gp145	12	13.0	68.9	homology to HCMV IRS1/TRS1; US22 superfamily
5	GP44	87	44.7	44.8	UL44 homolog, polymerase accessory protein

[a] See Figure 3.1 for approximate regions of the gel represented in each sample. [b] Number of peptides detected. [c] Percent coverage

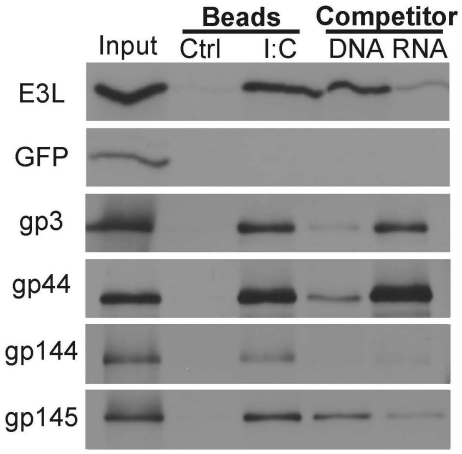

Figure 3.2. dsRNA-binding by *in vitro* translated GPCMV proteins. *In vitro* translated, radiolabeled GPCMV and control (E3L and EGFP) proteins were bound to either control or poly I:C conjugated agarose beads. To test the specificity of binding, samples were preincubated with or without DNA or poly I:C competitor prior to binding to poly I:C beads. 10% of the protein used in each binding reaction was run as an input control. The samples were analyzed by SDS-PAGE and phosphorimaging. The percent protein bound relative to the input control for each sample is shown below the bands.

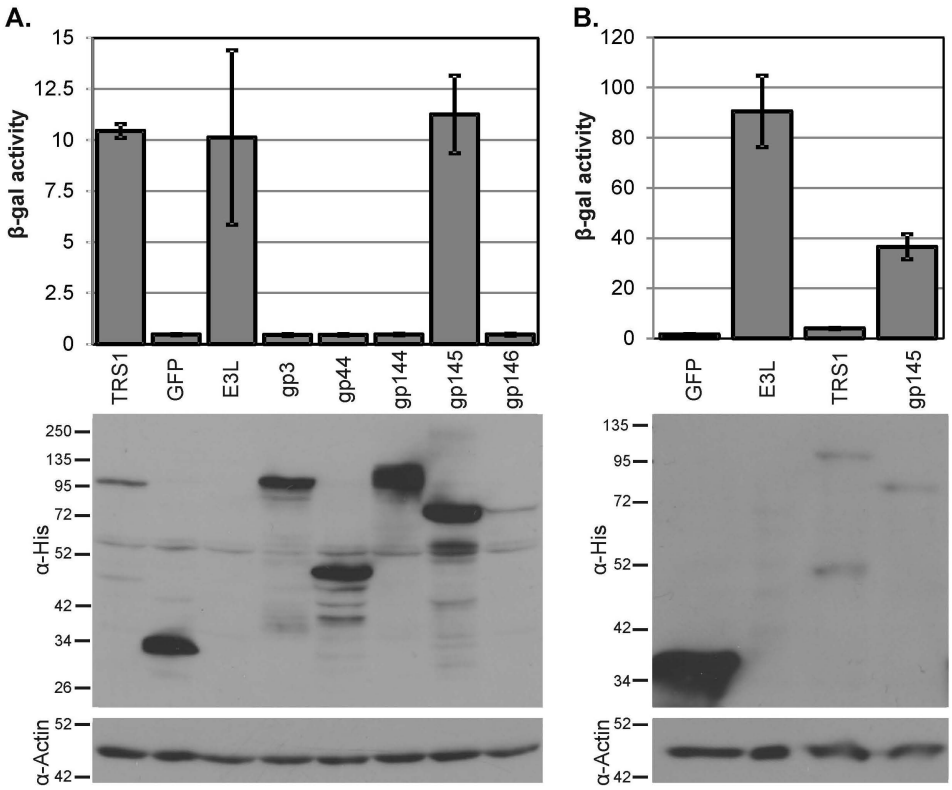

Figure 3.3. gp145 rescues VVΔE3L replication. (A) HeLa or (B) GPC-16 cells were transfected with the indicated plasmids and infected with VVΔE3L 24 hours later. Viral replication was measured at 24 hours post infection and the expression of the transfected proteins was measured by α-His immunoblot. E3L was not detectable in this blot because it is not 6X-His-tagged.

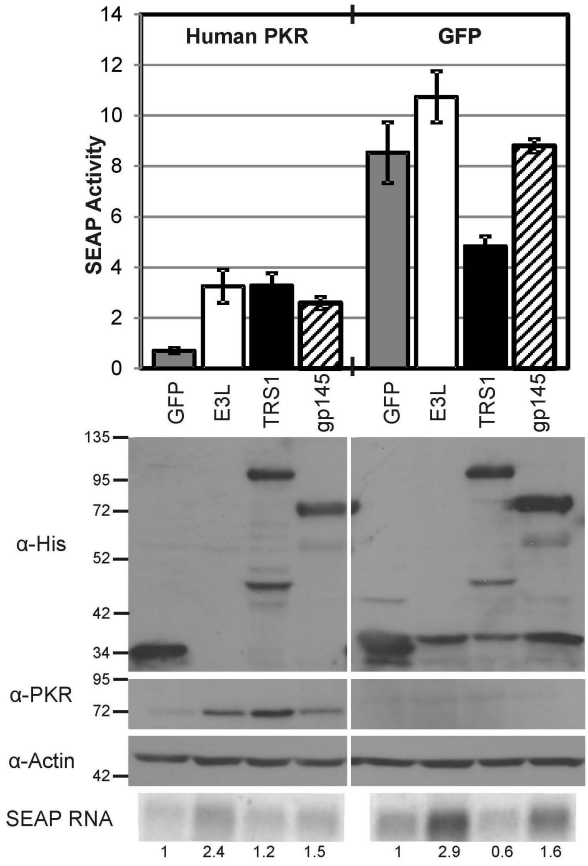

Figure 3.4. gp145 inhibits the activity of PKR. HeLa PKR knockdown cells were transfected with plasmids expressing SEAP, either knockdown-resistant human PKR or GFP, and GFP, E3L, TRS1, or gp145. SEAP activity of the medium was measured at 24 hours post transfection. Expression of the transfected proteins was measured by immunoblot. SEAP mRNA was detected by northern blot, and values indicate the amount of transcript relative to the GFP control in each set of transfections.

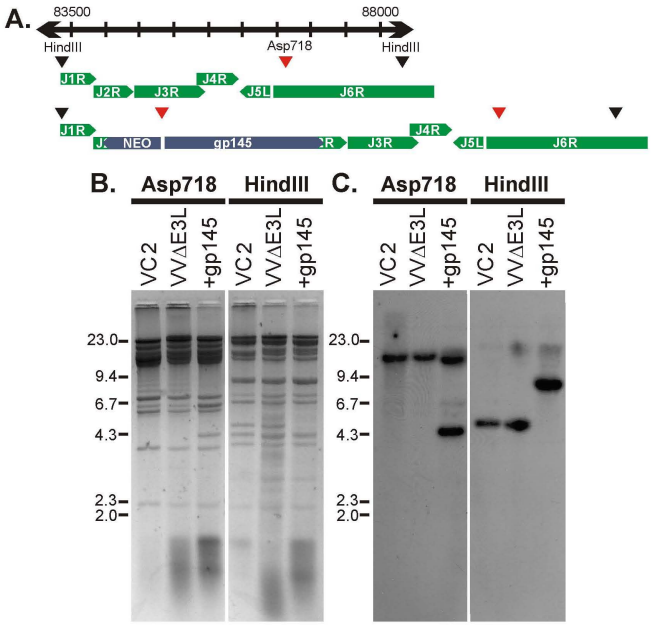

Figure 3.5. Characterization of VVΔE3L+gp145. (A) Map of the VC2 and VVΔE3L (top) genomes compared with VVΔE3L+gp145 (bottom) for the region flanking J2R. Vaccinia genes are shown in green while the recombination vector is blue. Black and red triangles indicate approximate HindIII and Asp718 restriction sites. (B) Viral DNA was isolated from cells infected with VC2, VVΔE3L, and VVΔE3L+gp145 viruses. After digestion with Asp718 or HindIII, viral DNA was separated by electrophoresis and visualized by ethidium staining. (C) Samples were then transferred to nitrocellulose and probed using a ^{32}P-labeled probe specific to the neomycin resistance and gp145 sequences plus J2R flanks.

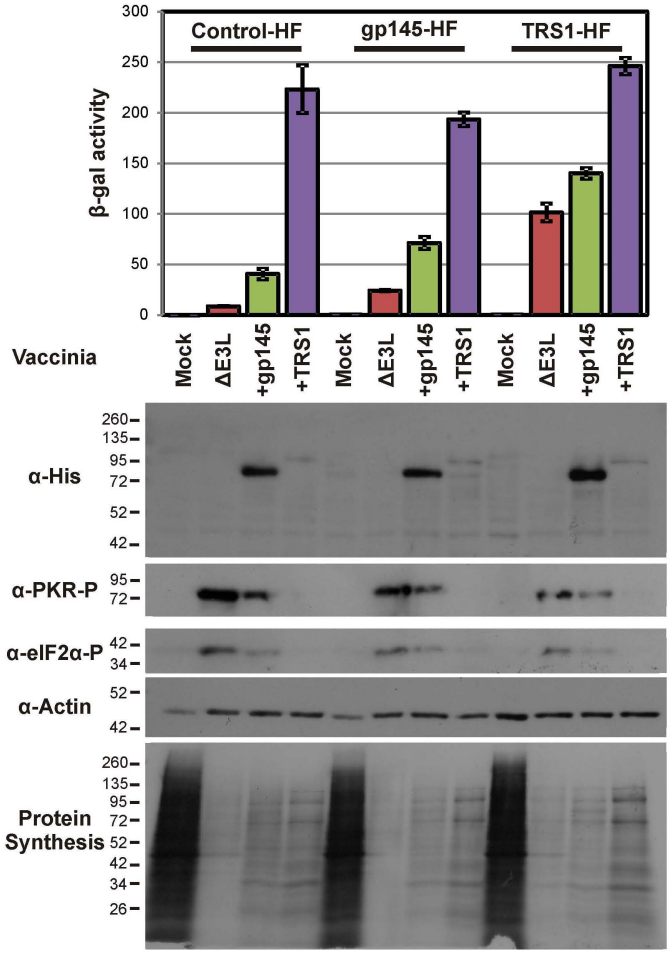

Figure 3.6. gp145 blocks PKR and eIF2α phosphorylation. Human fibroblasts transduced with control, gp145, or TRS1 expressing retroviral vectors were infected with VVΔE3L, VVΔE3L+gp145, VVΔE3L+TRS1, or mock infected. Cells were metabolically labeled and viral replication and total protein synthesis was measured at 24 hours post infection. Lysates were to immunoblotted with appropriate antibodies to assay the expression of His-tagged gp145 and TRS1 and to measure the levels of actin, phospho-PKR (T466) and phosphor-eIF2α (S51) present in cells after infection.

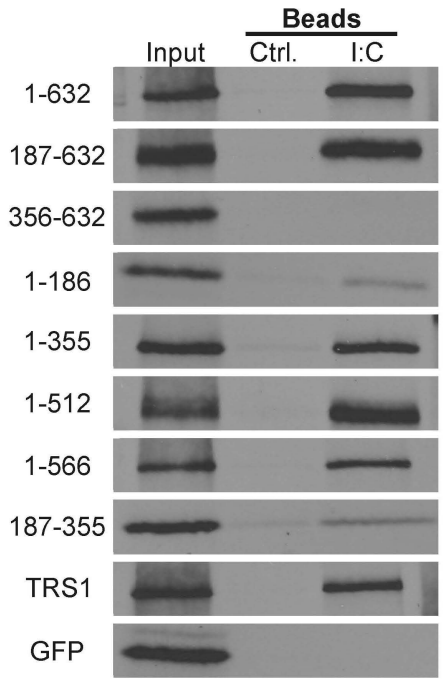

Figure 3.7. The core dsRNA-binding domain maps to gp145 amino acids 187-355.. gp145 N- and C- terminal truncations were expressed by in vitro translation and pulled down with either control or poly I:C beads. The numbers (left side) indicate the amino acid range included in each gp145 plasmid (diagramed in Figure 8). 10% of the protein used in each binding reaction was run as an input control, and the percent protein bound relative to the input control for each sample is shown below the bands.

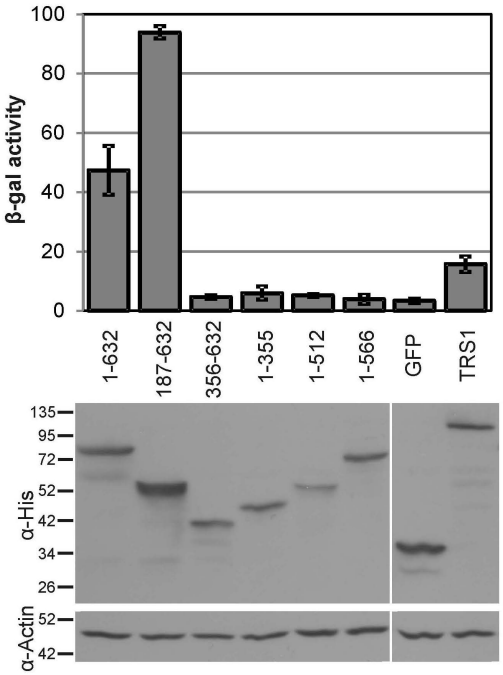

Figure 3.8. The gp145 dsRNA-binding domain is not sufficient to rescue VVΔE3L. COS-7 cells were transfected with gp145 truncations and infected with VVΔE3L 24 hours later. Viral replication was measured at 24 h.p.i. by β-gal expression and the expression of transfected proteins was monitored by α-His immunoblot.

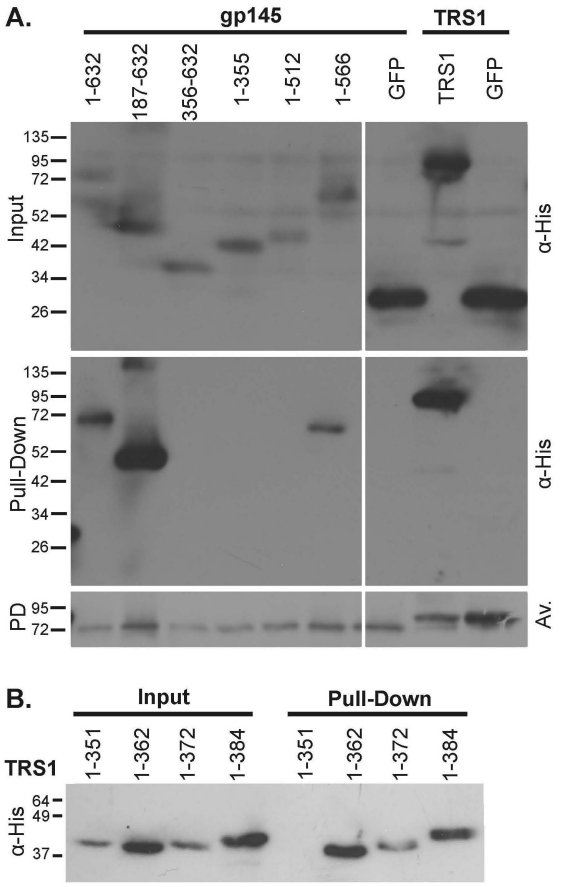

Figure 3.9. gp145 and TRS1 self-interact. COS-7 cells were transfected with plasmids expressing biotin ligase, biotin signal-tagged gp145 or TRS1 as indicated at the top, and with 6X-His tagged gp145 and TRS1 truncations, or GFP. Biotinylated proteins were pulled down by binding to avidin beads and detected with Avidex-AP (Av), while associated proteins were detected by α-His immunoblot. (A) Self-interaction by gp145 truncations and (B) Self-interaction by TRS1 truncations (biotinylated TRS1 not shown).

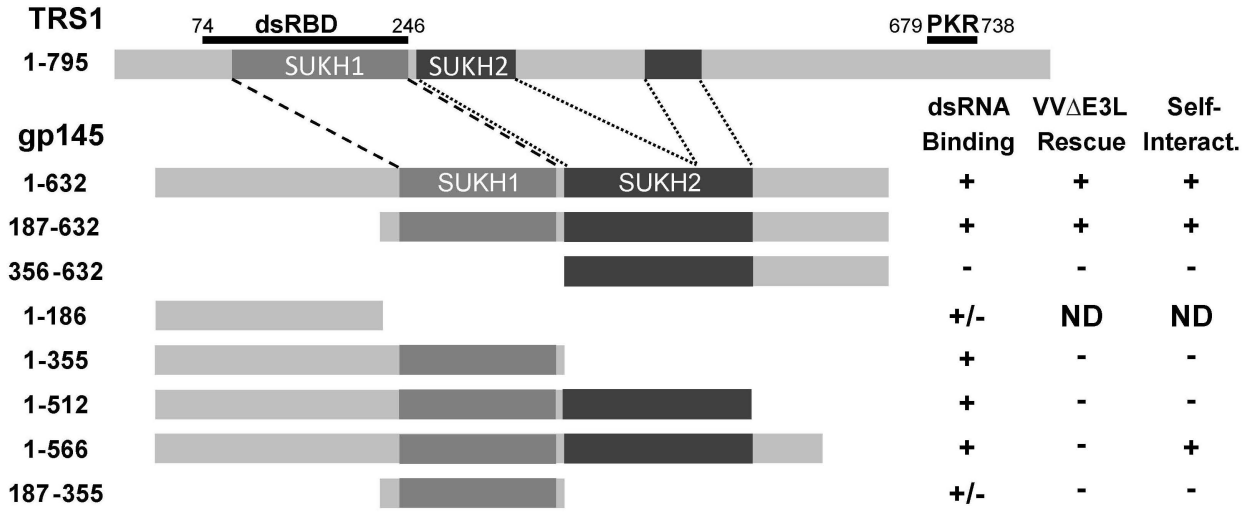

Figure 3.10. Summary of gp145 domain mapping experiments. Shown are diagrams of the approximate boundaries of the TRS1 and gp145 SUKH domains, along with two regions of TRS1—the minimal dsRNA-binding domain and C-terminal residues necessary for direct PKR-binding—that are essential for rescue of VVΔE3L. The gp145 truncations used in Figs. 3.7-9 and summaries from the dsRNA-binding, VVΔE3L rescue, and self-interaction experiments are also shown, unless not determined (ND).

CHAPTER 4

Discussion and Future Directions

Sensing of pathogen associated molecular patterns and the subsequent induction of an immune response is one of a cell's first lines of defense against infection (78). Double stranded RNA (dsRNA) is recognized by a number of mammalian immune pathways to induce an antiviral state and restrict viral replication (48). One of these pathways, protein kinase R (PKR), regulates translation initiation in response to dsRNA recognition and binding by phosphorylating eIF2 on its α-subunit and preventing the formation of eIF2α-$tRNA_i^{Met}$-GTP ternary complex (50). While some viruses utilize internal ribosome entry sites or other strategies to initiate translation in an eIF2-independent fashion, most viruses encode protein or nucleic acid factors to prevent or reverse PKR activity (102).

Human cytomegalovirus (HCMV) encodes two proteins that antagonize PKR: IRS1 and TRS1 (25). These proteins are essential for viral replication and their deletion allows the activation of PKR in infected cells (90). Previous studies have revealed that TRS1 and IRS1 bind dsRNA (54) and interact with PKR (55), and that disruption of either of these activities results in proteins that are inactive as PKR antagonists. Based on these results, we have hypothesized that TRS1 and IRS1 antagonize PKR by forming a trimolecular complex with dsRNA and PKR (90).

In this dissertation, we probed dsRNA binding by TRS1 to test the trimolecular model of TRS1 function and sought to identify the PKR antagonist of guinea pig cytomegalovirus (GPCMV). In Chapter 2, we investigated the formation of dsRNA during HCMV infection, and evaluated the dsRNA binding properties of TRS. In Chapter 3, we identified a PKR antagonist

encoded by GPCMV, gp145, and compared its function to TRS1. While these studies furthered our understanding of how CMVs antagonize PKR, much remains to be learned about the function of TRS1 and IRS1 during HCMV infection and how we can use this knowledge to treat or prevent HCMV disease.

What is the source of dsRNA during viral infection?

dsRNA has long been known to elicit an interferon response (97) and most viruses encode one or more factors to counteract dsRNA-triggered immune pathways such as PKR (79). Indirect evidence that dsRNA accumulates in infected cells exists. For example, viral transcripts isolated from infected cells have been found to either be duplexed or capable of annealing following purification (14, 65). Recently, dsRNA has been observed *in vivo* during viral infection (144) and we examined the kinetics of dsRNA accumulation during HCMV infection in this work (90). Despite these advances, the source of dsRNA accumulation during infection has yet to be identified for most viruses.

Among RNA viruses, dsRNA is assumed to either be the viral genome or a necessary intermediate of viral replication. dsRNA has been detected during dsRNA virus and (+)-stranded ssRNA virus infection, but, surprisingly, not during (-)-stranded ssRNA virus infection (144). These viruses nonetheless encode antagonists of PKR and other dsRNA activated pathways (85), This could indicate either that viral dsRNA is present at levels below the limits of immunofluorescence detection or that it is abundant but made inaccessible to antibody binding, and presumably cellular antiviral pathways, by viral dsRNA binding proteins. Alternatively, the Sendai virus C protein has been found to limit dsRNA production during replication, suggesting

that Sendai and other (-)-stranded ssRNA viruses tightly regulate dsRNA formation during infection (136).

dsRNA production is also widespread in cells infected with DNA viruses (144). Recent evidence suggests that dsRNA could originate from bidirectional overlapping transcription. The genomes of DNA viruses, including HCMV, are densely packed with open reading frames. Several studies of the HCMV transcriptome have found overlapping sense and antisense viral transcripts that could anneal *in vivo* (51, 149). Individual DNA virus transcripts could also have sufficient secondary structure to activate the cellular dsRNA response, as has been observed in RNA virus messages including the HIV TAR RNA (87),

Infected cells may intentionally synthesize dsRNA to stimulate an immune response. Cellular dsRNA is found in and contained to the nucleus during normal cell growth (10). Breakdown in this containment could cause the activation of dsRNA pathways. Additionally, RNA polymerase III is a sensor of cytoplasmic DNA, which it uses to template the synthesis of dsRNA to activate an interferon response (28). Thus, when trying to identify the nature of dsRNA that has been induced by viral infection it would be unwise to focus exclusively on viral transcripts.

Recent advances in high throughput sequencing and transcriptome profiling have facilitated the identification of dsRNA present in infected cells, but the detection of overlapping transcripts does not prove that the two strands were actually annealed in *in vivo.* It would be possible to sequence an sample enriched for dsRNA either after degrading ssRNA using ssRNA-specific ribonucleases such as RNase A or T1 (107) or by using one of several protocols that

specifically isolate dsRNA (29, 42). However, concentration and purification can cause the artificial annealing of RNAs that are not normally duplexed *in vivo* (65).

RNA immunoprecipitation (RIP) could be used to identify the *in vivo* dsRNA binding partners of both cellular and viral dsRNA binding proteins while lessening the problems of artificial annealing associated with RNA purification (37, 67). In particular, crosslinking dsRNA and dsRNA binding proteins before lysis would allow the use of stringent experimental conditions that could help avoid artificial RNA annealing and postlysis protein-RNA interactions (98). It would be particularly interesting to monitor changes in the protein-RNA associations following the disruption of the cellular or viral dsRNA binding proteins. For example, RIP might reveal that dsRNAs that normally bind to TRS1 during infection associate with PKR when TRS1 and IRS1 are deleted. Despite these technical hurdles, recent advances in RNA analyses may soon provide us with new knowledge on the nature of virally-induced dsRNA.

How does TRS1 antagonize PKR?

dsRNA accumulates during HCMV infection and activates PKR if TRS1 and IRS1 are not present (90). Previous work has demonstrated that TRS1 interacts with both PKR (55) and dsRNA (54). We have hypothesized that the three molecules form a trimolecular complex, wherein dsRNA binding stabilizes PKR-TRS1 interactions, that blocks PKR homodimerization and activation. To test this model of TRS1 function, we must understand how TRS1 interacts with dsRNA and PKR and whether the binding interactions are cooperative or separate functions of TRS1. Engineering mutants that disrupt either TRS1's dsRNA or PKR binding activity will allow us to test the importance of these functions during HCMV replication.

Perhaps the greatest limitation we face in our studies of TRS1 function is the lack of a TRS1 structure. As a US22 family protein, TRS1 lacks homology to proteins found outside of the betaherpesvirus subfamily, dsRNA binding or otherwise, that have had their structures solved. At the same time, functions have not been identified for most of the US22 family proteins despite their conservation across CMVs (94). Solving the TRS1 structure could provide valuable insights into TRS1 function as well as help us to understand the role of other US22 family genes during infection.

In this study, we describe the purification of TRS1 from baculovirus infected insect cells. Using this expression platform, TRS1 yield and purity have been approaching levels needed for crystallization trials. Further optimization of TRS1 production in suspension cell culture could make structural studies even more feasible. However, should TRS1 be refractory to structural studies, gp145 may be a reasonable alternative. As a somewhat smaller protein than TRS1 and rhTRS1, gp145 has a distinct advantage over m142/m143 in that, like TRS1, it is a stable, functional protein when expressed individually. While gp145 and TRS1 diverge outside of the US22 domain and a gp145 structure would be unlikely to provide information on the PKR-TRS1 interface, a gp145 structure would be a useful scaffold to model the structures of TRS1 and other US22 proteins. Alternatively, we could attempt to express and purify the US22 or dsRNA binding domains of TRS1 as truncations. Given the challenges we observed with expressing TRS1 truncations in bacteria, finding a stable and soluble TRS1 fragment could be problematic.

Without knowing the structure of TRS1, we pursued a better understanding of dsRNA binding by TRS1 as a means to evaluate the trimolecular model. Analyses of the affinity and length requirements of the TRS1-dsRNA interaction showed the TRS1 bound to dsRNAs that could activate PKR with slightly lower affinity than the kinase. If TRS1 and IRS1 were present

at equimolar concentrations during infection, TRS1 could not simply sequester dsRNA away from PKR. However, because TRS1 is much more abundant than PKR during late time points, we cannot exclude the possibility that TRS1 could act as a stoichiometric inhibitor of PKR and other dsRNA activated antiviral pathways.

Our current understanding of the TRS1 dsRNA binding domain came from studying TRS1 truncations. To map the TRS1 dsRNA binding domain, we incubated TRS1 truncations translated *in vitro* using rabbit reticulocyte lysate with poly I:C conjugated agarose beads (54). This assay identified a minimal dsRNA binding fragment, TRS1[74-246] (54). Because large truncations are more likely to either destroy protein structure or disrupt multiple functional domains, in this study we sought to identify point mutants in full length TRS1 that were deficient in dsRNA binding and test their effect on TRS1 function.

However, our recent experiments have been complicated by inconsistency in our poly I:C binding assay. In particular, TRS1[Δ86-246], an internal deletion missing the necessary and sufficient dsRNA binding domain delineated previously, now repeatedly interacted with poly I:C beads. Two main sources of experimental variation might account for these different results. Our initial experiments used commercial poly I:C beads that are no longer available (54), forcing us to use dsRNA agarose made in-house (81). Differences in the poly I:C length, density or end structure between these and the commercial beads could cause differential binding. Alternatively, variation between batches of rabbit reticulocyte lysate, which we used for *in vitro* translation, could account for the differences we observe in dsRNA binding activity (52).

As another means to evaluated dsRNA binding, we have recently begun using transiently transfected cell lysates, rather than *in vitro* translation, as the protein source for our dsRNA

binding assay (23) and have observed TRS1[Δ86-246] nonbinding consistent with our first experiments (54). This assay is very similar to the protocol we used to identify gp145 and other GPCMV dsRNA binding proteins and we have confidence that is detects dsRNA binding activity. How we reconcile the differences between results from our dsRNA binding assays remains an open question. We suspect that the *in vitro* translation based assay might be more sensitive and potentially be measuring the activity of a second dsRNA binding domain in TRS1. We are also interested in comparing the dsRNA binding activity of *in vitro* translated protein synthesized using either wheat germ extract to TRS1 produced either using rabbit reticulocyte lysate. This could help clarify whether dsRNA binding by TRS1[Δ86-246] is an artifact caused by some component of the reticulocyte lysate. As we continue to study TRS1 point mutants, it will be imperative that we improve our dsRNA binding assay.

Further improvements to TRS1 purification would allow us to examine the dsRNA binding of TRS1 in isolation from other cellular components. In this study, we successfully expressed full length TRS1 using baculovirus infection, enabling us to measure the dsRNA binding affinity of TRS1. Given our success purifying TRS1 from insect cells, we could use baculovirus expression vectors or drosophila S2 cells to transiently or stably express TRS1 variants (126). Alternatively, by improving the expression of TRS1 in transduced mammalian cells we would engineer cell lines that would not only be valuable for protein purification, but also useful for testing the *trans*-complementation of HCMV[ΔI/ΔT]. We are particularly eager to test lentiviral vectors that include chromatin opening elements to avoid the genomic silencing of the integrated vector (3). While the poly I:C binding assays is a valuable first screen for dsRNA binding activity, the electrophoretic mobility shift assay (EMSA) provides valuable information on the affinity of TRS1 for dsRNA (124). In this study, we successfully used EMSA

to study the kinetics and length requirement of full-length TRS1 binding to dsRNA. When purified TRS1 mutants are available, we would be able to accurately quantify the differences in their dsRNA binding activity using this assay.

Our experiments suggest that dsRNA and PKR binding by TRS1 map to two distinct domains of the protein. However, our current understanding of the PKR-TRS1 interface is limited, having only mapped the C-terminal boundary of the TRS1's PKR binding domain (55). Testing the function of mutants that are defective in PKR binding would allow us to test the involvement of TRS1 in other dsRNA activated antiviral pathways and the trimolecular model of TRS1 function.

TRS1 and PKR interact in a species specific manner as measured by the yeast two-hybrid assay (23). Because PKRs across species are comparatively well conserved, we can identify sequence differences between PKRs that do or do not bind to TRS1 and map PKR residues that are required for TRS1 binding. The reciprocal experiment to identify TRS1 residues required for PKR binding is more complicated. TRS1 is much less conserved than PKR, and there are considerable differences in the PKR binding activities of TRS1 homologues. Of note, rhTRS1 only binds phosphorylated PKR while TRS1 binds inactive PKR (23). So while a homology based screen helped identify residues important for dsRNA binding, it is less likely to be useful for studying the PKR binding domain.

One approach to identify the TRS1-PKR interaction domain would be to use charge-cluster-to-alanine mutational screening (131). Charged residues are typically found on the surface of proteins and their mutation is less likely to disrupt protein structure (30). This approach was useful in identifying TRS1 mutants defective in dsRNA binding and could limit

the number of TRS1 mutants to test for PKR binding in yeast two-hybrid or other assays. Similarly, it is possible to map surfaces involved in protein-protein or protein-nucleic acid interfaces by using mass spectrometry following covalent modification of surface residues (92, 95). In this study, we showed that modification of arginine with *p*-hydroxyphenylglyoxal (HPG) impacted TRS1 and PKR interactions with dsRNA. In preliminary mass spectometry studies, we successfully identified HPG modified residues in each protein. While a major limitation of this approach is achieving complete coverage of a protein sequence with mass spectrometry, we could use this study to identify regions of TRS1 that are at either the PKR or dsRNA binding interface..

What are the functions of TRS1 during CMV infection?

Many viral proteins are multifunction and several studies have demonstrated that TRS1 and IRS1 have several shared and divergent functions in addition to antagonizing PKR. The strong PKR activation phenotype we observe in cells infected with HCMV[ΔI/ΔT] has led us to believe that antagonizing PKR is the essential function of TRS1 and IRS1 during HCMV replication. However, additional TRS1 functions include a role in virion packaging, viral DNA replication, inhibition of autophagy, and interference in dsRNA activated pathways other than PKR. Additional experiments will be necessary to determine the relative importance of TRS1's many functions for HCMV replication.

One of the first functions of TRS1 or IRS1 to be identified was that either protein was required as one of a set of eleven genes needed for efficient DNA replication using the HCMV *ori*Lyt (110). While TRS1 does interact with the DNA polymerase processivity factor UL44 (134), subsequent studies indicated that the effect of TRS1 and IRS1 on replication was mediated

by the activity of either protein as a transcriptional transactivator of replication gene expression (62, 133). However, the role of TRS1 and IRS1 on transcription of viral messages has only been examined in transfection based assays. Transfection can cause a localized activation of PKR (72, 73). Therefore, TRS1 might be acting by derepressing translation rather stimulating transcription. This could be tested by examining the impact of TRS1 on mRNA levels by real time PCR or Southern blot or by testing whether TRS1 and IRS1 effect transcription in $PKR^{-/-}$ cells. A second open reading frame in the 3' end of the IRS1 gene is also expressed during infection and the resulting protein has been characterized as a regulator of immediate early gene transcription (121). However, because HCMV[ΔIRS1] has no replication defect in cell culture, this activity is nonessential (12).

Studies have found that TRS1 has functions in virion assembly and inhibition of autophagy that have yet to be found in IRS1. Unlike HCMV[ΔIRS1], which replicates to wild type titers, HCMV[ΔTRS1] has a moderate replication defect (12). Cells infected with HCMV[ΔTRS1] had defects in both normal HCMV-induced nuclear reorganization and DNA packaging into capsids (1). It is unclear whether IRS1 also plays a role in capsid assembly. TRS1 inhibits autophagy through interactions with Beclin 1 (20). This activity requires the N-terminal end of TRS1 that is dispensable for function as a PKR antagonist (54). The role of these TRS1 functions during HCMV replication is unclear. However, because HCMV[ΔI/ΔT] can be complemented by vaccinia E3L, which is unlikely to share this activity, these TRS1 functions are presumably not essential for replication. Nonetheless, we would be able to conclude that PKR inhibition is the primary essential role of TRS1 and IRS1 during infection if we found that HCMV[ΔI/ΔT] could replication in null or eIF2α S51A fibroblasts.

TRS1 and E3L share the ability to bind dsRNA. While E3L is known to interfere in multiple dsRNA activated antiviral pathways in addition to PKR (113), it is unclear whether TRS1 and IRS1 block these pathways during HCMV infection. We have observed that TRS1 can prevent the activation of the 2'-5'oligoadenylate synthetase/RNAse L pathway during VVΔE3L infection, but did not observe RNA degradation during HCMV[ΔI/ΔT] infection (90). While we cannot exclude the possibility that PKR activation shuts down replication before RNase L can be activated, this observation suggests either that HCMV encodes a second antagonist of the RNase L pathway or that the pathway simply isn't activated during infection. HCMV[ΔI/ΔT] infection of PKR null or eIF2α S51A fibroblasts could demonstrate which, if any, dsRNA activated pathways are inhibited by TRS1 in addition to the PKR pathway. The observation that MCMV mutant lacking m142 and m143 grew as well as wild type MCMV in $PKR^{-/-}$ mouse fibroblasts, leads us to suspect that PKR antagonism is the only essential function of the TRS1 homologues (16). However, if HCMV[ΔI/ΔT] were to have a replication defect in $PKR^{-/-}$ cells, we could look for increased interferon production as a sign of RIG-I like helicase activity or RNA degradation as a sign of RNase L activation.

What can we learn about TRS1 evolution?

PKR is one of a minority of cellular genes that has recently been evolving under strong positive selection (45, 123). Many rapidly evolving genes play a role in host immunity and have been driven to adapt by evolutionary pressure exerted by pathogens. The cytomegaloviruses are thought to have coevolved with their hosts (91) and over a dozen CMVs isolated from unique hosts have now had their genomes sequenced. After this study, the PKR antagonists from four of these virus—HCMV, MCMV, RhCMV, and GPCMV—have been characterized, and each utilizes a subtly different mechanism to inhibit PKR. Could the cytomegaloviruses, and

specifically their PKR antagonists, become a model system for the study of host-viral coevolution?

The herpesvirus genome includes approximately 40 conserved core genes that play essential roles in the viral life cycle that include DNA replication, capsid formation and virion assembly (142). Despite being essential for viral replication, the herpesvirus PKR antagonists are not strongly conserved and the viruses exploit a variety of strategies to antagonize PKR. While herpesvirus PKR antagonists include short-RNA inhibitors of PKR (32) and phosphatase recruiting factors (31), viral dsRNA-binding proteins are the most widespread PKR antagonists (54, 101, 115). The dsRNA-binding proteins of the alpha- and gammaherpesviruses have similar noncanonical dsRNA binding motifs (115). In contrast, TRS1 and it homologues are members of the US22 gene family, which is unique to betaherpesviruses.

Betaherpesviruses have the highest rate of gene gain of the herpesviruses, and gene duplication has led to the formation of viral gene families (142). US22 gene family members have been found in three of the four betaherpesvirus genera. The fourth genus, the proboscoviruses, are elephant viruses that represent the earliest branch in betaherpesvirus evolution (82). Unfortunately, a complete proboscovirus genome is not available and we cannot compare its coding content with the other genera. Of the remaining genera, roseolovirus genomes are significantly smaller but they nonetheless share several of the same gene families, including the US22 gene family, with the CMVs. However, the shared gene families generally include fewer members in roseoloviruses (40). For example, HCMV encodes thirteen US22 family genes while human herpesvirus 6 (HHV-6), a roseolovirus, encodes nine (40) (Fig. 4.1).

Noticeably absent from the roseolovirus genome is an obvious TRS1 homologue. Whether the roseoloviruses use a US22 family protein to antagonize PKR remains an unanswered question that could be addressed by screening for HHV-6 dsRNA binding proteins, an approach that was successful for identifying gp145 as the GPCMV antagonist. Alternatively, the HHV-6 US22 family proteins could be cloned and tested for activity against PKR. If none of the proteins antagonize PKR, we could test HHV-6 or a library of HHV-6 genes for their ability to rescue VVΔE3L replication to explore the possibility that the roseoloviruses antagonize PKR using a completely different mechanism than the cytomegaloviruses (25, 27).

The remaining betaherpesviruses form a single clade that includes the cytomegaloviruses, the muromegaloviruses, and the unassigned viruses GPCMV, tupaia herpesvirus, and *Miniopterus schreibersii* (bat) herpesvirus (150). These viruses each encode at least eleven US22 family proteins, including a known or predicted TRS1 homologue. The US22 gene family exemplifies the role of gene duplication in viral evolution. The US22 family ancestor is thought to have originated by the horizontal gene transfer of a bacterial SUKH gene into a herpesvirus followed by duplication and diversification into the family of proteins we observe today (148) (Fig. 4.1). While many of the US22 family genes are conserved across the cytomegaloviruses, it is interesting that the TRS1 homologue has been duplicated in great ape and new world monkey CMVs.

The ancestral betaherpesvirus likely had a class A genome structure, which has been maintained in most extant species (Fig. 4.1) (40). However, the great ape and new world monkey CMVs each have a class E genome, where the TRS1 homologue is encoded in repeat sequences, causing it to be partially or completely duplicated. The consequence of the TRS1/IRS1 duplication remains unclear. Duplication of PKR antagonists has been found to help

viruses adapt to nonpermissive cell types during experimental evolution (43). TRS1 duplication could confer a similar selective advantage to CMVs that has driven the adoption of the class E genome in some CMVs. Alternatively, as discussed above, HCMV TRS1 and IRS1 are somewhat functionally divergent, and the gene duplication could have been followed by the evolution of new functions other than inhibiting PKR (105).

Among the characterized CMV PKR antagonists, a complex pattern of species-specificity has emerged. TRS1 and rhTRS1 are species specific and can only antagonize the PKRs of primate species closely related to their natural host (23). In contrast, we observed that gp145 was active against guinea pig, human, and old world monkey PKR. To further complicate the matter, not only can m142/m143 antagonize human PKR (26), but MCMV[Δm142/Δm143] can be rescued by TRS1 (16). Characterizing additional TRS1 homologues will help clarify whether species specificity is a feature of the primate CMVs but not the rodent CMVs.

Developing a model to test the activity of TRS1 against PKRs from various species has been challenging. dsRNA binding proteins generally less dramatically rescue transgene expression in HeLa PKR^{KD} cells than eIF2α pseudosubstrates in reporter gene cotransfection assays (123). We have also attempted to test the activity of TRS1 homologues to rescue yeast growth after PKR expression without success (45). Significant differences in the kinetics of dsRNA formation and PKR activation between vaccinia and CMV infection may account for the observed differences in VVΔE3L rescue between TRS1 homologues that are not representative of the antagonists' actual activity against different PKRs.

Moving forward, it may be necessary to use a CMV background to test the species specificity of TRS1 homologues. We could transduce mouse $PKR^{-/-}$ cells to express different

TRS1 homologues and PKRs and test their ability to support the replication of MCMV[Δm142/Δm143] (16). Alternatively, if it becomes easier to genetically engineer CMVs, we could perform additional experiments to swap TRS1 homologues between different viruses (16). While the replication kinetics of CMVs differ somewhat, these experiments would have the advantage of testing the activity of TRS1 homologues under conditions more representative of what is found during natural infection and would help us clarify whether PKR is a determinant of CMV host range.

Can we develop a CMV vaccine?

The essential role of TRS1 and IRS1 during HCMV replication makes the proteins attractive targets for drug and vaccine development. Viruses such as VVΔE3L that lack a normal PKR response have been explored as vaccine candidates (68), and we feel HCMV[ΔI/ΔT] is a potential vaccine strain. Because HCMV[ΔI/ΔT] lacks the normal viral dsRNA binding proteins, free dsRNA is available to stimulate a robust interferon response in infected cells. This heightened interferon signaling could lead to a more robust adaptive immune response when compared to infections using viruses attenuated by disruption of other essential genes (68).

While a HCMV vaccine could help reduce the incidence of CMV disease in immunocompromised individuals, preventing congenital CMV infection is a primary motivator of vaccine development. HCMV is the most common viral congenital infection in the developed world, where the virus infects up to 2% of newborns *in utero* (127). Approximately 10% of newborns that are congenitally infected will develop clinically evident disease, which often results in neurodevelopmental sequelae, including mental retardation and hearing loss (127). Severe cases of congenital CMV infection result in approximately 150 deaths and 5500 cases of

permanent disability each year in the United States (5). The long term costs associated with the care of these children are estimated to be ~$2 billion annually (2). In a recent analysis by the Institutes of Medicine, the combined human and economic toll of congenital infection made HCMV the single most cost effective vaccine target identified by the study (135).

Vaccine trials with HCMV[ΔI/ΔT] would require prior demonstration of vaccine efficacy in an animal model of infection. However, HCMV has a restricted host range and we cannot study the virus in animal models of infection. This has led us to identify the PKR antagonists of animal CMVs including MCMV gene m142 and m143 and gp145. (16). However, MCMV is not transmitted across the placenta during the course of natural infection (128), limiting its utility as a model of congenital CMV infection. While guinea pigs have fewer genetic tools available than mice, the GPCMV model has several advantages over MCMV in addition to natural congenital infections (128). GPCMV is more genetically similar to primate CMVs than MCMV is (129). Additionally, where two MCMV proteins are required to antagonize PKR (140), gp145 alone, like TRS1, is sufficient to block the PKR pathway, simplifying studies of gp145 function.

Development of GPCMV[Δgp145] will allow us to study the role of gp145 during GPCMV infection and to determine whether the protein, like HCMV TRS1/IRS1 and MCMV m142/m143, is required for replication. gp145 may be dispensable in cell culture, as VVΔE3L, VVΔK3L, and VVΔE3L/ΔK3L all replicated to varying degrees in GPL cells. Additionally, a GPCMV mutant that includes deletion of gp145 replicates poorly in this cell type (35). These observations could reflect that PKR is poorly expression in GPL cells or may indicate that guinea pigs have a generally weaker PKR response than other mammals. Alternatively, GPCMV may encode a second, weak PKR antagonist that we have not yet identified, similar to how herpes simplex encodes US11 in addition to γ34.5 (101).

Ultimately, GPCMV[Δgp145] will be tested for efficacy in preventing the congenital transmission of GPCMV. However, successful vaccine trials in GPCMV will not necessarily indicate that a vaccine against HCMV is possible. Aside from differences in the underlying mechanisms of gp145 and TRS1 against PKR and in the biology and coding content of GPCMV and HCMV, HCMV is noteworthy for its capacity to cause superinfection despite preexisting immunity (56). HCMV reinfection has been found to be frequent in women and is thought to contribute to congenital CMV transmission in mothers that were seropositive prior to conception (122). Nonetheless, congenital CMV infection is generally less frequent and severe in mothers who seroconverted prior to pregnancy, so a HCMV vaccine could still significantly decrease the morbidity and mortality of congenital CMV even if it does not provide sterilizing immunity (5).

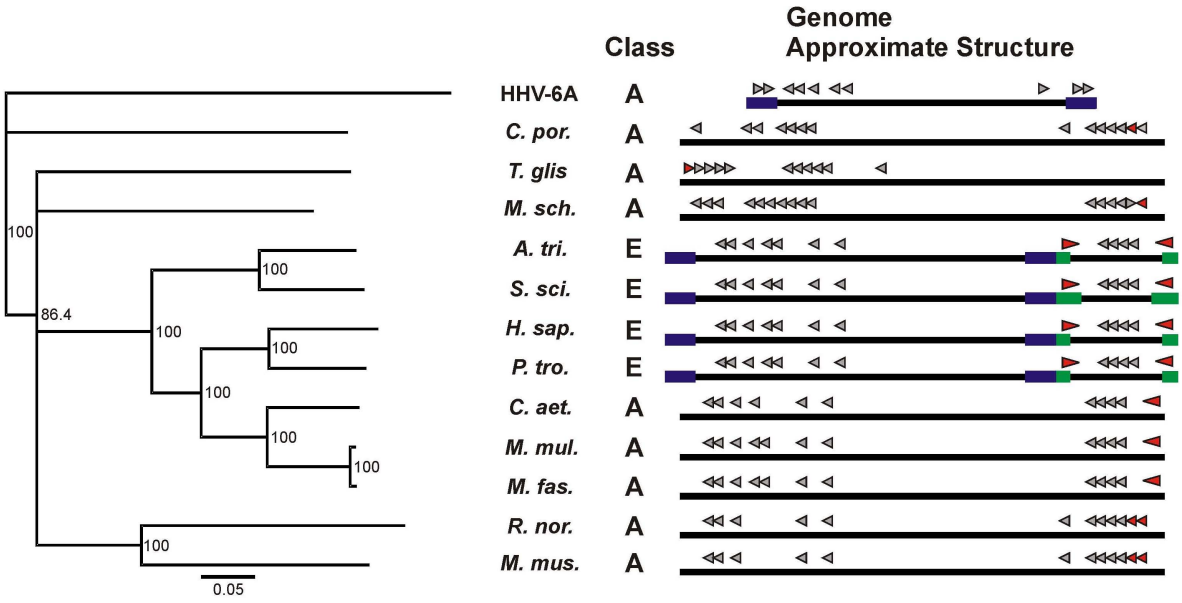

Figure 4.1. TRS1 and the US22 gene family. At left, a neighbor joining tree of cytomegalovirus Pol genes is shown, rooted with human herpesvirus 6, a roseolovirus. At right, each virus's genome is diagramed with number and approximate location of US22 genes. Blue and green bars indicate repeat sequences, while triangles signify US22 genes and their orientation, with red indicating predicted or known TRS1 homologues. Cytomegaloviruses originated from rat (*R. nor.*), mouse (*M. mus.*), three-striped night monkey (*A. tri.*), common squirrel monkey (*S. sci.*), grivet monkey (*C. aet.*), olive baboon (*P. cyn.*), rhesus macaque (*M. mul.*), crab-eating macaque (*M. fas.*), common chimpanzee (*P. tro.*), human (*H. sap.*), common treeshrew (*T. glis*), common bent-wing bat (*M. sch.*), and guinea pig (*C. por.*).

BIBLIOGRAPHY

1. **Adamo, J. E., J. Schroer, and T. Shenk.** 2004. Human cytomegalovirus TRS1 protein is required for efficient assembly of DNA-containing capsids. J Virol **78:**10221-9.
2. **Arvin, A. M., P. Fast, M. Myers, S. Plotkin, and R. Rabinovich.** 2004. Vaccine development to prevent cytomegalovirus disease: report from the National Vaccine Advisory Committee. Clin Infect Dis **39:**233-9.
3. **Bandaranayake, A. D., C. Correnti, B. Y. Ryu, M. Brault, R. K. Strong, and D. J. Rawlings.** 2011. Daedalus: a robust, turnkey platform for rapid production of decigram quantities of active recombinant proteins in human cell lines using novel lentiviral vectors. Nucleic Acids Res **39:**e143.
4. **Barry, P. A., K. M. Lockridge, S. Salamat, S. P. Tinling, Y. Yue, S. S. Zhou, S. M. Gospe, Jr., W. J. Britt, and A. F. Tarantal.** 2006. Nonhuman primate models of intrauterine cytomegalovirus infection. ILAR J **47:**49-64.
5. **Bate, S. L., S. C. Dollard, and M. J. Cannon.** 2010. Cytomegalovirus seroprevalence in the United States: the national health and nutrition examination surveys, 1988-2004. Clin Infect Dis **50:**1439-47.
6. **Beattie, E., K. L. Denzler, J. Tartaglia, M. E. Perkus, E. Paoletti, and B. L. Jacobs.** 1995. Reversal of the interferon-sensitive phenotype of a vaccinia virus lacking E3L by expression of the reovirus S4 gene. J Virol **69:**499-505.
7. **Beattie, E., E. B. Kauffman, H. Martinez, M. E. Perkus, B. L. Jacobs, E. Paoletti, and J. Tartaglia.** 1996. Host-range restriction of vaccinia virus E3L-specific deletion mutants. Virus Genes **12:**89-94.
8. **Beattie, E., J. Tartaglia, and E. Paoletti.** 1991. Vaccinia virus-encoded eIF-2 alpha homolog abrogates the antiviral effect of interferon. Virology **183:**419-22.
9. **Bevilacqua, P. C., and T. R. Cech.** 1996. Minor-groove recognition of double-stranded RNA by the double-stranded RNA-binding domain from the RNA-activated protein kinase PKR. Biochemistry **35:**9983-94.
10. **Bickel, K. S., and D. R. Morris.** 2006. Silencing the transcriptome's dark matter: mechanisms for suppressing translation of intergenic transcripts. Mol Cell **22:**309-16.
11. **Bierle, C. J., M. R. Schleiss, and A. P. Geballe.** 2012. Antagonism of the protein kinase R pathway by the guinea pig cytomegalovirus US22-family gene gp145. Virology **433:**157-66.
12. **Blankenship, C. A., and T. Shenk.** 2002. Mutant human cytomegalovirus lacking the immediate-early TRS1 coding region exhibits a late defect. J Virol **76:**12290-9.
13. **Bonin, M., J. Oberstrass, N. Lukacs, K. Ewert, E. Oesterschulze, R. Kassing, and W. Nellen.** 2000. Determination of preferential binding sites for anti-dsRNA antibodies on double-stranded RNA by scanning force microscopy. RNA **6:**563-70.
14. **Boone, R. F., R. P. Parr, and B. Moss.** 1979. Intermolecular duplexes formed from polyadenylylated vaccinia virus RNA. J Virol **30:**365-74.
15. **Buaas, F. W., K. Lee, S. Edelhoff, C. Disteche, and R. E. Braun.** 1999. Cloning and characterization of the mouse interleukin enhancer binding factor 3 (Ilf3) homolog in a screen for RNA binding proteins. Mamm Genome **10:**451-6.
16. **Budt, M., L. Niederstadt, R. S. Valchanova, S. Jonjic, and W. Brune.** 2009. Specific inhibition of the PKR-mediated antiviral response by the murine cytomegalovirus proteins m142 and m143. J Virol **83:**1260-70.

17. **Casey, J. L.** 2006. RNA editing in hepatitis delta virus. Curr Top Microbiol Immunol **307:**67-89.
18. **Chang, H. W., J. C. Watson, and B. L. Jacobs.** 1992. The E3L gene of vaccinia virus encodes an inhibitor of the interferon-induced, double-stranded RNA-dependent protein kinase. Proc Natl Acad Sci U S A **89:**4825-9.
19. **Chang, K. Y., and A. Ramos.** 2005. The double-stranded RNA-binding motif, a versatile macromolecular docking platform. FEBS J **272:**2109-17.
20. **Chaumorcel, M., M. Lussignol, L. Mouna, Y. Cavignac, K. Fahie, J. Cotte-Laffitte, A. Geballe, W. Brune, I. Beau, P. Codogno, and A. Esclatine.** 2012. The human cytomegalovirus protein TRS1 inhibits autophagy via its interaction with Beclin 1. J Virol **86:**2571-84.
21. **Chaumorcel, M., M. Lussignol, L. Mouna, Y. Cavignac, K. Fahie, J. Cotte-Laffitte, A. Geballe, W. Brune, I. Beau, P. Codogno, and A. Esclatine.** 2011. The Human Cytomegalovirus Protein TRS1 Inhibits Autophagy via Its Interaction with Beclin 1. J Virol.
22. **Chee, M. S., A. T. Bankier, S. Beck, R. Bohni, C. M. Brown, R. Cerny, T. Horsnell, C. A. Hutchison, 3rd, T. Kouzarides, J. A. Martignetti, and et al.** 1990. Analysis of the protein-coding content of the sequence of human cytomegalovirus strain AD169. Curr Top Microbiol Immunol **154:**125-69.
23. **Child, S. J., G. Brennan, J. E. Braggin, and A. P. Geballe.** 2012. Species specificity of protein kinase R antagonism by cytomegalovirus TRS1 genes. J Virol **86:**3880-9.
24. **Child, S. J., and A. P. Geballe.** 2009. Binding and relocalization of protein kinase R by murine cytomegalovirus. J Virol **83:**1790-9.
25. **Child, S. J., M. Hakki, K. L. De Niro, and A. P. Geballe.** 2004. Evasion of cellular antiviral responses by human cytomegalovirus TRS1 and IRS1. J Virol **78:**197-205.
26. **Child, S. J., L. K. Hanson, C. E. Brown, D. M. Janzen, and A. P. Geballe.** 2006. Double-stranded RNA binding by a heterodimeric complex of murine cytomegalovirus m142 and m143 proteins. J Virol **80:**10173-80.
27. **Child, S. J., S. Jarrahian, V. M. Harper, and A. P. Geballe.** 2002. Complementation of vaccinia virus lacking the double-stranded RNA-binding protein gene E3L by human cytomegalovirus. J Virol **76:**4912-8.
28. **Chiu, Y. H., J. B. Macmillan, and Z. J. Chen.** 2009. RNA polymerase III detects cytosolic DNA and induces type I interferons through the RIG-I pathway. Cell **138:**576-91.
29. **Choi, Y. G., and J. W. Randles.** 1997. Microgranular cellulose improves dsRNA recovery from plant nucleic acid extracts. Biotechniques **23:**610-1.
30. **Chothia, C.** 1976. The nature of the accessible and buried surfaces in proteins. J Mol Biol **105:**1-12.
31. **Chou, J., E. R. Kern, R. J. Whitley, and B. Roizman.** 1990. Mapping of herpes simplex virus-1 neurovirulence to gamma 134.5, a gene nonessential for growth in culture. Science **250:**1262-6.
32. **Clarke, P. A., M. Schwemmle, J. Schickinger, K. Hilse, and M. J. Clemens.** 1991. Binding of Epstein-Barr virus small RNA EBER-1 to the double-stranded RNA-activated protein kinase DAI. Nucleic Acids Res **19:**243-8.
33. **Conn, G. L.** 2003. Expression of active RNA-activated protein kinase (PKR) in bacteria. Biotechniques **35:**682-4, 686.

34. **Craig, R., and R. C. Beavis.** 2004. TANDEM: matching proteins with tandem mass spectra. Bioinformatics **20:**1466-7.
35. **Cui, X., A. McGregor, M. R. Schleiss, and M. A. McVoy.** 2009. The impact of genome length on replication and genome stability of the herpesvirus guinea pig cytomegalovirus. Virology **386:**132-8.
36. **Cullen, B. R.** 2006. Is RNA interference involved in intrinsic antiviral immunity in mammals? Nat Immunol **7:**563-7.
37. **Darnell, R. B.** 2010. HITS-CLIP: panoramic views of protein-RNA regulation in living cells. Wiley Interdiscip Rev RNA **1:**266-86.
38. **Davies, M. V., H. W. Chang, B. L. Jacobs, and R. J. Kaufman.** 1993. The E3L and K3L vaccinia virus gene products stimulate translation through inhibition of the double-stranded RNA-dependent protein kinase by different mechanisms. J Virol **67:**1688-92.
39. **Davison, A. J.** 2007. Comparative analysis of the genomes. *In* A. Arvin, G. Campadelli-Fiume, E. Mocarski, P. S. Moore, B. Roizman, R. Whitley, and K. Yamanishi (ed.), Human Herpesviruses: Biology, Therapy, and Immunoprophylaxis, 2011/02/25 ed. Cambridge University Press, Cambridge.
40. **Davison, A. J., and D. Bhella.** 2007. Comparative genome and virion structure. *In* A. Arvin, G. Campadelli-Fiume, E. Mocarski, P. S. Moore, B. Roizman, R. Whitley, and K. Yamanishi (ed.), Human Herpesviruses: Biology, Therapy, and Immunoprophylaxis, 2011/02/25 ed. Cambridge University Press, Cambridge.
41. **Demmler, G. J.** 1996. Congenital cytomegalovirus infection and disease. Adv Pediatr Infect Dis **11:**135-62.
42. **Diaz-Ruiz, J. R., and J. M. Kaper.** 1978. Isolation of viral double-stranded RNAs using a LiCl fractionation procedure. Prep Biochem **8:**1-17.
43. **Elde, N. C., S. J. Child, M. T. Eickbush, J. O. Kitzman, K. S. Rogers, J. Shendure, A. P. Geballe, and H. S. Malik.** 2012. Poxviruses deploy genomic accordions to adapt rapidly against host antiviral defenses. Cell **150:**831-41.
44. **Elde, N. C., S. J. Child, A. P. Geballe, and H. S. Malik.** 2008. Protein kinase R reveals an evolutionary model for defeating viral mimicry. Nature.
45. **Elde, N. C., S. J. Child, A. P. Geballe, and H. S. Malik.** 2009. Protein kinase R reveals an evolutionary model for defeating viral mimicry. Nature **457:**485-9.
46. **Fannin Rider, P. J., W. Dunn, E. Yang, and F. Liu.** 2008. Human cytomegalovirus microRNAs. Curr Top Microbiol Immunol **325:**21-39.
47. **Fierro-Monti, I., and M. B. Mathews.** 2000. Proteins binding to duplexed RNA: one motif, multiple functions. Trends Biochem Sci **25:**241-6.
48. **Gantier, M. P., and B. R. Williams.** 2007. The response of mammalian cells to double-stranded RNA. Cytokine Growth Factor Rev **18:**363-71.
49. **Garaigorta, U., and F. V. Chisari.** 2009. Hepatitis C virus blocks interferon effector function by inducing protein kinase R phosphorylation. Cell Host Microbe **6:**513-22.
50. **Garcia, M. A., J. Gil, I. Ventoso, S. Guerra, E. Domingo, C. Rivas, and M. Esteban.** 2006. Impact of protein kinase PKR in cell biology: from antiviral to antiproliferative action. Microbiol Mol Biol Rev **70:**1032-60.
51. **Gatherer, D., S. Seirafian, C. Cunningham, M. Holton, D. J. Dargan, K. Baluchova, R. D. Hector, J. Galbraith, P. Herzyk, G. W. Wilkinson, and A. J. Davison.** 2011. High-resolution human cytomegalovirus transcriptome. Proc Natl Acad Sci U S A **108:**19755-60.

52. **Geballe, A. P., and M. K. Gray.** 1992. Variable inhibition of cell-free translation by HIV-1 transcript leader sequences. Nucleic Acids Res **20:**4291-7.
53. **Geballe, A. P., and E. S. Mocarski.** 1988. Translational control of cytomegalovirus gene expression is mediated by upstream AUG codons. J Virol **62:**3334-40.
54. **Hakki, M., and A. P. Geballe.** 2005. Double-stranded RNA binding by human cytomegalovirus pTRS1. J Virol **79:**7311-8.
55. **Hakki, M., E. E. Marshall, K. L. De Niro, and A. P. Geballe.** 2006. Binding and nuclear relocalization of protein kinase R by human cytomegalovirus TRS1. J Virol **80:**11817-26.
56. **Hansen, S. G., C. J. Powers, R. Richards, A. B. Ventura, J. C. Ford, D. Siess, M. K. Axthelm, J. A. Nelson, M. A. Jarvis, L. J. Picker, and K. Fruh.** 2010. Evasion of CD8+ T cells is critical for superinfection by cytomegalovirus. Science **328:**102-6.
57. **Hansen, S. G., L. I. Strelow, D. C. Franchi, D. G. Anders, and S. W. Wong.** 2003. Complete sequence and genomic analysis of rhesus cytomegalovirus. J Virol **77:**6620-36.
58. **Hewitt, L., and J. M. McDonnell.** 2004. Screening and optimizing protein production in E. coli. Methods Mol Biol **278:**1-16.
59. **Hinnebusch, A. G., and J. R. Lorsch.** 2012. The Mechanism of Eukaryotic Translation Initiation: New Insights and Challenges. Cold Spring Harb Perspect Biol.
60. **Hornung, V., J. Ellegast, S. Kim, K. Brzozka, A. Jung, H. Kato, H. Poeck, S. Akira, K. K. Conzelmann, M. Schlee, S. Endres, and G. Hartmann.** 2006. 5'-Triphosphate RNA is the ligand for RIG-I. Science **314:**994-7.
61. **Hovanessian, A. G., and J. Justesen.** 2007. The human 2'-5'oligoadenylate synthetase family: unique interferon-inducible enzymes catalyzing 2'-5' instead of 3'-5' phosphodiester bond formation. Biochimie **89:**779-88.
62. **Iskenderian, A. C., L. Huang, A. Reilly, R. M. Stenberg, and D. G. Anders.** 1996. Four of eleven loci required for transient complementation of human cytomegalovirus DNA replication cooperate to activate expression of replication genes. J Virol **70:**383-92.
63. **Jacobs, B. L., and J. O. Langland.** 1996. When two strands are better than one: the mediators and modulators of the cellular responses to double-stranded RNA. Virology **219:**339-49.
64. **Jacobs, B. L., J. O. Langland, and T. Brandt.** 1998. Characterization of viral double-stranded RNA-binding proteins. Methods **15:**225-32.
65. **Jacquemont, B., and B. Roizman.** 1975. RNA synthesis in cells infected with herpes simplex virus. X. Properties of viral symmetric transcripts and of double-stranded RNA prepared from them. J Virol **15:**707-13.
66. **Janzen, D. M., and A. P. Geballe.** 2004. The effect of eukaryotic release factor depletion on translation termination in human cell lines. Nucleic Acids Res **32:**4491-502.
67. **Jensen, K. B., and R. B. Darnell.** 2008. CLIP: crosslinking and immunoprecipitation of in vivo RNA targets of RNA-binding proteins. Methods Mol Biol **488:**85-98.
68. **Jentarra, G. M., M. C. Heck, J. W. Youn, K. Kibler, J. O. Langland, C. R. Baskin, O. Ananieva, Y. Chang, and B. L. Jacobs.** 2008. Vaccinia viruses with mutations in the E3L gene as potential replication-competent, attenuated vaccines: scarification vaccination. Vaccine **26:**2860-72.
69. **Jopling, C. L., M. Yi, A. M. Lancaster, S. M. Lemon, and P. Sarnow.** 2005. Modulation of hepatitis C virus RNA abundance by a liver-specific MicroRNA. Science **309:**1577-81.

70. **Juanjuan, C., F. Yan, C. Li, L. Haizhi, W. Ling, W. Xinrong, X. Juan, L. Tao, Y. Zongzhi, and C. Suhua.** 2011. Murine model for congenital CMV infection and hearing impairment. Virol J **8:**70.
71. **Kato, H., O. Takeuchi, E. Mikamo-Satoh, R. Hirai, T. Kawai, K. Matsushita, A. Hiiragi, T. S. Dermody, T. Fujita, and S. Akira.** 2008. Length-dependent recognition of double-stranded ribonucleic acids by retinoic acid-inducible gene-I and melanoma differentiation-associated gene 5. J Exp Med **205:**1601-10.
72. **Kaufman, R. J., M. V. Davies, V. K. Pathak, and J. W. Hershey.** 1989. The phosphorylation state of eucaryotic initiation factor 2 alters translational efficiency of specific mRNAs. Mol Cell Biol **9:**946-58.
73. **Kaufman, R. J., and P. Murtha.** 1987. Translational control mediated by eucaryotic initiation factor-2 is restricted to specific mRNAs in transfected cells. Mol Cell Biol **7:**1568-71.
74. **Kawagishi-Kobayashi, M., C. Cao, J. Lu, K. Ozato, and T. E. Dever.** 2000. Pseudosubstrate inhibition of protein kinase PKR by swine pox virus C8L gene product. Virology **276:**424-34.
75. **Khoo, D., C. Perez, and I. Mohr.** 2002. Characterization of RNA determinants recognized by the arginine- and proline-rich region of Us11, a herpes simplex virus type 1-encoded double-stranded RNA binding protein that prevents PKR activation. J Virol **76:**11971-81.
76. **Kitajewski, J., R. J. Schneider, B. Safer, S. M. Munemitsu, C. E. Samuel, B. Thimmappaya, and T. Shenk.** 1986. Adenovirus VAI RNA antagonizes the antiviral action of interferon by preventing activation of the interferon-induced eIF-2 alpha kinase. Cell **45:**195-200.
77. **Kost, T. A., J. P. Condreay, and D. L. Jarvis.** 2005. Baculovirus as versatile vectors for protein expression in insect and mammalian cells. Nat Biotechnol **23:**567-75.
78. **Kumar, H., T. Kawai, and S. Akira.** 2011. Pathogen recognition by the innate immune system. Int Rev Immunol **30:**16-34.
79. **Langland, J. O., J. M. Cameron, M. C. Heck, J. K. Jancovich, and B. L. Jacobs.** 2006. Inhibition of PKR by RNA and DNA viruses. Virus Res **119:**100-10.
80. **Langland, J. O., and B. L. Jacobs.** 2002. The role of the PKR-inhibitory genes, E3L and K3L, in determining vaccinia virus host range. Virology **299:**133-41.
81. **Langland, J. O., S. M. Pettiford, and B. L. Jacobs.** 1995. Nucleic acid affinity chromatography: preparation and characterization of double-stranded RNA agarose. Protein Expr Purif **6:**25-32.
82. **Latimer, E., J. C. Zong, S. Y. Heaggans, L. K. Richman, and G. S. Hayward.** 2011. Detection and evaluation of novel herpesviruses in routine and pathological samples from Asian and African elephants: identification of two new probosciviruses (EEHV5 and EEHV6) and two new gammaherpesviruses (EGHV3B and EGHV5). Vet Microbiol **147:**28-41.
83. **Li, S., J. Y. Min, R. M. Krug, and G. C. Sen.** 2006. Binding of the influenza A virus NS1 protein to PKR mediates the inhibition of its activation by either PACT or double-stranded RNA. Virology **349:**13-21.
84. **Licklider, L. J., C. C. Thoreen, J. Peng, and S. P. Gygi.** 2002. Automation of nanoscale microcapillary liquid chromatography-tandem mass spectrometry with a vented column. Anal Chem **74:**3076-83.

85. **Lu, Y., M. Wambach, M. G. Katze, and R. M. Krug.** 1995. Binding of the influenza virus NS1 protein to double-stranded RNA inhibits the activation of the protein kinase that phosphorylates the elF-2 translation initiation factor. Virology **214:**222-8.
86. **Luckow, V. A., S. C. Lee, G. F. Barry, and P. O. Olins.** 1993. Efficient generation of infectious recombinant baculoviruses by site-specific transposon-mediated insertion of foreign genes into a baculovirus genome propagated in Escherichia coli. J Virol **67:**4566-79.
87. **Maitra, R. K., N. A. McMillan, S. Desai, J. McSwiggen, A. G. Hovanessian, G. Sen, B. R. Williams, and R. H. Silverman.** 1994. HIV-1 TAR RNA has an intrinsic ability to activate interferon-inducible enzymes. Virology **204:**823-7.
88. **Manche, L., S. R. Green, C. Schmedt, and M. B. Mathews.** 1992. Interactions between double-stranded RNA regulators and the protein kinase DAI. Mol Cell Biol **12:**5238-48.
89. **Marcus, P. I., and M. J. Sekellick.** 1977. Defective interfering particles with covalently linked [+/-]RNA induce interferon. Nature **266:**815-9.
90. **Marshall, E. E., C. J. Bierle, W. Brune, and A. P. Geballe.** 2009. Essential role for either TRS1 or IRS1 in human cytomegalovirus replication. J Virol **83:**4112-20.
91. **McGeoch, D. J., F. J. Rixon, and A. J. Davison.** 2006. Topics in herpesvirus genomics and evolution. Virus Res **117:**90-104.
92. **McKee, C. J., J. J. Kessl, J. O. Norris, N. Shkriabai, and M. Kvaratskhelia.** 2009. Mass spectrometry-based footprinting of protein-protein interactions. Methods **47:**304-7.
93. **McKenna, S. A., D. A. Lindhout, T. Shimoike, C. E. Aitken, and J. D. Puglisi.** 2007. Viral dsRNA inhibitors prevent self-association and autophosphorylation of PKR. J Mol Biol **372:**103-13.
94. **Menard, C., M. Wagner, Z. Ruzsics, K. Holak, W. Brune, A. E. Campbell, and U. H. Koszinowski.** 2003. Role of murine cytomegalovirus US22 gene family members in replication in macrophages. J Virol **77:**5557-70.
95. **Mendoza, V. L., and R. W. Vachet.** 2009. Probing protein structure by amino acid-specific covalent labeling and mass spectrometry. Mass Spectrom Rev **28:**785-815.
96. **Meredith, R. W., J. E. Janecka, J. Gatesy, O. A. Ryder, C. A. Fisher, E. C. Teeling, A. Goodbla, E. Eizirik, T. L. Simao, T. Stadler, D. L. Rabosky, R. L. Honeycutt, J. J. Flynn, C. M. Ingram, C. Steiner, T. L. Williams, T. J. Robinson, A. Burk-Herrick, M. Westerman, N. A. Ayoub, M. S. Springer, and W. J. Murphy.** 2011. Impacts of the Cretaceous Terrestrial Revolution and KPg extinction on mammal diversification. Science **334:**521-4.
97. **Merigan, T. C.** 1970. Interferon stimulated by double stranded RNA. Nature **228:**219-22.
98. **Mili, S., and J. A. Steitz.** 2004. Evidence for reassociation of RNA-binding proteins after cell lysis: implications for the interpretation of immunoprecipitation analyses. RNA **10:**1692-4.
99. **Miller, A. D., D. G. Miller, J. V. Garcia, and C. M. Lynch.** 1993. Use of retroviral vectors for gene transfer and expression. Methods Enzymol **217:**581-99.
100. **Mocarski, E. S., Jr, T. Shenk, and R. F. Pass.** 2007. Cytomegaloviruses, p. 2702-2772. *In* B. N. Fields, D. M. Knipe, and P. M. Howley (ed.), Fields' virology, 5th ed. Wolters Kluwer Health/Lippincott Williams & Wilkins, Philadelphia.
101. **Mohr, I., and Y. Gluzman.** 1996. A herpesvirus genetic element which affects translation in the absence of the viral GADD34 function. EMBO J **15:**4759-66.

102. **Mohr, I., T. Pe'ery, and M. B. Mathews.** 2007. Protein Synthesis and Translational Control during Viral Infection, p. 545–599. *In* M. B. Mathews, N. Sonenberg, and J. W. B. Hershey (ed.), Translational Control in Biology and Medicine, 3rd ed. Cold Spring Harbor Laboratory Press, Cold Spring Harbor, NY.
103. **Murphy, E., and T. Shenk.** 2008. Human cytomegalovirus genome. Curr Top Microbiol Immunol **325:**1-19.
104. **Nallagatla, S. R., J. Hwang, R. Toroney, X. Zheng, C. E. Cameron, and P. C. Bevilacqua.** 2007. 5'-triphosphate-dependent activation of PKR by RNAs with short stem-loops. Science **318:**1455-8.
105. **Nasvall, J., L. Sun, J. R. Roth, and D. I. Andersson.** 2012. Real-time evolution of new genes by innovation, amplification, and divergence. Science **338:**384-7.
106. **Nesvizhskii, A. I., A. Keller, E. Kolker, and R. Aebersold.** 2003. A statistical model for identifying proteins by tandem mass spectrometry. Anal Chem **75:**4646-58.
107. **Nichols, N. M., and D. Yue.** 2008. Ribonucleases. Curr Protoc Mol Biol **Chapter 3:**Unit3 13.
108. **Nozawa, N., Y. Yamamoto, Y. Fukui, H. Katano, Y. Tsutsui, Y. Sato, S. Yamada, Y. Inami, K. Nakamura, M. Yokoi, I. Kurane, and N. Inoue.** 2008. Identification of a 1.6 kb genome locus of guinea pig cytomegalovirus required for efficient viral growth in animals but not in cell culture. Virology **379:**45-54.
109. **Obbard, D. J., K. H. Gordon, A. H. Buck, and F. M. Jiggins.** 2009. The evolution of RNAi as a defence against viruses and transposable elements. Philos Trans R Soc Lond B Biol Sci **364:**99-115.
110. **Pari, G. S., and D. G. Anders.** 1993. Eleven loci encoding trans-acting factors are required for transient complementation of human cytomegalovirus oriLyt-dependent DNA replication. J Virol **67:**6979-88.
111. **Pari, G. S., M. A. Kacica, and D. G. Anders.** 1993. Open reading frames UL44, IRS1/TRS1, and UL36-38 are required for transient complementation of human cytomegalovirus oriLyt-dependent DNA synthesis. J Virol **67:**2575-82.
112. **Pellett, P. E., and B. Roizman.** 2007. The Family Herpesviridae: A Brief Introduction, p. 2480-2499. *In* B. N. Fields, D. M. Knipe, and P. M. Howley (ed.), Fields' virology, 5th ed. Wolters Kluwer Health/Lippincott Williams & Wilkins, Philadelphia.
113. **Perdiguero, B., and M. Esteban.** 2009. The interferon system and vaccinia virus evasion mechanisms. J Interferon Cytokine Res **29:**581-98.
114. **Pettersson, U., and L. Philipson.** 1974. Synthesis of complementary RNA sequences during productive adenovirus infection. Proc Natl Acad Sci U S A **71:**4887-91.
115. **Poppers, J., M. Mulvey, C. Perez, D. Khoo, and I. Mohr.** 2003. Identification of a lytic-cycle Epstein-Barr virus gene product that can regulate PKR activation. J Virol **77:**228-36.
116. **Powers, C., and K. Fruh.** 2008. Rhesus CMV: an emerging animal model for human CMV. Med Microbiol Immunol **197:**109-15.
117. **Ramos, A., S. Grunert, J. Adams, D. R. Micklem, M. R. Proctor, S. Freund, M. Bycroft, D. St Johnston, and G. Varani.** 2000. RNA recognition by a Staufen double-stranded RNA-binding domain. EMBO J **19:**997-1009.
118. **Rauch, A., M. Bellew, J. Eng, M. Fitzgibbon, T. Holzman, P. Hussey, M. Igra, B. Maclean, C. W. Lin, A. Detter, R. Fang, V. Faca, P. Gafken, H. Zhang, J. Whiteaker, D. States, S. Hanash, A. Paulovich, and M. W. McIntosh.** 2006.

Computational Proteomics Analysis System (CPAS): an extensible, open-source analytic system for evaluating and publishing proteomic data and high throughput biological experiments. J Proteome Res **5:**112-21.

119. **Rawlinson, W. D., H. E. Farrell, and B. G. Barrell.** 1996. Analysis of the complete DNA sequence of murine cytomegalovirus. J Virol **70:**8833-49.
120. **Romanowski, M. J., E. Garrido-Guerrero, and T. Shenk.** 1997. pIRS1 and pTRS1 are present in human cytomegalovirus virions. J Virol **71:**5703-5.
121. **Romanowski, M. J., and T. Shenk.** 1997. Characterization of the human cytomegalovirus irs1 and trs1 genes: a second immediate-early transcription unit within irs1 whose product antagonizes transcriptional activation. J Virol **71:**1485-96.
122. **Ross, S. A., N. Arora, Z. Novak, K. B. Fowler, W. J. Britt, and S. B. Boppana.** 2010. Cytomegalovirus reinfections in healthy seroimmune women. J Infect Dis **201:**386-9.
123. **Rothenburg, S., E. J. Seo, J. S. Gibbs, T. E. Dever, and K. Dittmar.** 2009. Rapid evolution of protein kinase PKR alters sensitivity to viral inhibitors. Nat Struct Mol Biol **16:**63-70.
124. **Ryder, S. P., M. I. Recht, and J. R. Williamson.** 2008. Quantitative analysis of protein-RNA interactions by gel mobility shift. Methods Mol Biol **488:**99-115.
125. **Samuel, C. E.** 2011. Adenosine deaminases acting on RNA (ADARs) are both antiviral and proviral. Virology **411:**180-93.
126. **Schetz, J. A., and E. P. Shankar.** 2004. Protein expression in the Drosophila Schneider 2 cell system. Curr Protoc Neurosci **Chapter 4:**Unit 4 16.
127. **Schleiss, M. R.** 2008. Cytomegalovirus vaccine development. Curr Top Microbiol Immunol **325:**361-82.
128. **Schleiss, M. R.** 2006. Nonprimate models of congenital cytomegalovirus (CMV) infection: gaining insight into pathogenesis and prevention of disease in newborns. ILAR J **47:**65-72.
129. **Schleiss, M. R., A. McGregor, K. Y. Choi, S. V. Date, X. Cui, and M. A. McVoy.** 2008. Analysis of the nucleotide sequence of the guinea pig cytomegalovirus (GPCMV) genome. Virol J **5:**139.
130. **Schonborn, J., J. Oberstrass, E. Breyel, J. Tittgen, J. Schumacher, and N. Lukacs.** 1991. Monoclonal antibodies to double-stranded RNA as probes of RNA structure in crude nucleic acid extracts. Nucleic Acids Res **19:**2993-3000.
131. **Schuessler, A., K. L. Sampaio, L. Scrivano, and C. Sinzger.** 2010. Mutational mapping of UL130 of human cytomegalovirus defines peptide motifs within the C-terminal third as essential for endothelial cell infection. J Virol **84:**9019-26.
132. **Shors, T., K. V. Kibler, K. B. Perkins, R. Seidler-Wulff, M. P. Banaszak, and B. L. Jacobs.** 1997. Complementation of vaccinia virus deleted of the E3L gene by mutants of E3L. Virology **239:**269-76.
133. **Stasiak, P. C., and E. S. Mocarski.** 1992. Transactivation of the cytomegalovirus ICP36 gene promoter requires the alpha gene product TRS1 in addition to IE1 and IE2. J Virol **66:**1050-8.
134. **Strang, B. L., A. P. Geballe, and D. M. Coen.** 2010. Association of human cytomegalovirus proteins IRS1 and TRS1 with the viral DNA polymerase accessory subunit UL44. J Gen Virol **91:**2167-75.
135. **Stratton, K. R., J. Durch, and R. S. Lawrence.** 2000. Vaccines for the 21st century : a tool for decisionmaking. National Academy Press, Washington, D.C.

136. **Takeuchi, K., T. Komatsu, Y. Kitagawa, K. Sada, and B. Gotoh.** 2008. Sendai virus C protein plays a role in restricting PKR activation by limiting the generation of intracellular double-stranded RNA. J Virol **82:**10102-10.
137. **Tartaglia, J., M. E. Perkus, J. Taylor, E. K. Norton, J. C. Audonnet, W. I. Cox, S. W. Davis, J. van der Hoeven, B. Meignier, M. Riviere, and et al.** 1992. NYVAC: a highly attenuated strain of vaccinia virus. Virology **188:**217-32.
138. **Thompson, A. J., and S. A. Locarnini.** 2007. Toll-like receptors, RIG-I-like RNA helicases and the antiviral innate immune response. Immunol Cell Biol **85:**435-45.
139. **Toroney, R., C. M. Hull, J. E. Sokoloski, and P. C. Bevilacqua.** 2012. Mechanistic characterization of the 5'-triphosphate-dependent activation of PKR: Lack of 5'-end nucleobase specificity, evidence for a distinct triphosphate binding site, and a critical role for the dsRBD. RNA **18:**1862-74.
140. **Valchanova, R. S., M. Picard-Maureau, M. Budt, and W. Brune.** 2006. Murine cytomegalovirus m142 and m143 are both required to block protein kinase R-mediated shutdown of protein synthesis. J Virol **80:**10181-90.
141. **Vercammen, E., J. Staal, and R. Beyaert.** 2008. Sensing of viral infection and activation of innate immunity by toll-like receptor 3. Clin Microbiol Rev **21:**13-25.
142. **Wang, N., P. F. Baldi, and B. S. Gaut.** 2007. Phylogenetic analysis, genome evolution and the rate of gene gain in the Herpesviridae. Mol Phylogenet Evol **43:**1066-75.
143. **Wang, W., K. Riedel, P. Lynch, C. Y. Chien, G. T. Montelione, and R. M. Krug.** 1999. RNA binding by the novel helical domain of the influenza virus NS1 protein requires its dimer structure and a small number of specific basic amino acids. RNA **5:**195-205.
144. **Weber, F., V. Wagner, S. B. Rasmussen, R. Hartmann, and S. R. Paludan.** 2006. Double-stranded RNA is produced by positive-strand RNA viruses and DNA viruses but not in detectable amounts by negative-strand RNA viruses. J Virol **80:**5059-64.
145. **Weston, K., and B. G. Barrell.** 1986. Sequence of the short unique region, short repeats, and part of the long repeats of human cytomegalovirus. J Mol Biol **192:**177-208.
146. **Wiesen, J. L., and T. B. Tomasi.** 2009. Dicer is regulated by cellular stresses and interferons. Mol Immunol **46:**1222-8.
147. **Wohnsland, A., W. P. Hofmann, and C. Sarrazin.** 2007. Viral determinants of resistance to treatment in patients with hepatitis C. Clin Microbiol Rev **20:**23-38.
148. **Zhang, D., L. M. Iyer, and L. Aravind.** 2011. A novel immunity system for bacterial nucleic acid degrading toxins and its recruitment in various eukaryotic and DNA viral systems. Nucleic Acids Res **39:**4532-52.
149. **Zhang, G., B. Raghavan, M. Kotur, J. Cheatham, D. Sedmak, C. Cook, J. Waldman, and J. Trgovcich.** 2007. Antisense transcription in the human cytomegalovirus transcriptome. J Virol **81:**11267-81.
150. **Zhang, H., S. Todd, M. Tachedjian, J. A. Barr, M. Luo, M. Yu, G. A. Marsh, G. Crameri, and L. F. Wang.** 2012. A novel bat herpesvirus encodes homologues of MHC classes I and II, C-type lectin, and a unique family of immune-related genes. J Virol.
151. **Zhang, P., and C. E. Samuel.** 2007. Protein kinase PKR plays a stimulus- and virus-dependent role in apoptotic death and virus multiplication in human cells. J Virol **81:**8192-200.

Craig John Bierle

Fred Hutchinson Cancer Research Center
1100 Fairview Avenue North, C2-023
Seattle, WA 98109

e-mail: cjb57@u.washington.edu
phone: 206-667-5199
fax: 206-667- 6523

EDUCATION

University of Washington — Seattle, WA
Ph.D., Molecular and Cellular Biology — Expected Dec. 2012

Cornell University — Ithaca, NY
B.S., Biological Sciences — 2006
Cum Laude with Distinction in Research
Honors Thesis Title: Anaerobic Cellulose Degradation in Chicago Bog, an Acidic Peat Bog, and the Isolation and Characterization of Associated Peatland Bacteria

DISSERTATION RESEARCH — 2007-present

Mentor:
Adam Geballe, MD — Fred Hutchinson Cancer Research Center, Seattle, WA

Double-stranded RNA (dsRNA) serves as a pathogen associated molecular pattern that alerts the host cell to infection and triggers an antiviral response. Protein kinase R (PKR) is part of this antiviral response and PKR blocks translation initiation after it is activated by dsRNA. My research has focused on understanding the accumulation of viral dsRNA during cytomegalovirus infection and characterizing the function of the dsRNA-binding PKR antagonists encoded by human and guinea pig cytomegaloviruses.

OTHER RESEARCH EXPERIENCE

LABORATORY ROTATIONS — 2006-2007
Mentors:

Maxine Linial, Ph. D. — Fred Hutchinson Cancer Research Center, Seattle, WA
Foamy virus biology

Raymond Monnat, M.D — University of Washington, Seattle, WA
Engineering of homing endonucleases

Hans-Peter Kiem, M.D. — Fred Hutchinson Cancer Research Center, Seattle, WA
Retroviral gene therapy

UNDERGRADUATE RESEARCH
Mentors:

Stephen Zinder, Ph.D. 2003-2006
Microbial ecology of northern peatlands Cornell University, Ithaca, NY

Andrew Sykes, Ph. D. Summer 2003
Design of chemical pH sensors University of South Dakota, Vermillion, SD

TEACHING ASSISTANTSHIPS

2007-2008

Introductory Genetics University of Washington
Genome 371 Seattle, WA

Molecular, Cellular, and Developmental Biology University of Washington
Biology 200 Seattle, WA

PUBLICATIONS

1. **Bierle, C. J.,** Schleiss, M. R., and Geballe, A. P. (2012). Antagonism of the protein kinase R pathway by the guinea pig cytomegalovirus US22-family gene gp145. Virology **433**(1), 157-66.

2. Marshall, E. E., **Bierle, C. J**., Brune, W., and Geballe, A. P. (2009). Essential role for either TRS1 or IRS1 in human cytomegalovirus replication. *J Virol* **83**(9)**,** 4112-20.

PRESENTATIONS

1. **Bierle, C. J**., M. R. Schleiss, and A. P. Geballe. 2011. The guinea pig cytomegalovirus US22 family gene gp145 antagonizes PKR. *American Society for Virology Meeting*. Minneapolis, Minnesota. Talk.

2. **Bierle, C. J**., S. J. Child, G. Brennan, M. R. Schleiss, and A. P. Geballe. 2010. Species-Specific Adaptation of Cytomegaloviruses to Protein Kinase R. *CSHL Meeting on Translation Control*. Cold Spring Harbor, New York. Poster.

AWARDS AND HONORS

2008	NSF Graduate Research Fellowship Program, Honorable Mention
2004	Robert L. Strickler Scholarship
2004	Cornell University Hughes Scholar
2003	Seal & Serpent Scholarship
2002-2006	James E. Casey Scholarship
2002-2006	Cornell Tradition Fellow

REFERENCES

Adam Geballe, M.D.—Ph.D. Mentor
Member of Human Biology Faculty
Fred Hutchinson Cancer Research Center
1100 Fairview Avenue North, C2-023
Seattle, WA 98109
(206) 667-5122
ageballe@fhcrc.org

Michael Lagunoff, Ph.D.—Graduate Committee Member
Associate Professor of Microbiology
University of Washington
Box 357735
Seattle WA 98195-7735
(206) 616-4285
lagunoff@u.washington.edu

Mark Schleiss, M.D.—Collaborator
Director, Division of Pediatric Infectious Diseases and Immunology
Center for Infectious Diseases and Microbiology Translational Research
University of Minnesota
2001 6th Street SE
3-214 MTRF
Minneapolis, MN 55455
(612) 626-9913
schleiss@umn.edu

Stephen Zinder, Ph.D.—Undergraduate Research Mentor
Professor of Microbiology
Cornell University
272 Wing Hall
Ithaca, NY 14853
(607) 255-2415
shz1@cornell.edu